Studies of Alfven and Lower Hybrid Waves in Plasma and Complex Plasma

THESIS SUBMITTED TO
DELHI TECHNOLOGICAL UNIVERSITY
For the Award of the Degree of

DOCTOR OF PHILOSOPHY
IN PHYSICS

By

Mr. Rajesh Gupta
(2K18/PhD/AP/29)

Under the supervision of
PROF. SURESH C. SHARMA
And
Joint-supervision of
PROF. RUBY GUPTA

Department of Applied Physics

DELHI TECHNOLOGICAL UNIVERSITY
Delhi-110042, India

(June, 2023)

Dedicated

To

My Son-Skanda

Delhi Technological University

(Govt. of National Capital Territory of Delhi)
Shahbad Daulatpur, Bawana Road, Delhi-110042

CERTIFICATE

This is to certify that the thesis titled ***"Studies of Alfven and Lower Hybrid Waves in Plasma and Complex Plasma"*** submitted by **Mr. Rajesh Gupta (2K18/PhD/AP/29)** to Delhi Technological University (DTU), Delhi, India for the degree of Doctor of Philosophy, is a bonafide record of the research work carried out by him under our supervision and guidance. The work embodied in this thesis has been carried out in the Plasma & Nano Simulation Research Lab, Department of Applied Physics, Delhi Technological University (DTU), Delhi, India. The work of this thesis is original and has not been submitted in parts or fully to any other Institute or University for the award of any other degree or diploma.

_____

Prof. Suresh C. Sharma
Supervisor
Department of Applied Physics,
Delhi Technological University,
Shahbad Daulatpur, Bawana Road,
Delhi-110042, India.

_____

Prof. Ruby Gupta
Joint -Supervisor
Department of Physics,
Swami Shraddhanand College,
University of Delhi, Alipur,
Delhi-110036, India.

Delhi Technological University

(Govt. of National Capital Territory of Delhi)
Shahbad Daulatpur, Bawana Road, Delhi-110042

DECLARATION BY THE CANDIDATE

I, **Rajesh Gupta**, hereby certify that the thesis titled ***"Studies of Alfven and Lower Hybrid Waves in Plasma and Complex Plasma"*** submitted in the fulfillment of the requirements for the award of thedegreeofDoctorofPhilosophyisanauthenticrecordofmyresearchworkcarriedoutunderthesupervisionof**Prof.Suresh C. Sharma,** Department of Applied Physics, Delhi Technological University (DTU) and Joint-supervision of **Prof. Ruby Gupta,** Department of Physics, Swami Shraddhanand College, University of Delhi (DU), Delhi. I further declare that I have not submitted any part of this thesis for the award of any other degree from any other university in India or abroad.

_____

Rajesh Gupta
(2K18/PhD/AP/29)
Delhi Technological University,
Shahbad Daulatpur, Bawana Road,
Delhi-110042, India.

ACKNOWLEDGEMENTS

It brings me great pleasure to express my responsibilities, heartfelt appreciation, and sense of duty to those whose assistance made in any way in finishing my doctoral thesis. Numerous individuals, including my university, supervisor, joint-supervisor, colleagues, friends, and family, provided me with a great deal of direction, support, and encouragement in order to finish this thesis. I feel incredibly fortunate to extend my gratitude to everyone who has helped me throughout the course of my work, in whatever capacity.

Firstly, and prior to all, the greatest appreciation and gratitude go out to **Prof. Suresh C. Sharma**, my supervisor, not only for his kindness, patience, and extensive knowledge, which have all been helpful to me, but also for giving me a flexible and peaceful environment for my research work. I would like to thank him for all of his help, advice, support, and excellent supervision while I was earning my research degree. He and I have had several chats, and each time he has given me precise explanations, healthy criticism and innovative suggestions that have really helped me to improve my thesis. For his thoughtful advice on subjects outside the purview of my research and for his kind support, I am grateful and thank him.

I would like to extend my sincere appreciation to **Prof. Ruby Gupta**, Swami Shraddhanand College, University of Delhi, Delhi, who is my joint - supervisor and she kept me motivated during my research work. Being her pupil is a privilege, and I feel extremely fortunate to have had such understanding. She is incredibly knowledgeable and experienced in plasma physics in general and dusty plasma in particular, and I have benefited significantly from her work. Her compassion, insight, and inspiration have always been present. She gave me access to research resources at her institute, and I want to thank her sincerely for that.

I would like to use this opportunity to express my gratitude to the DTU authorities especially Hon'ble **Vice Chancellor** Sir for his invaluable assistance and provision of the necessary research facilities to carry out this study.

I would like to thank all the faculty and staff members of Department of Applied Physics, DTU for their help and cooperation throughout my study period. I also want to extend a sincere and heartfelt thanks to my lab mates at the Plasma and Nano-Simulation Research Laboratory for the thought-provoking conversations, unselfish assistance, and all the fun we had while conducting the study.

At this time, I'd also like to express my gratitude to **Prof. D. N. Gupta,** Department of Physics and Astrophysics, University of Delhi and **Prof. R. P. Sharma, Former Head, CES, IIT,** Delhi for their insightful remarks and recommendations.

Since I would not be where I am now without the guidance, blessings, motivation and support of all my teachers since I was a young child. I would like to express my gratitude to all of them.

I would not have been able to accomplish this study work with my full devotion without the blessings, encouragement, and moral support of my parents, **Smt. Bimla Gupta** and **Dr. Ramesh Chandra Gupta**, for which I am very grateful.

I would like to express my deep appreciation to my brothers **Nitin Gupta, Sumit Gupta,** and **Rajiv Gupta** with a special word of appreciation for their unwavering support and encouragement. I am very thankful to **Rajiv Gupta** especially not only for a lot of friendly help but also for being there to listen when I needed an ear. He has always been there for me, and I sincerely appreciate that. During my studies, there were periods when nothing seemed to have any chance of success. But I have to be honest and state that his perseverance and unceasing support were the only things that allowed me to complete this research work.

I am really indebted and grateful to my son, **Skanda Gupta** and daughter **Shreeja Gupta**, both my little children who gave no hindrance in my studies and allowed me to complete the thesis work during the time they greatly needed me in their infancy for their entertainment and proper fondling and remained deprived of all.

Last but not the least; I am highly indebted to my wife, **Mrs. Sonal K. Gupta** who has been by my side in every difficult situation. Her co-operation, understanding, and sincere encouragement were the sustaining factors in accomplishing this thesis successfully.

I above all express my gratitude to the Almighty, whose mercy made it possible for me to complete my research work entirely. I am grateful to God for granting me the capacity for endurance and strength as well for eradicating every obstacle in my way.

Place: Delhi ***Rajesh Gupta***

Dated: 30 June, 2023

ABSTRACT

The excitation of waves, may be electromagnetic or electrostatic, in plasmas or dusty plasmas by electron or ion beams (relativistic or non-relativistic) has also attracted considerable attention. Beam-plasma interaction involves many physical aspects, including, for example, mechanisms of wave radiation, collective processes leading to instabilities, plasma and beam dynamics, as well as several applications, such as communications between two spacecraft or between spacecraft and the earth. An electron mode depends on the mass of the electrons, but the ions may be assumed to be infinitely massive, i.e., stationary while an ion mode depends on the ion mass, but the electrons are assumed to be massless and redistribute themselves instantaneously according to Boltzmann relation. Only rarely, for example, in the lower hybrid oscillation, will a mode depend on both the electron and the ion mass. The various wave modes can also be classified according to whether they propagate in an un-magnetized plasma or parallel, perpendicular, or oblique to the static magnetic field. Moreover, the presence of highly charged dust particles in a plasma can have significant influence on the collective properties of the plasma, and hence wave mode properties. The waves and instabilities can be excited either by the free sources of energy such as plasma currents produced by the electromagnetic and electrostatic fields present within the plasma or by an external beam source propagating inside it. Hence, we aim at the theoretical investigations of waves and instabilities in plasmas or dusty plasmas.

We have studied, analytically, abnormal Doppler resonance with an electron beam in a magnetized plasma that causes a plane polarized Alfven wave to decay nonlinearly. There are two different wave propagation modes namely, the Alfven wave mode, with a frequency lesser than plasma ion frequency ω_{ci} and the electron cyclotron wave mode, with a frequency approaching electron cyclotron frequency ω_{ce}. The plane polarized Alfven waves and electron beam communicate through both normal and abnormal Doppler resonance. The frequency does not fluctuate and the wave stabilizes in anomalous resonance contact in contrast to the case of normal Doppler resonance. It is also described in this work, how the frequency and growth rate of plasma electrons vary with magnetic field and number density.

Rajesh Gupta
Delhi Technological University, Delhi, India

The Shear Alfven waves are only affected by the beam's particles when they counter-propagate one-another and destabilize left-hand polarized modes for parallel waves and left-hand as well as right-hand polarized modes for oblique waves via an action called fast cyclotron interaction. Right-hand (RH) and left-hand (LH) polarized oblique Alfven modes are affected differentially by collisions between beam ions and plasma constituents in terms of the growth rate and frequency of produced Alfven waves. We have also observed that the polarized oblique Alfven modes exhibit a polarization reversal after resonance. The growth rates are correlated with the increase in propagation angle and because of the obliquity of the wave, the maximum growth rate rises in the presence or absence of the beam. The frequency and growth rate of the waves both are affected by the collision of beam ions with plasma constituents. As the beam velocity drops, the significance of collisions increases and they damp the Alfven waves more and more.

We have also given a theoretical analysis on the generation of an obliquely propagating shear Alfven wave in dusty plasma by hydrogen ion beam. When the ion beam particles counter-propagate with a shear Alfven wave, they interact with through cyclotron interaction with the wave whereas through Cerenkov interaction with a co-propagating wave. It has been discussed about how the beam speed, magnetic field, wave number, dust particle density, and dust charge fluctuations affect the situation. As the beam velocity increases, both the wave frequency and maximum growth rate decrease, with the changes being different for parallel and perpendicular wave numbers. The findings and experimental observations are well congruent.

A problem based on fluid theory of beam driven growth of lower hybrid wave (LHW) in a magnetized relativistic beam plasma system is also has been studied. The decay of large amplitude lower hybrid wave, the pump or mother wave into lower-hybrid sideband wave and beam mode drives the instability. A ponderomotive force is applied to plasma electrons by the excited sideband wave when it interacts with the pump wave. The dependence of parametric instabilities on the local plasma characteristics has been used to determine the rate of growth of the beam driven instability in various beam density regions. The results indicate that electron dynamics in the presence of a relativistic electron beam play a major role in the beam coupling those results in parametric instability of the LH wave.

The present research work can be extended to study waves and instabilities in plasmas and findings of the present research work may be useful in investigating astrophysical situations, near earth environment, and fusion plasma devices, etc.

CONTENTS

	Page No.
Acknowledgement …..…….	**iii**
Abstract……...……...	**vi**
List of Publications …...……	**xiii**
List of Figures……...	**xv**
List of Tables…….	**xix**

Chapter 1:		**Introduction……..**	**1-23**
1.1	Background……		2
1.2	Plasmas……..……		3
1.3	Dusty or complex Plasmas……..……..		4
	1.3.1	Characteristics……...	5
		1.3.1.1 Quasi-Neutrality……	6
		1.3.1.2 Debye Shielding……	6
	1.3.2	Methods of Production……..	7
	1.3.3	Charging of the dust grains……	8
	1.3.4	Dust charge Fluctuations……...	9
1.4	Waves In Plasmas Or Dusty Plasmas And Instabilities……		9
	1.4.1 Alfven wave mode……...		11
	1.4.2 Lower Hybrid Wave mode……..		12

1.5	Dusty Plasma in Space and Laboratory…….…….....	13
	1.5.1 Dusty Plasma in Space……...	13
	1.5.2 Dusty Plasma In Laboratory …….	14
1.6	Beam Plasma Interaction…….…….....	14
1.7	Phase Synchronism**…….**	15
1.8	Assumptions……	16
1.9	Dynamics……....	17
1.9	Objectives & Thesis Layout……..	18
References		21

Chapter 2: Stabilization of Plane Polarized Alfven Waves by Anomalous Doppler Resonance……...…….…….....24- 34

2.1	Introduction……	24
2.2	Instability Analysis……..……..	26
2.3	Determination Of Growth Rate……..	29
2.4	Results and Discussion……..	30
2.5	Conclusion……...……...	32
References		33

Chapter 3: Polarization Reversal of Oblique Electromagnetic Wave in Collisional Beam-Hydrogen Plasma……35- 53

3.1	Introduction……..	35
3.2	Instability Analysis……..……..	37
	3.2.1 Oblique Shear Alfven Wave……	38
3.3	Conclusion …….	48
References		50

Chapter 4: Generation of Obliquely Propagating Shear Alfven Wave in Dusty Plasma by Ion Beam…….....54-74

4.1	Introduction……..	54
4.2	InstabilityAnalysis……..……..	56
	4.2.1 For Cyclotron interaction……	60
	4.2.2 For Cerenkov interaction**……**	62
4.3	Results and Discussion…….	62
4.4	Conclusion……...……...	71
References		72

Chapter 5: Beam-driven Growth of Lower Hybrid Wave in a Magnetized Relativistic Beam-Plasma System……...75-89

5.1	Introduction……..	75
5.2	Analytical Mode ……	77
	5.1.1 Compton Regime……	80

	5.1.2 Raman Regime……...	83
5.3	Conclusion……...……....	86
References		88

Chapter 6: Conclusion and Future Prospective…..... 90-96

LIST OF PUBLICATIONS

International Journals

1. **Rajesh Gupta**, Ruby Gupta and Suresh C. Sharma, "Polarization Reversal of Oblique Electromagnetic Wave in Collisional Beam-Hydrogen Plasma", *Progress in Electromagnetics Research C*, Vol. 127, 49-59 (2022) Impact Score: 1.68 doi:10.2528/PIERC22092526
2. **Rajesh Gupta**, Ruby Gupta, Suresh C. Sharma, "Generation of Obliquely Propagating Shear Alfven Wave in Dusty Plasma by Ion Beam" *Contributions to Plasma Physics*, Vol. 63, 1-13 (2023) (IF 1.255). https://doi.org/10.1002/ctpp.202200178
3. **Rajesh Gupta**, Suresh C. Sharma, Ruby Gupta, Devki Nandan Gupta, "Beam-driven Growth of Lower Hybrid Wave in a Magnetized Relativistic Beam-Plasma System" *Journal of Fusion Energy* Vol. 42, 25 (2023) (IF 1.793). https://doi.org/10.1007/s10894-023-00365-9

International /National Conference Publications

1. **Rajesh Gupta**, Suresh C. Sharma, Ruby Gupta, "Stabilization of plane polarized Alfven waves by anomalous Doppler resonance", presented at the **International Conference on Photonics, Metamaterials & Plasmonics (PMP-2019)**", held at the Department of Physics and Materials Science & Engineering, JIIT, Noida, Uttar Pradesh, India. *AIP Conference Proceedings* 2136, 060015 (2019) https://doi.org/10.1063/1.5120961

International / National Conference Presentations and Symposium / Workshops Attended

1. Poster Presented a paper titled, "Cyclotron Interaction of Alfven wave and Electron beam" in the ***National Conference on Smart Energy Resources and Sustainable Engineering (2019)*** at SSN College, University of Delhi, India (28-29 March, 2019).
2. **Virtual Symposium on "*International Day of Light 2020 (IDL-20)*"**, Department of Physics, organized by IEEE Photonics society and SPIE student chapters IIT Guwahati (16 May, 2020).
3. **Faculty Development Program on "*Research Techniques in Science and Technology*"** organized by K.R. Mangalam University, Gurugram in collaboration with Gargi College, University of Delhi (18-23 July, 2022).
4. Presented a paper titled, "Effect of Collisions on Interaction of Particle Beam with Alfven wave in Magnetoplasma" in the ***International conference on Advanced Futuristic Materials for Sustainable Society (ICAFM),*** Chandigarh School of Business, Jhanjeri, Mohali (22-23 August, 2022).
5. Presented a paper titled, "Collisional Damping of Pure and Shear Alfven Modes in Beam Plasma System" in the ***1st International Conference on Innovations & Future Prospects of Advanced Materials (IFPAM-2023)***, School of Basic and Applied Sciences, K.R. Mangalam University (SBAS- KRMU), Gurugram (23-24 March, 2023).

List of Figures

Fig. No.		Page No.
Chapter: 1		
1.1	Debye Shielding…….....	5
Chapter: 2		
2.1	Alfven wave frequency ω_1 (rad/s) as a function of k_z (cm^{-1})……....	30
2.2	Alfven wave frequency ω_1 (rad/sec) as a function of static magnetic field B (in Gauss)……	31
2.3	Growth rate γ (sec^{-1}) of the unstable mode as a function of wave number k_z (cm^{-1}) for anomalous Doppler resonance.....	31
2.4	Growth rate γ (sec^{-1}) of unstable mode as a function of static magnetic field B (in Gauss) for anomalous Doppler resonance.....	32
Chapter: 3		
3.1	Dispersion curves of oblique shear Alfven wave for different angles of propagation θ (a) 0º, (b) 30º, (c) 45º, (d) 60º and (e) 80º and the beam mode (f) with velocity 1.69×10^8 cms^{-1}……....	42
3.2	Growth rate γ_{wc} (in sec^{-1}) of the unstable mode as a function of k_z (in cm^{-1}) for different angles (a) 80^0, (b) 60^0, (c) 45^0, (d) 30^0 and (e) 0^0 of propagation of shear Alfven wave in the presence of beam-plasma collisions ……	44
3.3	Growth rate γ (in sec^{-1}) of the unstable mode as a function of k_z (in cm^{-1}) for different angles (a) 80^0, (b) 60^0, (c) 45^0 and (d) 30^0 of propagation of shear Alfven wave …….	45
3.4	Growth rates (a) γ and (b) γ_{wc} (in sec^{-1}) of the unstable mode as a function	

of k_z (in cm^{-1}) for an angle of propagation of shear Alfven wave 60^0 in the absence and presence of beam-plasma collisions…….. 46

3.5 Growth rate γ (in sec^{-1}) of the unstable mode as a function of B (in Gauss) for different angles (a) 30^0, (b) 45^0, (c) 60^0 and (d) 80^0 of propagation of shear Alfven wave…….. 47

3.6 Growth rate γ_{wc} (in sec^{-1}) of the unstable mode as a function of B (in gauss) for different angles (a) 0^0, (b) 30^0, (c) 45^0, (d) 60^0 and (e) 80^0 of propagation of shear Alfven wave in the presence of beam-plasma collisions……. 47

3.7 Growth rate γ (in sec^{-1}) of the unstable mode as a function of n_{eo} (in cm^{-3}) for different angles (a) 30^0, (b) 45^0, (c) 60^0 and (d) 80^0 of propagation of shear Alfven wave……..... 48

3.8 Growth rate γ_{wc} (in sec^{-1}) of the unstable mode as a function of n_{eo} (in cm^{-3}) for different angles (a) 0^0, (b) 30^0, (c) 45^0, (d) 60^0 and (e) 80^0 of propagation of shear Alfven wave in the presence of beam-plasma collisions…..... 48

Chapter: 4

4.1 Dispersion curve (a) of Shear Alfven wave and various beam modes with beam ion velocities (b) $v_{b0} = 1.84 \times 10^8$ cm/s (c) $v_{b0} = 1.69 \times 10^8$ cm/s (d) $v_{b0} = 9 \times 10^7$ cm/s (e) $v_{b0} = 6 \times 10^7$ cm/s (f) $v_{b0} = 2.8 \times 10^7$ cm/s for cyclotron interaction between wave and beam. 64

4.2 Normalized growth rate γ^{cyc}/ω_{ci} versus normalized parallel and perpendicular wave numbers……. 64

4.3 Normalized growth rate γ^{cyc}/ω_{ci} versus normalized parallel wave number for different beam velocities (a) 2.8×10^7 cms^{-1} (b) 6.0×10^7 cms^{-1} (c) 9.0×10^7 cms^{-1} (d) 1.69×10^8 cms^{-1} (e) 1.84×10^8 cms^{-1}……..... 65

4.4 Normalized growth rate γ^{cyc}_{max} versus static magnetic field B in Gauss for different parallel wave numbers (a) 0.001 (b) 0.002 (c) 0.004 (d) 0.006 (e) 0.0075 (in cm^{-1}) of unstable shear Alfven wave……..... 65

4.5 Normalized wave frequency ω/ω_{ci} of the shear Alfven wave versus beam velocity (cm/s) for different parallel wave number k_z (Cyclotron interaction) (a) 0.008 (b) 0.009 (c) 0.010 (d) 0.015 (in cm^{-1})……..... 66

4.6 Normalized dispersion curve (a) of Shear Alfven wave for various beam modes with different beam ion velocities (b) v_{b0} =1.84 × 10^8 cm/s (c) v_{b0} = 1.69 × 10^8 cm/s (d) v_{b0} = 9 × 10^7 cm/s (e) v_{b0} = 6 × 10^7 cm/s (f) v_{b0} = 2.8 × 10^7 cm/s for Cerenkov interaction……. 66

4.7 Normalized growth rates γ^{cer}/ω_{ci} versus normalized perpendicular wave numbers for various normalized parallel wave numbers $k_z\times c/\omega_{pi}$ (a) = 0.12 (b) = 0.35 (c) = 0.59 (d) = 0.82……..... 67

4.8 Normalized maximum growth rate γ_{max}^{cyc} versus normalized perpendicular wave number for different beam velocities,v_{b0} (a) 2.8×10^7 cm/s (b) 6×10^7 cm/s (c) 9×10^7 cm/s (d) 1.6×10^8 cm/s (e) 1.84 × 10^8 cm/s……... 68

4.9 Normalized shear Alfven wave frequency ω/ω_{ci} versus normalized perpendicular wave numbers $k_x\times c/\omega_{pi}$ at different normalized parallel wave numbers, $k_z\times c/\omega_{pi}$ (a)= 0.12 (b) = 0.35 (c) = 0.59 (d) = 0.82……... 68

4.10 Dispersion curves of shear Alfven wave frequency in dusty plasma at (a) δ = 1 (b) δ = 2 (c) δ = 5 (d) δ = 7……..... 69

4.11 Decrease in frequency of shear Alfven wave due to dust charge fluctuations in plasma for (a) δ = 7 (b) δ = 5 (c) δ = 3 (d) δ = 2…….. 69

4.12 Normalized maximum growth rate for cyclotron interaction versus normalized wave number at (a) δ = 1 (b) δ = 2 (c) δ = 5 (d) δ = 7……... 70

4.13 Normalized maximum growth rate for Cerenkov interaction versus normalized wave number at (a) δ = 1 (b) δ = 2 (c) δ = 5 (d) δ = 7……... 71

Chapter: 5

5.1 Variation of instability growth rate of LH wave in the Compton regime for different wave frequencies, (a) $\boldsymbol{\omega_p = 0.2\omega_{pe}}$ and (b) $\boldsymbol{\omega_p = 0.1\omega_{pe}}$……. 81

5.2 Variation of instability growth rate of LH wave in the Compton regime for

different beam density, (a) $\boldsymbol{\omega_{pB} = 0.2\ \omega_{pe}}$, (b) $\boldsymbol{\omega_{pB} = 0.4\ \omega_{pe}}$, and (c) $\boldsymbol{\omega_{pB} = 0.6\ \omega_{pe}}$……..... 81

5.3 Instability growth rate of LH wave in the Compton regime with the wave number of the beam mode for different beam velocities, (a) $\boldsymbol{v_B = -0.1c}$, (b) $\boldsymbol{v_B = -0.3c}$, (c) $\boldsymbol{v_B = -0.6c}$, and (d) $\boldsymbol{v_B = -0.8c}$**…….....** 82

5.4 Instability growth rate of LH wave in the Compton regime for different magnetic field strength, (a) **B = 10 kG**, (b) **B = 20 kG**, (c) **B = 30 kG**, and (d) **B = 50 kG**……..... 83

5.5 Instability growth rate of LH wave in Raman regime for different plasma frequencies, (a) $\boldsymbol{\omega_p = 0.1\omega_{pe}}$, (b) $\boldsymbol{\omega_p = 0.8\omega_{pe}}$, and (c) $\boldsymbol{\omega_p = 2\omega_{pe}}$.. 84

5.6 Instability growth rate of LH wave in Raman regime for different beam frequencies, (a) $\boldsymbol{\omega_{pB} = 0.2\ \omega_{pe}}$, (b) $\boldsymbol{\omega_{pB} = 0.4\ \omega_{pe}}$, and (c) $\boldsymbol{\omega_{pB} = 0.6\ \omega_{pe}}$……..... 85

5.7 Instability growth rate of LH wave in Raman regime for different beam velocities, (a) $\boldsymbol{v_B = -0.1c}$, (b) $\boldsymbol{v_B = -0.2c}$, (c) $\boldsymbol{v_B = -0.4c}$, and (d) $\boldsymbol{v_B = -0.6c}$……. 85

5.8 Instability growth rate LH Wave in Raman regime for different magnetic field, (a) B = 5 kG, (b) B = 10 kG, (c) B = 20 kG, and (d) B = 50 kG……. 86

LIST OF TABLES

Table No.		Page No.
Chapter 2		
2.1	Angle of propagation, unstable wave numbers and frequencies of oblique shear Alfven waves and maximum growth rates of wave in the absence and presence of beam-plasma collisions…….....	43

CHAPTER1

INTRODUCTION

1.1 BACKGROUND

The term "plasma" refers to a neutral gas that contains neutrals, ions, and electrons and it is the most abumdant form of matter in the universe. Dust, in the form of microscopic grains of solid material, is an omnipresent component of this plasma. Therefore, dusty plasmas may be considered as a complex mixture of charged dust or micro particulates, ions, electrons, and neutral atoms. These particulates range in size from microns to nanometers, and may be either positively or negatively charged. Currents and magnetic fields are produced as a result of electromagnetic forces exerted by the charged system of numerous interacting particles. With the development of a variety of wave phenomena of remarkable complexity and significant practical utility, these fields play a significant role in the dynamics of plasmas. Plasma is present throughout the universe, including interstellar medium, solar wind, planetary rings, Earth's atmosphere, and magnetosphere. It can also be prepared in laboratories through DC and RF discharges.

The laboratory discovery of plasma crystals triggered a vast increase of interest in complex plasmas. Complex plasma physics is an emerging field of study that includes solid states, the kinetics of phase transitions, hydrodynamics, non-linear physics, and a variety of fundamental features of plasma physics. It is also used in engineering, astronomy, and other industrial applications. Involvement in the topic has increased steadily among research organizations throughout the globe, and so has the quantity of scholarly publications.

The charge on a dust particle changes with the surrounding plasma potential rather than being constant, as is the case with plasma or plasmas containing negative ions. This leads to new damping effects and new mechanisms for wave growth. Depending on whether an oscillating magnetic field is present or not, waves can be categorized as electromagnetic or electrostatic. An electrostatic wave must be fully longitudinal, according to Faraday's law of induction applied to plane waves. A transverse component is required for an electromagnetic wave, although it can also partially be a longitudinal wave. In the present thesis, we study the electromagnetic Alfven wave and electrostatic lower hybrid waves in plasma and complex plasma.

1.2 PLASMA

Plasma, considered as fourth state of matter, constitutes nearly 99% of matter known in the universe, mostly associated with stars. It was firstly identified that the existence of fourth state of matter by W. Crookes [1] in 1879. The term “plasma” as a description of ionized gas, was introduced by I. Langmuir [2] in 1929. Plasma means something moldable and it is characterized by presence of ions or electrons in any combination and in a significant portion. This leads to some peculiar properties. The interactions between particles in a solid, liquid, or gas are much weaker than those in a plasma. In plasma, electric and magnetic fields interact to create strong forces between particles, allowing them to interact in ways that are not possible in the other states of matter. The plasma as a whole remains electrically neutral. However, any ionized gas can’t be called a plasma unless it has a significant degree of ionization. Plasma is an ionized state of matter that develops as a result of the heating continuously of a solid material and passes through phase transitions until an ionized gaseous state develops.

Plasmas are electrically conducted gases composed of ions and electrons that produce magnetic fields and electric currents, and respond strongly to electromagnetic forces. The degree of ionization, the ratio of ionized to neutral particles in a volume of space, and other variables like density, temperature etc. affect the characteristics of plasma. Probably the most important general property is that the morphology of plasma is dictated by electromagnetic forces (Maxwell’s Equations). The charged particles align and accelerate within self-generated electromagnetic fields, resulting in a current flow. One of the primary characteristics of plasma is the collective effect [3], in which charged particles interact with one another via coulomb force. Any single moving

charged particle will also interact with its neighbours, resulting in polarization of the medium and the establishment of a local electric field. It turns, nearby particles will move collectively to reduce this electric field. This is the “collective effect.” An essential parameter to describe plasma is the Debye length. It gives an indication of the distance at which the other charged particles in the plasma are affected by a single charged particle's electric field. Debye length is important for shielding electrostatic fields, as the arrangement of the charged particles efficiently blocks any electrostatic fields at this distance. Quasi-neutrality is another key characteristics of plasmas. Any deviation from neutrality will be compensated for locally by an electric field or current created by the electrostatic interaction between ions and electrons. Almost everywhere in the universe is made of plasma. It might appear as diffuse interstellar clouds, stellar coronas, or dense star interiors. One may see many other plasma phenomena, both man-made and natural, on earth as well. Natural plasmas like lightning and fire are well-known, and even non-physicists are familiar with numerous manmade plasmas like neon lights and street lamps.

1.3 DUSTY OR COMPLEX PLASMA

Plasmas that contain charged liquid or solid particles as dust are referred to as "complex" or "dusty" plasmas. Depending on how the plasmas' charging processes are functioning, the charges may be negative or positive. In space, it's common to encounter dust and dusty plasma. They can be found in planetary rings, comet tails, interplanetary and interstellar clouds [4-6], close to man-made satellites and space stations [7-8]. Additionally, laboratories are currently researching dusty plasmas. Researchers have used the term “complex plasmas” to differentiate dusty plasmas specially “designed” for such investigations. Dust grain size ranges from nm to mm, is around 10^{12} times heavier than that of a proton. Usually, the dust grains become negatively charged due to their numerous encounters with electrons rather than with the cumbersome ions of the plasma, as electrons are highly mobile. This fact makes the field intriguing and technologically significant. The magnitude of this charge is 10^3 -10^4 times of electronic charge for 1μm sized particles. Dust grains isolate in plasma if their size $a << \lambda_D < a_d$, and remain non-isolated if $a << a_d < \lambda_D$, where λ_D is the Debye length and a_d is the distance between two dust particles. Non-isolated dust

particles lead to collective phenomena in plasma while charged dust particles have no effect on the characteristics of plasma.

Massive charged particles must be present for the collective processes to occur in complicated plasma. In addition to altering the charge composition of a plasma, micron-sized particles immersed in it can also cause novel physical processes, such as variations in particle charges and the effects of dissipation and plasma recombination on the particle surface. New methods for energy inflow into the system are implied by these activities. Thus, complex plasmas represent a novel class of non-Hamiltonian systems with potential characteristics that are entirely distinct from those of conventional multicomponent plasmas.

In a number of laboratory apparatuses and industrial operations, dusty plasmas have their common occurrence. Dust plays an exceptionally important role in technological plasma applications, associated with the utilization of plasma deposition and etching technologies in microelectronics, as well as with production of thin films and nanoparticles [9-11]. Understanding the fundamental mechanisms governing, for example, the transit of dust particles, the impact of dust on plasma properties, etc.is important to manage these processes. The physics of dusty plasmas has been studied intensively because of its importance for a number of applications in space and laboratory plasmas [4, 12].

The grains often carry thousands of elementary charges for a micron-sized particle, which results in a tremendously high electrostatic energy for the mutual interaction. As a result, it is considerably simpler to create significant electrostatic coupling in the dust subsystem than it is in the electron-ion subsystem. One may see the production of structured formations of dust particles called plasma crystals. In 1959, Wuerker et al. [13] published the first experimental observation of the ordered (quasi crystalline) structures of charged micro-particles formed in a modified Paul's trap.

1.3.1 Characteristics

The following are some of the ways that the dust grains in the plasma change the plasma's typical properties:

1.3.1.1 Quasi-Neutrality

Dusty plasmas behave like normal plasmas in the absence of outside forces and are macroscopically neutral. Therefore, the charge neutrality requirement reads as follows in equilibrium

$$en_{e0} = Q_d n_{d0} + en_{i0}, \quad (1.1)$$

where n_{i0}, n_{e0} and n_{d0} is the equilibrium i o n density, electron density and dust grain density, e is the electronic charge and Q_d ($= \pm Z_d\, e$) is the charge of positively/ negatively charged dust particles while, Z_d is the number of electrons stuck on one dust particle ~ 10^3 - 10^4. However, charging of dust grains may result in a virtually complete depletion of electron number density in many space and experimental plasmas.

1.3.1.1 Debye Shielding

Plasma is a unique state of matter consisting of free-moving ions and electrons. It generally does not contain strong electric fields in its rest frame, due to its high conductivity. This shielding of an external electric field from the interior of a plasma can be viewed as a result of the free flow of plasma current. This current is able to effectively short out any interior electric fields, thus keeping the plasma in a more stable state. Debye length is the length-scale associated with such shielding (the radius of Debye sphere) (Fig.1.1).

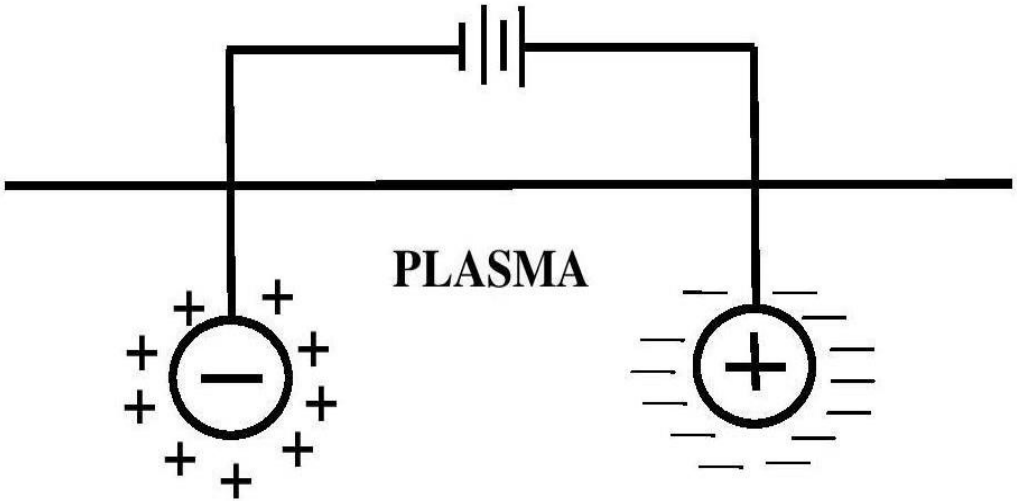

Fig. 1.1 Debye Shielding [3]

A cloud of electrons and negatively charged dust particles would surround a positive potential given to the dusty plasma, while a cloud of ions and positively charged dust particles, if present, would surround a negative potential. A cold plasma results from perfect shielding since there is no charge agitation on the cloud. The charged particles do, however, have a tendency of escaping from the edge of the clouds at specific temperatures, and thus create a potential of the order of $k_B T/e$ in the plasma, leading to insufficient shielding. Debye length is another name for the approximate thickness of such a charged cloud or sheath. The mathematical relation for Debye length as discussed by Shukla and Mamun [14] is

$$\lambda_D = \frac{\lambda_{De}\lambda_{Di}}{\sqrt{\lambda_{De}^2+\lambda_{Di}^2}}, \qquad (1.2)$$

where $\lambda_{De} = \sqrt{T_e/4\pi n_{e0}e^2}$ and $\lambda_{Di} = \sqrt{T_i/4\pi n_{i0}e^2}$ are electron and ion Debye lengths, respectively.

1.3.2 Methods of Production

If an external electrostatic or electromagnetic field isn't introduced to lift and confine the dust grains, they will just sink to the bottom of a plasma under the influence of gravity [18]. The majority of laboratory plasmas, meanwhile, don't seem to be very concerned about this issue because the normal relaxation period for microparticles is significantly longer than the charging time. Thus, by simply sprinkling dust into the plasma, it was easy to create a dusty plasma. Depending on the uses, many methods have been developed to date to make a dusty plasma. Dusty plasmas can be created in a variety of ways, including by suspending negatively charged, 40 m diameter Silica (SiO_2) particles in an argon glow discharge [19], dispersing dust grains into a plasma in a Q-machine [20, 21], and growing dust in plasma created from certain chemically reactive gases, such as silane (SiH_4) and oxygen (O_2).A magnetized dusty plasma experiment (MDPX) has recently been developed to investigate the dynamics of completely magnetized dusty plasmas [22] with a greater focus on fusion plasmas and astrophysical plasmas.

1.3.3 CHARGING OF THE DUST GRAINS

Charging of dust grains basically involves three processes [14] namely (a) Interaction of dust grains with plasma constituents (b) Interaction of dust grains with energetic particles such as electrons and ions (c) Interaction of dust particles with photons. The mechanisms involving charging of dust grains in the interstellar medium were initially described by Spitzer in 1941[23].

The accumulation of electrons and ions from the plasma, photoelectron emission by UV radiation, thermionic emission, secondary electron emission, and ion sputtering, among other processes, cause the dust grains submerged in a plasma to become charged [24]. The electron flow is large as compared to the flux of ions through plasma. Therefore, the equilibrium dust charge on dust particles is negative in plasma. If electron emission is significant than the equilibrium charge becomes positive. Additionally, both laboratory and space plasmas can contain both positively and negatively charged particles. This is feasible because when exposed to UV light, grains can emit electrons as a source.

The charge of a grain results from a variety of mechanisms. If all processes are taken into account, calculating the equilibrium charge on a grain can become quite difficult. The dust charge Q and its surface potential ϕ_s will be negative for dust particles in a plasma with temperatures T_e for electrons and T_i for ions. This is because the electrons being lighter have a thermal velocity v_{te} which is much larger than the thermal velocity v_{ti} of the heavy ions. The plasma particles can also cause ion and electron currents on dust grain surface. The total of the currents resulting from various charging processes determines the charging rate $\frac{dQ}{dT}$ of the grain. These currents vary with the surface potential of a dust particle. A particle submerged in a plasma with no charge will progressively charge up by gathering the electron and ion currents in accordance with the relationship [25, 26].

$$\frac{dQ}{dT} = I_e + I_i \qquad (1.3)$$

and when $I_e + I_i = 0$, charge equilibrium establishes. $\phi_s = -2.51\, k_B T_e / e$ for an

electron-ion plasma. The relation between charge and surface potential is $Q = C\phi_s$, where C refers to the capacitance of a dust particle in plasma. The dust grain experiences a positive charge after absorbing plasma ions, which tends to increase the surface potential. The potential on dust particle is influenced by the electron and ion currents. Generally, the potential at surface is negative, which repels electrons and attracts ions. Then, in order to achieve equilibrium with no net current, the electron current is decreased and the ion current is increased. The variability of the grain charge is a significant characteristic of dusty plasma [27, 28]. Consequently, the dust particle's electric charge varies with time and it should be studied as a dynamic variable.

1.3.4 DUST CHARGE FLUCTUATIONS

It is obvious that any changes in plasma currents might cause changes in dust charge, which could then bring further collective effects [29]. The dust charge fluctuations have been given by

$$\frac{dQ_{d1}}{dt} + \eta\, Q_{d1} = -\left|I_{e0}\right|\left(\frac{n_{i1}}{n_{i0}} - \frac{n_{e1}}{n_{e0}}\right), \tag{1.4}$$

where $\eta = -\dfrac{\left|I_{c0}\right|\, e}{C_g}\left(\dfrac{1}{T_e} - \dfrac{1}{T_i - \phi_{g0}}\right)$

and $Q_{d1} = Q_d - Q_{d0}$ is the perturbed dust grain charge.

The capacitance of the dust grain is $C_g = \left[a(1 + a/\lambda_{De}\right]$.

Substituting $\dfrac{d}{dt} = -i\omega$, we can calculate the dust charge fluctuation as

$$Q_{d1} = \frac{i\left|I_{e0}\right|}{(\omega + i\eta)}\left(\frac{n_{i1}}{n_{i0}} - \frac{n_{e1}}{n_{e0}}\right). \tag{1.5}$$

In this charging model, the effects of the size and shape of dust particles are not taken into consideration. This model is reasonably valid provided $a << \lambda_{De} << \lambda$, where a is the radius of dust particle, λ_{De} is the Debye length and λ is the wavelength of the fluctuation fields. The spread in Q_d/m_d (dust charge to mass ratio) for the dust particles is considered negligible. Moreover, Jana *et al*. [26]have given the limits of the theory for magnetized dusty plasma, that the charging equation for dust grains can be

valid if $a \ll \rho_L$ $\left[\text{where } \rho_L = \frac{v_{te}}{\omega_{ce}} \right]$ is the electron Larmor radius.

It is obvious that the dust charge fluctuations are determined by the electron and ion density perturbations in a plasma and natural decay rate η. Physically, the charge fluctuations decay because any deviation in grain potential from equilibrium floating potential is opposed by the plasma currents [30].

1.4 WAVES IN PLASMAS OR DUSTY PLASMAS AND INSTABILITIES

Plasma is a state of matter composed of charged particles that has unique electrical conductivity properties. This allows it to couple with both electric and magnetic fields. This complex supports various waves, both electromagnetic and electrostatic. Waves can be further classified by the oscillating species, i.e., electrons or ions. The electron temperature is often equal to or higher than the temperature of other plasma components in plasmas of relevance. Moreover, due to the small mass of the electron, the electrons are much faster than the other plasma components. For an electron wave mode, the ions may be assumed to be infinitely massive or even stationary and depends only on electron mass. While an ion wave mode depends on the ion mass, and the electrons are considered massless. The plasma components redistribute themselves instantaneously following Boltzmann relation. Exceptionally, a mode which depends on both the electron and ion masses is the lower hybrid oscillation. The different modes may also be divided into groups based on how they move through a magnetized plasma or whether they move parallel, perpendicular, or oblique to the static magnetic field. Electrostatic waves in plasma include lower hybrid wave, Langmuir wave, ion acoustic wave, ion cyclotron wave, etc. and electromagnetic waves include magnetosonic wave, surface plasma wave, light wave, whistler wave, Alfven wave, etc. Each of the numerous wave propagation modes may be classified by its polarisation and by its dispersion relation, i.e., mathematical expression between the wave frequency and the wave number. Plasma diagnostics benefit greatly from the knowledge on plasma characteristics that may be gleaned from the study of plasma waves. Many of the modes are made unstable by either the plasma's intrinsic free energy or externally launched electron and ion beams.

The wave amplitude is dampened by dissipative processes like collisions. In other words, the wave field transmits energy to the plasma particles. In a plasma, a wave attenuation process called Landau damping, which is fundamentally non collisional, also exists. The energy potential well of the wave traps certain plasma particles that are travelling at speeds near to the wave phase velocity, which causes energy to be transferred from the wave to the particles as a result of Landau damping. Additionally, instabilities that transmit energy from the plasma particles to the wave field may result in modes with increasing amplitudes. Instability phenomena are significant in many plasma processes. The containment of a hot plasma in the laboratory is significantly made more difficult by the occurrence of several distinct forms of instabilities in plasma. For the study of controlled thermonuclear fusion, the analysis of these instabilities is crucial and significant.

The dust charge fluctuations and the dust grain dynamics alters the present wave modes and introduces novel modes as well as some instabilities. An electron-ion plasma is well known to sustain both longitudinal and transverse wave modes [14]. Because of density and potential fluctuations, only longitudinal modes can exist in an ideal un-magnetized plasma, but both longitudinal and transverse wave modes can be excited in a magnetized plasma. Furthermore, the behaviour of wave modes is also impacted by the strong coupling between dust grains. While the addition of the dust inertia causes some entirely novel modes [31], the presence of static charged dust in a plasma can affect the usual linear and non-linear plasma modes. The dust grains have a wide range of sizes, masses and charges and considering the effects of all these parameters is cumbersome. Thus, we assumed the dust grains to have a constant mass, m_d, but their charges and sizes may vary.

1.4.1 ALFVEN WAVE MODES

. Of all known electromagnetic waves, Afven waves are the slowest and have the lowest frequency. Alfven waves, which are transverse magnetic tension waves that move along magnetic field lines, may be excited in an electrically conducting fluid saturated by a magnetic field. The Alfven waves are compressional, which means that magnetic field variations of Alfven waves are in the direction of wave motion. The trajectories of the charged particles passing through plasma with these waves have very little alteration. The Alfven wave may be categorized as pure Alfven wave and shear Alfven wave

depending upon their direction of propagation and orientation of electric vectors with respect to magnetic field. Pure or plane polarized Alfven wave travels along the magnetic field direction, displaying a continuous spectrum and accelerates particles. Transverse plane polarized fluctuations in ideal infinitely conducting plasma are defined as perturbations where magnetic field fluctuations and velocity fluctuations are perpendicular to magnetic field. In the shear Alfven wave the current along the magnetic field is carried by electrons while the current across the magnetic field is carried by ions due to the ion polarization drift and it propagates with the wave magnetic field vector perpendicular to the background field. In the standard Magneto-Hydro-Dynamic concept, the shear Alfven wave is more interesting because wave energy is transported directly along field lines. In interstellar space, the particle acceleration over considerable distances can be caused by shear waves. Gekelman *et al.* [32] have studied that the properties of shear Alfven waves emitted from the sources with the cross field size of the order of the electron inertial length, are different from planar magneto-hydrodynamic waves. The waves that propagate at an angle can also be important in the nonlinear evolution of the system. Additionally, the properties of Alfven waves can be modified by increasing their frequency and modifying the dispersion relation if there are charged dust grains present in the plasma. The discovery of powerful Alfven waves is important because they could provide an explanation for the elevated solar wind velocity and coronal temperature.

1.4.2 LOWER HYBRID WAVE MODES

The lower hybrid oscillations are the longitudinal oscillations of ions and electrons in a magnetized plasma. They involve oscillations of both the ions and electrons in plasma or dusty plasma. These are highly electrostatic in nature and the modes propagation direction must almost be perpendicular to the fixed magnetic field. Because the required exact alignment in relation to the magnetic field is rarely attained, this mode is rather irrelevant in practice. There are certain exceptions, such as when lower hybrid waves are used to heat and drive current in fusion plasmas. Due to their ability to interact efficiently with electrons propagating along the magnetic field and with ions in the transverse plane, they are considered as important for space and laboratory plasma. LHWs can transfer energy from the perpendicular motion of ions to the parallel motion of electrons or vice versa, either accelerating the electrons or

heating the ions. The plasma conditions, particularly the plasma beta and the pump wave's amplitude and polarization—also known as the mother wave's properties—have an impact on the growth rates of parametric instabilities. Numerous non-linear phenomena are caused by the LH waves, including modulational instabilities, harmonic production, and parametric instabilities

1.5 DUSTY PLASMA IN SPACE AND LABORATORY

With sizes of the dust cloud ranging from a few millimetres to astrophysical systems (such as planetary rings, interstellar medium, nebula, comet tails and noctilucent clouds) with an enormous range of sizes, they can be formed under laboratory conditions (such as plasma processing reactors, laboratory experiments, rocket exhaust, and fusion experiments).

1.5.1 DUSTY PLASMA IN SPACE

The solar system, planets, cometary tails, planetary rings, and noctilucent clouds are just a few examples of the many different things that include dust. Dust is also present practically everywhere in the universe. It is possible for spacecraft to sustain physical damage as well as electrical issues due to the presence of charged dust grains, which are frequent in the interplanetary medium and low earth orbit. The development of planets, planetary rings, comet tails, and nebulae may be explained in part by charged dust particles in space plasmas. It is critical to comprehend the physical characteristics of this plasma system in space given the range of contexts in which dusty plasma may be involved. The "interstellar medium" -- a mixture of cosmic dust, hydrogen, and helium -- fills the space between the stars. Atoms of hydrogen make up the vast majority of the interstellar medium. Also present in the interstellar medium is cosmic dust. These particles dwarf hydrogen atoms in size. However, there are far fewer particles of cosmic dust than there are hydrogen atoms in the same volume of space. In the interstellar medium, hydrogen atoms are thought to be 1000 times more frequent than cosmic dust. The dust particles in the circumstellar or interstellar clouds are metallic (graphite, magnetite, amorphous carbons, etc.) and dielectric (ices, silicates, etc.). There are theories as to why our solar system, which is made up of the sun and all the things that circle it, may also include a significant number of dust grains. The

theories include the possibility that micrometeoroids, space debris, human-made pollution, lunar ejecta, and other types of debris may be to blame.

1.5.1 DUSTY PLASMA IN LABORATORY

There are two main characteristics that set laboratory dusty plasmas apart from astrophysical and space plasmas. Firstly, laboratory plasmas are bounded and the characteristics, such as structure, temperature, and conductivity, can affect the dusty plasma formation. Secondly, the external circuit that sustains the dusty plasma also imposes different boundary effects on the dusty plasma. Dust particles interact with the plasma in which they are suspended and their study is known as "dusty plasma research." The primary objective of early experiments with dusty plasma was to achieve a good control of contamination in plasma-processing reactors, either by removing dust particles from the gaseous phase or by preventing them from coming into contact with the surface. This provides a wide range of particle processing options, including surface modification (coating, etching), bulk modification (melting, crystallization), and many more.

1.6 BEAM PLASMA INTERACTION

The complexity of charged particle beams interacting with plasma has been a major topic of theoretical and experimental research. There have been attempts to harness the process of beam instabilities as an efficient way for collisionnless plasma heating, despite the fact that in many devices used for controlled thermonuclear fusion, the charged particle beams begin to exhibit instabilities and anomalous particle diffusion.

There are a variety of oscillation modes into which the plasma may be stimulated, some of which gain amplitude at the cost of the beam energy. The subject of shifting energy from a particle beam to electromagnetic wave energy has received a lot of research in several disciplines of physics. Beam-energy interactions necessitate the preservation of phase matching between waves and particles for as long as feasible. Cerenkov and cyclotron resonances are widely recognized for their important feature of preserving synchronization. The notion of exciting waves in the ionospheric or magnetospheric plasma using a controlled electron or ion beam was presented in the 1970s, which led to the French-Soviet ARAKS experiment [32]. It is not a novel

concept to introduce a charged particle beam into the ionosphere in order to generate waves [33, 34]. Moreover, beam-plasma interaction has also received a lot of interest as a result of in-force experiments used to examine the characteristics of the ionosphere and magnetosphere. The density of the beam was modified to analyze electrostatic [35] and electromagnetic [36–39] wave emissions by the electron or ion beam in order to employ the beam as an antenna radiating plasma modes.

Through momentum and energy conservation, a relativistic beam-plasma system may sustain a number of different plasma modes. As the relativistic electron beam may have a high energy that can be effectively transmitted to the target plasma, the interaction of a relativistic electron beam with the plasma has been employed for plasma heating in fusion and numerous additional applications [40-42]. A relativistic beam-plasma instabilities have garnered a lot of practical [43, 44] and theoretical research [45-47] due to their ability to generate plasma waves and couple energy between the beam and plasma.

1.7 PHASE SYNCHRONISM

We analyse the interaction between an ensemble of relativistic electrons with velocity v_b and an electromagnetic wave with phase velocity, $v_{ph} = \omega / k_z$ near to the electron velocity in order to better understand the phase synchronism requirement. There are three relevant cases:

Case I: If $v_b \approx \omega / k_z$ then the beam velocity is approximately equal to the phase velocity of the EM wave and hence the EM wave appears to relativistic electrons as a static field that may speed up or slow them down. No net energy transfer occurs when an equal number of electrons, which were originally distributed in phase randomly, are accelerated and decelerated if the beam velocity perfectly matches the phase velocity of the electromagnetic wavethe beam velocity is almost equal to the phase velocity of EM wave.

Case II: If $v_b < \omega / k_z$, or the beam velocity, is only slightly slower than the wave's phase velocity; the electrons are bundled together in the wave's accelerated phase, increasing their kinetic energy at the cost of the wave amplitude.

Case III: If $v_b > \omega / k_z$, the beam velocity exceeds the wave's phase velocity. The electrons in the accelerated zone (-eE > 0) then migrate swiftly to the decelerating zone (-eE<0), whereas the electrons in the decelerating zone are retarded and remain there for a longer period of time. In this approach, electrons accumulate in the retarding zone, and energy is transferred from the electrons to the wave. The radiation from distinct bunches of electrons combines coherently, resulting in increased output radiation from the device. The Cerenkov condition, often known as phase synchronism, is given by

$$\omega = \mathbf{k} \cdot \mathbf{v_b}, \qquad (1.6)$$

where 'k' and 'ω' represents wave vector and the frequency of the slow EM mode, respectively and v_b represents the beam velocity. Eq. (1.6) also gives the frequency of operation of the device for fixed beam energy.

1.8 ASSUMPTIONS

Plasma, in its most basic form, is a combination of gases containing both charged and neutral particles, the mobility of which is controlled by electromagnetic fields that are both internal and external to the system. We focus, usually, on the most basic case, in which the plasma is composed entirely of electrons and one type of ion, with no neutral component present. Due to its quasi-neutrality, the plasma can be regarded as neutral when only slow large- scale movements are analysed. Charge components with equal densities can travel at various speeds; therefore, the lack of charge does not always imply the absence of current. Electrons contribute in a current which can be present in plasma and their contribution in the mass flux can be neglected as ion mass is much greater than electron mass. Further, in fast-varying fields only light electrons have time to react to the field variations while massive ions remain practically motionless. Our study involves the interaction of electron or ion beam with the Alfven wave which are low frequency wave.

In a magnetised relativistic beam plasma system, our work also examines the parametric decay of lower hybrid waves (LHW), which are low frequency waves. The generation of these waves depends on both ion and electron mobility. In order to analyse their instability, we have taken into account both the ion density and the electron contribution. The investigation described here is limited to waves of small

amplitude. The study will, thus, be based on a linear perturbation theory with the presumption that the fluctuations in the plasma parameters caused by the presence of waves, are minimal (to the first order) as compared to the undistributed parameters. It is assumed that the magnetic field being applied externally is constant and uniform and that the plasma is homogenous.

1.9 DYNAMICS

Transport equations for the entire plasma as a conducting fluid, supplemented by the electrodynamic equations, can be used in place of the set of macroscopic transport equations for each particular species in a plasma. The magneto hydrodynamic (MHD) equations are the general name for these entire macroscopic equations for a conducting fluid.The MHD equations include the fundamental conservation laws of mass, momentum, and energy as well as the induction equation for the magnetic field in its conventional nonrelativistic form. These are

$$\frac{\partial n}{\partial t} + \nabla \cdot (n\mathbf{v}) = 0, \tag{1.7}$$

the equation of motion in the form

$$m\frac{dv}{dt} = -e\mathbf{E} - e(\mathbf{v} \times \mathbf{B}), \tag{1.8}$$

and the motion of the fluid can be described by the current density expressed as

$$\mathbf{J} = -ne\mathbf{v} \tag{1.9}$$

where n is the number density, $\mathbf{v}$ is the velocity, $\mathbf{E}$ is the electric field of the wave, $\mathbf{B}$ is the external magnetic field and $\mathbf{J}$ is the current density. The fluid equations that describe the motion of the particles are solved along with Maxwell's equations. In this instance, a wave equation is not explicitly derived. Instead, we discover a dispersion relation, which connects the wave frequency ‘ω’ and the wave number ‘k’. The suitable dispersion relation contains all the data on the propagation of a specific wave mode.

1.10 OBJECTIVES & THESIS LAYOUT

The objectives of the research are motivated by the application of Alfven waves and lower Hybrid waves in space and astronomical plasma. Our main focus of research is to investigate the growth or damping of electromagnetic wave, the Alfven wave and electrostatic wave, the Lower Hybrid wave during the beam plasma interaction in plasma and complex plasma. The effect of collision between plasma species, beam velocity, dust parameters number density and dust charge fluctuations, etc. on the propagation of Alfven and Lower Hybrid waves in plasma and complex plasma also have been studied. The mode frequencies and growth rate at various experimental settings have been calculated using a theoretical model that has been constructed to examine excitation of waves and instabilities in dusty plasmas. The theoretical findings have been contrasted with those from the experiments, and their potential use in diverse dusty plasma environments has been examined.

The present research work is motivated by the science and technology of plasma in different fields such as microelectronics, material processing, study of earth's ionosphere, geophysical phenomena like solar wind and various stellar phenomenon like discovery of the dust spokes in Saturn's B ring, where dust component plays a significant role in exciting waves and instabilities and hence modifies the system properties.

The overall goal of this thesis is to provide deeper insight into the physics of Alfven wave and LH waves instabilities/stabilities in the presence of plasma environments. For this, a fluid model will be developed using the first order perturbation theory. Our theoretical model would pave the way in understanding the experimental observations regarding growth and decay of Alfven wave and LH wave in plasma and complex plasma.

The following key goals, which are described below, serve as the foundation for the current research work:

1. Stabilization of plane polarized Alfven waves by anomalous Doppler resonance.

2. Polarization Reversal of Oblique Electromagnetic Wave in Collisional Beam-Hydrogen Plasma

3. Generation of Obliquely Propagating Shear Alfven Wave in Dusty Plasma by Ion Beam

4. Beam-driven Growth of Lower Hybrid Wave in a Magnetized Relativistic Beam-Plasma System.

THESIS LAY OUT

The entire research work divides the thesis into seven chapters which areas discussed below:

Chapter 1: This chapter deals with the introduction to dusty plasmas, production, charging mechanisms and Coupling between the dust grains. Moreover, background of the Alfven waves, LH waves in plasmas and their possible applications in laboratory and space plasmas have been discussed in detail.

Chapter 2: This chapter contains the theoretical model for interaction of plane polarized Alfven wave with the electron beam in a plasma. Fluid treatment is employed to study plasma and beam response. The growth rate of instability/stability has been obtained using first order perturbation theory. The waves interact with the electron beam via normal and anomalous Doppler resonance. The variation of frequency and growth rate with magnetic field and number density of plasma electrons is also discussed.

Chapter 3: In this chapter, a theoretical model based on fluid treatment has been developed to study polarization reversal of oblique shear Alfven wave in collisional beam-hydrogen plasma. It has been shown that an ion beam can efficiently transfer its energy to plasma through wave generation. The effects of collisions between beam ions with plasma components and collisions between plasma components on growth rate as well as frequency of generated waves have been studied.

Chapter 4: An analytical model based on the fluid treatment on plasmas species and ion beam have been developed to study the interaction of obliquely propagating Shear Alfven wave by an ion beam in a magnetized dusty plasma. Ion beam interacts via cyclotron and Cerenkov interaction with shear Alfven wave only if they counter propagate and co-propagate, respectively. The effect of beam velocity, magnetic field, wave number, dust particle density and dust charge fluctuations have been analyzed in detail. The outcomes and the experimental findings are well-aligned.

Chapter 5: In this chapter, a problem based on fluid theory of parametric decay of lower hybrid wave in a magnetized relativistic beam plasma system has been

studied. The nonlinear coupling of lower hybrid wave via beam mode excitation is numerically analyzed. The growth rates of beam driven instability in different beam density regions namely Compton regime and Raman regime have been obtained with the dependency of parametric instabilities on the local plasma parameters.

Chapter 6: The major findings of different investigations and their significance have been summarized in this chapter. Moreover, the future possibilities have also been highlighted.

REFERENCES

[1] W. Crookes, Phil. Trans. R. Soc. Lond.**170**, 135 (1879).

[2] L. Tonkand I. Langmuir, Phy. Rev. **33**,195(1929).

[3] F.F. Chen, "*Introduction to Plasma Physics and Controlled Fusion"* Second edition, Vol. **1 (**1974): Plasma Physics, Los Angeles.

[4] C.K. Goertz, Dusty plasmas in the solar system, Rev. Geophys. **27** (1989) 271–292.

[5] T.G. Northrop, "Dusty plasmas", *Phys. Scripta.* **45** (1992) 475–490.

[6] V.N. Tsytovich, Dust plasma crystals, drops, and clouds, Phys. Usp. **40** (1997) 53–94.

[7] E.C. Whipple, Potentials of surfaces in space, Rep. Prog. Phys. 44 (1981) 1197–1250.

[8] P.A. Robinson, P. Coakley, Spacecraft charging-progress in the study of dielectrics and plasmas, IEEE Trans. Electr. Insul. **27** (1992) 944.

[9] G.S. Selwyn, J. Singh, R.S. Bennett, In situ laser diagnostic studies of plasma-generated particulate contamination, J. Vac. Sci. Technol. A 7 (1989) 2758–2765.

[10] A. Bouchoule, Technological impacts of dusty plasmas, in: A. Bouchoule (Ed.), Dusty Plasmas: Physics, Chemistry and Technological Impacts in Plasma Processing, Wiley, Chichester, 1999, pp. 305–396.

[11] H. Kersten, H. Deutsch, E. Stoffels, W.W. Stoffels, G.M.W. Kroesen, R. Hippler, Micro-disperse particles in plasmas: from disturbing side effects to new applications, Contrib. Plasma Phys. **41** (2001) 598–609.

[12] D. A. Mendis and M. Rosenberg, Anu. Rev. Astron. Astrophys. **32**, 419 (1994).

[13] R. F. Wuerker, H. Shelton, R.V. Langmuir, Electrodynamic containment of charged particles, J. Appl. Phys. **30** (1959) 342–349.

[14] P. K. Shuklaand A. A. Mamun, "*Series in Plasma Physics: Introduction to Dusty Plasma Physics"* Institute of Physics Publishing Ltd., Bristol and Philadelphia (2002), Chapter I.

[15] S. Ichimaru, Rev. Mod. Phys. **54**, 1017 (1982).

[16] E. Thomas Jr, R. Fisher, and R.L. Merlino, Phys Plasmas **14**, 123701 (2007).

[17] S. Hamaguchi, R. T. Farouki, and D. H.E. Dubin, Phys. Rev. E **56,** 4671 (1997).

[18] L. Boufendi, A. Bouchoule, Plasma Sources Sci. Tech. **3,** 262 (1994).

[19] E. Thomas Jr., Phys. Plasmas. **7**, 3194 (2000).

[20] W. Xu, B. Song, R. L. Merlino, and N. D' Angelo, Rev. Sci. Instrum. **63**, 5266

(1992).

[21] R.L. Merlino, "*Plasma Physics Applied" Trans world research network, India*, Chapter-V (2006),73-110.

[22] E. Thomas Jr. U. Konopka, D. Artis, B. Lynch, S. Leblane, S. Adams, R. L. Merlino, and M. Rosenberg, *J. Plasma Phys.* **81**, 345810206 (2015).

[23] L. Spitzer, "*Physical Processes in the Interstellar Medium,*" (1978) John Wiley, New York.

[24] A. Barkan, N. D' Angelo, and R. L. Merlino, Phys. Rev. Lett.**73,** 3093 (1994).

[25] E. C. Whipple, T. G. Northrop and D. A. Mendis, J. Geophys. Res. **90**, 7405 (1985).

[26] M. R. Jana, A. Sen and P. K. Kaw, Phys. Rev. E **48**, 3930 (1993).

[27] S. V. Vladimirov, Phys. Plasmas, **1**, 2762 (1994).

[28] C. Cui and J. Goree, IEEE Trans. Plasma Science **22**, 151 (1994).

[29] A. Sharma and V. K. Tripathi, Phy. Fluids **31**, 3697 (1988).

[30] E.C. Whipple, T.G. Northdrop and D.A.Mendis, J. Geophys. Res. **90**,7405(1985).

[31] P. K. Shukla, Phys. Scripta **45**, 504 (1992).

[32] J. Lavergnat and R. Pellat, J. Geophys. Res. **84**, 7223 (1979).

[33] R. L. Dowden, J. Geophys. Res. **78**, 684 (1973).

[34] T. F. Bell and T. N. C. Wang, IEEE Trans. Antennas Propag. **19**, 517 (1971).

[35] S. C. Sharma, M.P. Srivastava, M. Sugawa and V.K. Tripathi, Phys. Plasmas **5**, 3161 (1998).

[36] A. Volokitin, C. Krafft and G. Matthieussent, Phys. Plasmas **2**, 4297 (1995).

[37] C. Krafft, G. Matthieussent, P. Thevenet and S. Bresson, Phys. Plasmas **1**, 2163 (1994).

[38] J. Lavergnat, T. Lehner and G. Matthieussent, Phys. Fluids **27**, 1632 (1984).

[39] C. Krafft, A. Volokitin and G. Matthieussent, Phys. Plasmas **3**, 1120 (1996).

[40] N. J. Sircombe, R. Bingham, M. Sherlock, T. Mendonca, and P. Norreys, Plasma Phys. Control. Fusion **50** 065005 (2008).

[41] G. Praburam, V. K.Tripathi, and V. K. Jain, Phys. Fluids, **31** 3145 (1988).

[42] D. N. Gupta and A. K. Sharma, Laser and Particle Beams **22** 89 (2004).

[43] R. Kodama et al., Nat. **412** 798 (2001).

[44] J. Hornubia et al., Laser Part. Beams **22** 129 (2004).

[45] T. Neubert and B. E. Gilchrist, Adv. Space Res. **34** 2409-2412 (2004).

[46] M. Tabak et al., Phys. Plasmas. **12** 057305 (2005).

[47] H. Saberi and B. Maraghechi, Plasma Phys. Controlled Fus. **55** 055011 (2009).

CHAPTER 2

Stabilization of Plane Polarized Alfven Waves by Anomalous Doppler Resonance

This work presents non-linear decay of plane polarized Alfven wave via anomalous Doppler resonance with an electron beam in a magnetized plasma. There exists two modes of wave propagation, one having frequency $<\omega_{ci}$ corresponds to Alfven wave, and the other has frequency approaching ω_{ce} which corresponds to electron cyclotron wave. The waves interact with the electron beam via normal and anomalous Doppler resonance. The normal resonance interaction increases the frequency of plane polarized Alfven wave but shows no growth or decay in amplitude. However, in anomalous resonance interaction the frequency remains unchanged and the wave stabilizes. The variation of frequency and the growth rate with magnetic field and number density of plasma electrons is also discussed in the chapter. The phase velocity and the unstable frequency of the wave decrease with an increase in the number density of plasma electrons. These results can be applied to explain some of the experimental observations.

2.1 INTRODUCTION

In 1942 Hannes Alfven proposed the existence of an Electromagnetic-Hydrodynamic wave which would carry energy from the photosphere to heat up the corona and the solar wind in nature. After the Argus Nuclear Test, Berthold Harris and Hope detected Alfven waves in the ionosphere in 1958. Alfven waves are the slowest and have the lowest frequencies of any known electromagnetic wave. Such waves require the presence of magnetic field. The Alfven wave is the dominant low frequency

transverse mode of magnetized plasma. The Alfven wave propagates along the magnetic field and displays a continuous spectrum. This wave may play an important role in energy transport, in driving field-aligned currents, in particle acceleration and heating, and in explaining Inverted-V structure in magnetosphere – ionosphere coupling [1].

The interaction of electron beam or ion beam with plasma waves in magnetized plasma can excite many instabilities, which are helpful for understanding the stability confinement and heating of the plasma [2, 3]. In plasma, with an electron beam introduced parallel to the magnetic field, electrostatic ion cyclotron wave can easily be destabilised [4]. Gupta *et al* [5] have discussed analytically the whistler wave interaction with an electron beam propagating through magnetized plasma for oblique as well as parallel propagation. Shevchenko et al [6] have studied low frequency Alfven wave excitation, saturation and subsequent nonlinear evolution by an ion beam in a plasma. They also studied how the steepened wave profiles grew out of low frequency Alfven fluctuations. Gupta *et al* [7] have shown that growth rate of the instability increases with the beam density via Cerenkov interaction and fast cyclotron interaction when surface plasma waves are excited. Yin *et al* [8] have investigated, the generation of kinetic Alfven waves by ion-ion streaming along the magnetic field at relatively low Alfven speed and low beta plasma. They have found electron parallel heating increases both the wave growth rates and the range of unstable modes of the instability. Shukla and Stenflo [9] have shown that Alfven and magnetosonic wave can be non-linearly excited by a high frequency external pump wave. They have illustrated that finite amplitude Alfven waves can either interact with the background plasma or with themselves, giving rise to a number of nonlinear phenomena such as wave amplitude modulation or filamentation, density profile modification as well as self organization in vortical structure. Voitenko *et al* [10] have studied non-linear excitation of kinetic Alfven wave and whistler wave by electron driven Langmuir waves. They have shown that the resonant pairs of Kinetic Alfven wave and whistler wave are nonlinearly coupled to the pump Langmuir waves and their amplitude undergo exponential growth from the thermal level. Tripathi *et al* [11] have experimentally demonstrated the excitation of travelling shear Alfven Wave in a laboratory magnetoplasma. They found that the ambient plasma density and electron temperature were significantly enhanced by the beam. Chen *et al* [2] have investigated kinetic Alfven wave driven by a fast electron beam in finite beta plasma. Their results show that the kinetic resonant

interaction of beam electron is the driving source for kinetic Alfven Wave instability. Shukla and Sharma [12] have studied non-linear decay of a beam driven plasma mode into an Alfven wave plus a circularly polarized electromagnetic wave near the electron plasma frequency.

In the present paper, we study the excitation of Alfven waves by an electron beam injected parallel to the magnetic field in magnetized plasma. In section 2, we study instability analysis and calculate the growth rate of Alfven waves for slow and fast cyclotron interactions with electron beam. Results and discussion are given in section 3 and finally the conclusion is given in section 4.

2.2 INSTABILITY ANALYSIS

Consider a plasma immersed in a dc magnetic field $\mathbf{B_s} \parallel \hat{\mathbf{z}}$, with electron number density n_{eo}, ion number density n_{io}, electron mass m_e, ion mass m_{io}, electron charge -e and ion charge e. An electromagnetic Alfven wave propagates through it, with electric field

$$\mathbf{E} = A e^{-i(\omega t - k_z z)}.$$

The magnetic field of the wave $\mathbf{B} = c\mathbf{k_z} \times \mathbf{E}/\omega$.

An electron beam with density n_{bo} flows through the plasma along the z-direction, parallel to magnetic field.

The equation of motion, governing the drift velocity of plasma electrons, plasma ions and beam electrons is

$$m\left[\frac{\partial \mathbf{v}}{\partial t} + \mathbf{v}\cdot\nabla\,\mathbf{v}\right] = -e\,\mathbf{E} - \frac{e}{c}\mathbf{v}\times(\mathbf{B_S} + \mathbf{B}). \qquad (2.1)$$

In equilibrium (i.e., in the absence of the wave), $\mathbf{v_e} = 0$ and $\mathbf{v_i} = 0$. When wave is present, **E** and **B** of the wave are treated as small or perturbed quantities and result in perturbed velocities $\mathbf{v_{1e}}$, $\mathbf{v_{1o}}$ and $\mathbf{v_{1be}}$ for plasma electrons, plasma ions and beam electrons, respectively.

On linearizing Eq. (1), we obtain

$$\frac{\partial \mathbf{v_1}}{\partial t} = -\frac{e\,\mathbf{E}}{m} - \mathbf{v_1}\times\hat{\mathbf{z}}\,\omega_{ce}, \qquad (2.2)$$

where $\omega_{ce} = \dfrac{e\mathbf{B_s}}{m_e c}$.

The number density of electrons and ions have been calculated by using equation of continuity

$$\frac{\partial n}{\partial t}+\nabla.(n\mathbf{v})=0\,. \tag{2.3}$$

Current densities of different components have been calculated by formula

$$\mathbf{J}=ne\mathbf{v}\,. \tag{2.4}$$

The wave equation used for obtaining dispersion relation is

$$\nabla^2\mathbf{E}-\nabla(\nabla.\mathbf{E})+\frac{\omega^2}{c^2}\mathbf{E}=-\frac{4\pi i\omega}{c^2}\mathbf{J}\,. \tag{2.5}$$

Now we consider a plane polarized Alfven wave propagating along the magnetic field i.e., $\mathbf{E} = E_x\hat{\mathbf{x}}$ and $\mathbf{k}= k_z\hat{\mathbf{z}}$. Writing x, y, z-components of Eq. (2), we obtain the perturbed plasma electron velocities as

$$v_{1ex}=-\frac{e(-i\omega)E_x}{m_e\left(\omega_{ce}^2-\omega^2\right)}, \tag{2.6}$$

$$v_{1ey}=-\frac{e\,E_x\omega_{ce}}{m_e\left(\omega_{ce}^2-\omega^2\right)}, \tag{2.7}$$

and $v_{1ez} = 0$. (2.8)

Substituting Eqs. (6), (7) and (8) in Eq. (4), we get the perturbed plasma electron current densities as

$$J_{1ex}=n_{eo}\frac{e^2}{m_e}\frac{(-i\omega)E_x}{\left(\omega_{ce}^2-\omega^2\right)}, \tag{2.9}$$

$$\text{and } J_{1ey}=n_{eo}\frac{e^2}{m_e}\frac{\omega_{ce}E_x}{\left(\omega_{ce}^2-\omega^2\right)}. \tag{2.10}$$

The perturbed plasma ion current densities are obtained from Eqs. (2.9) & (2.10), by replacing e by -e, ω_{ce} by $-\omega_{ce}$, and m_e by m_i.

Similarly, the perturbed beam electron velocities are obtained using Eq. (2.2) as:

$$v_{1bx}=-\frac{e}{m_e}\frac{\left(-i\bar{\omega}^2\right)E_x}{\omega\left(\omega_{ce}^2-\omega^2\right)}, \tag{2.11}$$

$$v_{1by}=-\frac{e}{m_e}\frac{\bar{\omega}\omega_{ce}E_x}{\omega\left(\omega_{ce}^2-\omega^2\right)}, \tag{2.12}$$

and $v_{1ez} = 0$. (2.13)

where $\bar{\omega} = \omega - k_z v_{bo}$.

The perturbed beam electron current densities obtained using Eq. (4) are

$$J_{1bx} = \frac{e^2}{m_e} \frac{n_{bo}\left(-i\bar{\omega}^2\right)E_x}{\omega\left(\omega_{ce}^2 - \omega^2\right)}, \tag{2.14}$$

$$\text{and } J_{1by} = \frac{e^2}{m_e} \frac{n_{bo}\bar{\omega}\omega_{ce}E_x}{\omega\left(\omega_{ce}^2 - \omega^2\right)}. \tag{2.15}$$

Substituting Eqs. (2.9), (2.10), (2.14) and (2.15) in Eq. (2.5),

we get

$$\left[-k_z^2 + \frac{\omega^2}{c^2} + \frac{\omega_{pe}^2\omega^2}{c^2\left(\omega_{ce}^2 - \omega^2\right)} + \frac{\omega_{pi}^2\omega^2}{c^2\left(\omega_{ce}^2 - \omega^2\right)} + \frac{\omega_{pb}^2\bar{\omega}^2}{c^2\left(\omega_{ce}^2 - \omega^2\right)}\right] E_x = 0$$

or

$$\omega^2\left[P + \frac{\omega_{pi}^2}{\left(\omega_{ce}^2 - \omega^2\right)}\right] - k_z^2c^2 = \frac{\omega_{pb}^2\bar{\omega}^2}{\left(\omega_{ce}^2 - \bar{\omega}^2\right)}, \tag{2.16}$$

where $P = 1 + \frac{\omega_{pe}^2}{\omega^2}$.

For Alfven waves $\omega_{ce} << \omega$, Eq. (2.16) becomes

$$-P\omega^4 + (P\omega_{ci}^2 + \omega_{pi}^2 + k_z^2c^2)\omega^2 - k_z^2c^2\omega_{ci}^2 = \frac{\omega_{pb}^2\bar{\omega}^2}{\left(\omega_{ce}^2 - \bar{\omega}^2\right)}$$

$$\text{or} \left(\omega^2 - \omega_1^2\right)\left(\omega^2 - \omega_2^2\right) = \frac{\omega_{pb}^2\bar{\omega}^2}{\left(\omega_{ce}^2 - \bar{\omega}^2\right)}, \tag{2.17}$$

where ω_1 and ω_2 are roots of Eq.(2.17) given as

$$\omega_1 = \left[\frac{P\omega_{ci}^2 + \omega_{pi}^2 + k_z^2 c^2}{2P} - \frac{\left[\sqrt{\left(P\omega_{ci}^2 + \omega_{pi}^2 + k_z^2 c^2 \right)^2 - 4Pk_z^2 c^2 \omega_{ci}^2} \right]}{2P} \right]^{1/2}$$

$$\omega_2 = \left[\frac{P\omega_{ci}^2 + \omega_{pi}^2 + k_z^2 c^2}{2P} + \frac{\left[\sqrt{\left(P\omega_{ci}^2 + \omega_{pi}^2 + k_z^2 c^2 \right)^2 - 4Pk_z^2 c^2 \omega_{ci}^2} \right]}{2P} \right]^{1/2} \quad (2.18)$$

Here ω_1 corresponds to Alfven wave frequency and ω_2 corresponds to electron cyclotron frequency.

2.3 DETERMINATION OF GROWTH RATE

In cyclotron interaction $\bar{\omega}^2 = \omega_{ce}^2$; we have slow cyclotron interaction or anomalous Doppler resonance for $\bar{\omega} \approx -\omega_{ce}$, and fast cyclotron interaction or normal resonance for $\bar{\omega} \approx \omega_{ce}$. Considering fast cyclotron interaction, we rewrite Eq. (2.17) as

$$\left(\omega - \omega_1\right)\left(\bar{\omega} - \omega_{ce}\right) = -\frac{\omega_{pb}^2 \bar{\omega}}{2\left(\omega + \omega_1\right)\left(\omega_1^2 - \omega_2^2\right)}. \quad (2.19)$$

Assuming perturbed quantities $\omega = \omega_1 + \Delta$ and $\bar{\omega} = \omega_{ce} + \Delta$, we get from Eq. (2.19)

$$\Delta = \left[-\frac{\omega_{pb}^2 \omega_{ce}}{4\omega_1\left(\omega_1^2 - \omega_2^2\right)} \right]^{1/2}. \quad (2.20)$$

As $\omega_1 < \omega_2$, there is no imaginary part of Δ, hence there is no growth rate and only the Alfven wave frequency gets changed.

Now, considering slow cyclotron interaction and assuming perturbed quantities $\omega = \omega_1 + \Delta$ and $\bar{\omega} = \omega_{ce}$, we get from Eq. (2.19)

$$\Delta = \left[\frac{\omega_{pb}^2 \omega_{ce}}{4\omega_1\left(\omega_1^2 - \omega_2^2\right)} \right]^{1/2}$$

As $\omega_1 < \omega_2$, Δ has an imaginary part and there is a growth rate given as

$$\gamma = \left[\frac{\omega_{pb}^2 \omega_{ce}}{4\omega_1 \left(\omega_1^2 - \omega_2^2 \right)} \right]^{1/2} . \qquad (2.21)$$

2.4 RESULTS AND DISCUSSION

The numerical calculations have been carried out using the typical parameters of plasma: electron number density $n_{eo}=10^{13}$ cm^{-3} and 10^{14} cm^{-3}, mass of electron $m_e= 9.1\times10^{-28}$ g, charge of electron e = 4.8×10^{-10}ergs, magnetic field $\mathbf{B_s}$ = 0-1000 G and beam density $n_{bo} = 2.8\times10^{9}$ cm^{-3}.

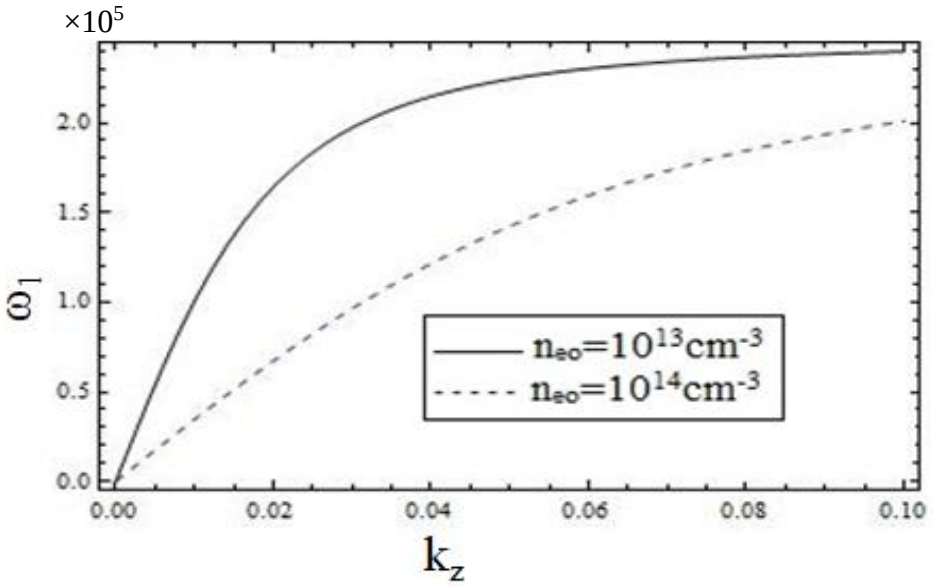

Fig. 2.1 Alfven wave frequency ω_1(rad/s) as a function of k_z (cm^{-1})

Fig. 2.1 shows the variation of the Alfven wave frequency ω_1 as a function of parallel wave number k_z using Eq. (2.18) for two values of electron number density $n_{e0}=10^{13}$cm^{-3} and 10^{14} cm^{-3} via slow cyclotron interaction with electron beam. From Fig. 2.1, it is clear that the Alfven wave frequency increases with increase in the value of k_z and saturates below the ion cyclotron frequency. The saturation value of wave frequency is also less for higher number density of electrons in plasma. Thus the phase velocity (ω_1/k_z) of Alfven wave decreases with an increase in number density of electrons or ions.

In Fig.2.2, we have plotted the Alfven wave frequency as the function of magnetic field (in Gauss) by taking k_z = 0.02 cm^{-1} and for electron number density n_{eo} = 10^{13} cm^{-3}

and 10^{14} cm^{-3}. The Alfven wave frequency rises with rise in magnetic field. The slope of curve of ω_1 vs. **B** for lesser electron number density is more than that for higher electron density i.e. ω_1 increases more rapidly with magnetic field with decrease in number density of electrons of plasma.

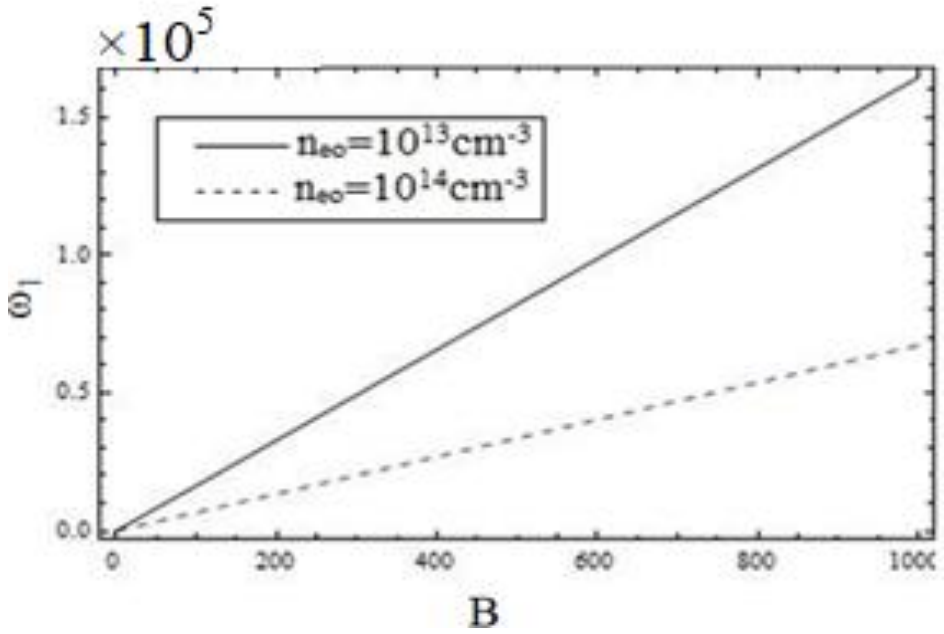

Figure 2.2 Alfven wave frequency ω_1 (rad/sec) as a function of static magnetic field B (in Gauss).

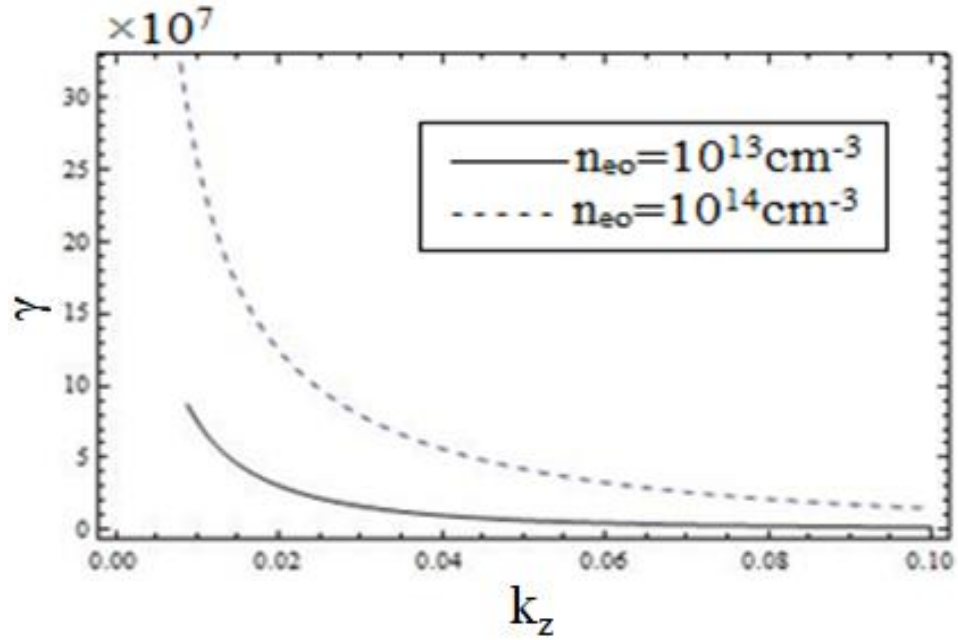

Figure 2.3 Growth rate γ (sec^{-1}) of the unstable mode as a function of wave number k_z (cm^{-1}) for anomalous Doppler resonance.

Fig. 2.3 shows the variation of growth rate γ (in sec^{-1}) for slow cyclotron interaction with wave number k_z (cm^{-1}) for different electron number densities of plasma $n_{eo} = 10^{13}$ cm^{-3} and 10^{14} cm^{-3} plotted using Eq. (2.21). The growth rate for slow cyclotron interaction decreases with increase in parallel wave number. In fast cyclotron interaction, the beam is not able to interact with the plane polarized Alfven wave for the unstable mode and therefore, no excitation or growth is obtained (cf.Eq.2.20).

Fig. 2.4 shows the variation of growth rate γ (sec^{-1}) for slow cyclotron interaction with static magnetic field B (in Gauss) for different electron plasma densities. The growth rate decreases with increase in value of static magnetic field.

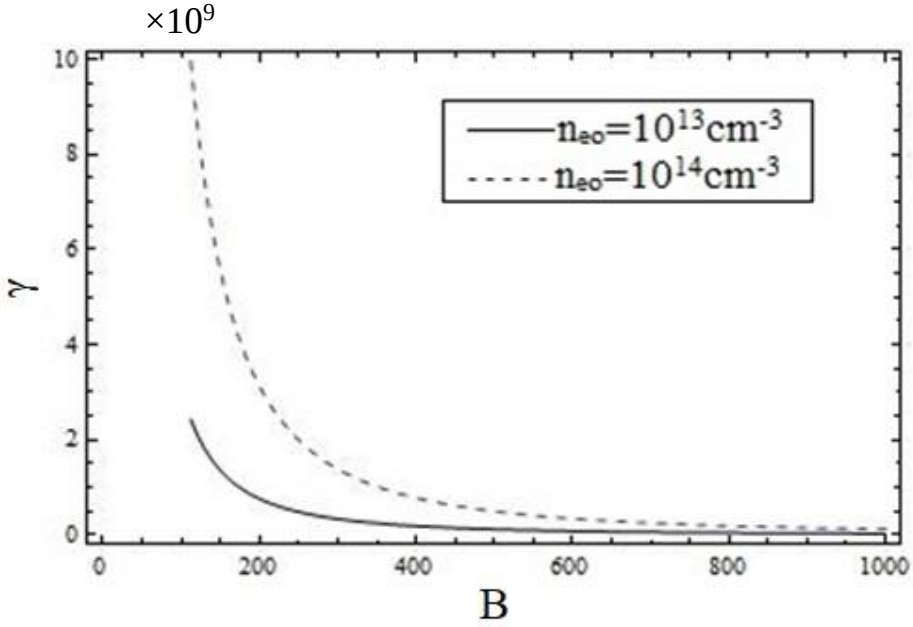

Figure 2.4. Growth rate γ (sec^{-1}) of unstable mode as a function of static magnetic field B (in Gauss) for anomalous Doppler resonance.

2.5 CONCLUSION

The plane polarized Alfven wave shows only cyclotron interaction with the beam mode and Cerenkov interaction is absent in the present case. For fast cyclotron interaction, the Alfven wave neither grows nor damps but there is an increment in Alfven wave frequency. However, for slow cyclotron interaction or anomalous Doppler resonance, the wave stabilizes with growth rate directly proportional to the beam density and inversely proportional to the external magnetic field. The wave frequency remains unaltered in the case of slow cyclotron interaction.

REFERENCES

[1] J. Shrivastava and M. S. Tiwari, "Alfven wave in dusty magnetosphere", Indian Journal of Radio & Space Physics **33**, 25 (2004).

[2] L. Chen, D. J. Wu, G. Q. Zhao, J. F. Tang, and J. Huang, "Excitation of Kinetic Alfven waves by fast electron beams", The Astrophysical Journal, 793:13 (5pp) (2014).

[3] P. K. Shukla and R. P. Sharma, "Alfven wave generation in a beam plasma system", Physical Review **A 25**, 2816 (1982).

[4] V. Prakash, S. C. Sharma, Vijayshri and R. Gupta "Ion beam driven resonant ion – cyclotron instability in magnetized dusty plasma", Phys. Plasmas **21**, 33701 (2014).

[5] R. Gupta, V. Prakash, S. C. Sharma and Vijayshri, "Interaction of an electron beam with whistler waves in magnetoplasma", Laser and particle beams **33**, 455 (2015).

[6] V. I. Shevchenko, V. L. Galinsky and S. K. Ride, "Excitation of left-hand-polarized nonlinear Alfven waves by an ion beam in a plasmas", Journal of Geophysical Research **107**, A11, 1367 (2002).

[7] R. Gupta, S. C. Sharma and V. Prakash, "Excitation of surface plasma waves by a density-modulated electron beam in a magnetized plasma cylinder", Physics of Plasmas **17**, 122105 (2010).

[8] L. Yin, D. Winske, W. Daughton, and K. J. Bowers, "Kinetic Alfven waves and electron physics. I. Generation from ion-ion streaming", Physics of Plasma, 14, 62104 (2007).

[9] P. K. Shukla and L. Stenflo, "Decay of a magnetic-field-aligned Alfven wave into inertial and kinetic Alfven waves in plasmas", Physics of Plasma **12**, 84502 (2005).

[10] Yu. Voitenko, M. Goossens, O. Sirenko, and A. C.-L. Chian, "Nonlinear excitation of kinetic Alfven waves and whistler waves by electron beam-driven Langmuir waves in the solar corona", EDP Sciences, A&A 409, 331, (2003).

[11] S.K.P. Tripathi, B. Van Compernolle, W. Gekelman, P. Pribyl, and W. Heidbrink. "Excitation of shear Alfven waves by a spiraling ion beam in a large magnetoplasma", Physical Review E **91**, 13109 (2015).

[12] P. K. Shukla and R. P. Sharma, "Alfven waves generation in a beam plasma system", Physical Review **A 25**, 2816 (1982).

CHAPTER 3

Polarization Reversal of Oblique Electromagnetic Wave in Collisional Beam-Hydrogen Plasma

In this chapter, a theoretical model based on fluid treatment has been presented to study polarization reversal of oblique shear Alfven wave in collisional beam-hydrogen plasma. It has been shown that an ion beam can efficiently transfer its energy to plasma through wave generation. The effects of collisions between beam ions with plasma components and collisions between plasma components on growth rate as well as frequency of generated waves have been studied.

3.1 INTRODUCTION

Alfven waves are a type of magneto hydrodynamic (MHD) waves which are low frequency waves below the ion cyclotron frequency travelling in a magnetized conducting fluid like plasma existing in space. These waves transport electromagnetic energy and communicate information concerning changes in plasma currents and magnetic field topology. At low frequencies, there are two different modes of electromagnetic propagation i) a compressional wave in which magnetic field strength and density change and ii) a shear wave in which only the direction of magnetic field varies. In the present paper, we are concerned with shear Alfven wave only. The shear Alfven wave propagates with the wave magnetic field vector perpendicular to background field. Gekelmanet al. [1] have studied various properties related to shear Alfven waves.

The shear Alfven wave is nearly incompressible and hence, more readily excitable

by either external perturbations e.g., solar wind, antenna or intrinsic collective instabilities (Chen and Zonca [2]. In a cylindrical column, the dispersion of shear wave was determined by Jephcott and Stocker [3]. Since last three decades, many experiments on Alfven waves have been done where some fundamental properties of shear Alfven wave have been explored. Oblique shear Alfven wave which is transverse with strong magnetic field variation perpendicular to the wave motion, can trade energy between the different frequencies which might propagate through plasma. This also means that energy can be exchanged with the particles in the plasma, in some cases, trapping particles in the troughs of the wave and carrying them along.

Plasma instabilities are caused by the energetic ion or electron beams. These beams are ever-present in the variety of space and astrophysical plasmas. Ion beam and interaction of radiation with plasma allocate a free energy source which can excite different wave modes in a plasma. Plasma waves can be stabilized or destabilized when they interact with electron or ion beams [4-11] and collisions generally have a stabilizing effect on the plasma waves [12-13]. An ion beam can destabilize Alfven waves and whistler waves if the beam speed is sufficiently large. The shear Alfven wave instability depends on the free energy stored in the particle distribution function in a velocity space and in a magnetized plasma, ion neutral collisions result in change of its dispersion relation [14]. For study of Alfven waves employing parallel ion beams, several laboratory experiments have been performed. In a laboratory magnetoplasma, Tripathi et al. [15] demonstrated excitation of propagating shear Alfven wave and established that the ambient plasma density and electron temperature were increased significantly by the ions beam. Zhang et al. [16] have experimentally explained the Doppler shifted cyclotron resonance between fast Lithium ions and shear Alfven waves in the helium plasma of the Large Plasma Device. In the partially ionized solar chromospheres, the collisions between various particles are an efficient dissipative mechanism for Alfven waves [16-17].

Many physicists showed that both Alfven waves and magnetosonic waves can be excited nonlinearly [18-21] and have explained about interactions of Alfven waves with ions [20]. Hollweg and Markovskii [21] have studied analytically, the instabilities generated by cyclotron resonances of ions with obliquely propagating waves in coronal holes and solar wind. Li and Lu [22] have investigated the interaction between oblique propagating Alfven waves and minor ions in the fast solar wind stream. Hellinger and Mangeney [23] found structure of an oblique shock wave by means of numerical

simulations and they studied that proton beam generates whistler waves at slightly oblique propagation. They also showed that for dense proton beams, the oblique modes have an important role in the nonlinear stage of electromagnetic instability [24]. Verscharen and Chandran [25] studied the polarization properties of both oblique and parallel propagating waves in the presence of ion beam and found that minimum beam speed required to excite such instabilities is significantly smaller for the former mode than for latter mode with $\mathbf{k} \times \mathbf{B_0} = 0$. Maneva et al. [26] examined the comparative behavior of parallel vs oblique Alfven cyclotron waves in the observed heating and acceleration alpha particles in the fast solar wind. They aimed to find which propagation angles are the most efficient in preferentially heating the alpha particles within the considered low frequency turbulent wave spectra. Gao et al. [27] found that the obliquely propagating Alfven waves can be excited by alpha/proton instability and background proton component & alpha component can be heated resonantly by Alfven waves. The study of oblique modes is very important in the thermodynamics of minor ions in the solar wind and may also find application within the Earth's bow shock as well as to basic plasma processes.

In the present paper, we study the reaction of oblique shear Alfven waves with an ion beam forced into magnetized plasma parallel to the magnetic field. In Section 2, instability analysis is given. The dispersion relation and growth rate of Alfven waves for fast and slow cyclotron interactions are derived in the absence as well as in the presence of plasma and beam collisions and the results are discussed. Finally, the conclusion part is given in Section 3.

3.2 INSTABILITY ANALYSIS

Assume a plasma in a dc background magnetic field $B_s \| \hat{z}$, with electron density n_{eo}, ion density n_{io}, electron mass m_e, ion mass m_i, electron charge -e and ion charge e. A positively charged particle-beam having mass m_b, charge q_b, and density n_{bo} passes parallel to the magnetic field, through the plasma along the z-direction with velocity v_{bo}. Consider an electromagnetic Alfven wave is propagating through the plasma with electric field

$\vec{E} = Ae^{-i(\omega t - \vec{k}.\vec{r})}$, where $\vec{k} = k_x \hat{x} + k_z \hat{z}$.

The magnetic field of the electromagnetic wave is given as $\vec{B} = c\vec{k} \times \vec{E}/\omega$.

The equation of motion, governing the drift velocity of plasma ions, plasma electrons, and beam particles is

$$m\left[\frac{\partial\vec{\upsilon}}{\partial t}+\vec{\upsilon}\cdot\nabla\vec{\upsilon}\right]=-e\,\vec{E}-\frac{e}{c}\vec{\upsilon}\times(\vec{B}_s+\vec{B})-\nu m\vec{\upsilon}, \tag{3.1}$$

where ν is the collision frequency of beam particles and plasma components. In equilibrium (i.e. in the absence of the wave), $\mathbf{v_i}=0$ and $\mathbf{v_e}=0$. When wave is present, $\vec{E}$ and $\vec{B}$ of the wave are treated as small or perturbed quantities and result in perturbed velocities $\upsilon_{\mathbf{i1}}$, $\upsilon_{\mathbf{e1}}$, and $\upsilon_{\mathbf{b1}}$ for plasma ions, plasma electrons and beam particles, respectively.

On linearizing Eq. (3.1), we obtain

$$\frac{\partial\vec{\upsilon}_1}{\partial t}=-\frac{e\,\vec{E}}{m}-\vec{\upsilon}_1\times\hat{\mathbf{z}}\,\omega_{ce}-\nu\vec{\upsilon}_1, \tag{3.2}$$

where $\omega_{ce}=\frac{eB_s}{mc}$ is the electron cyclotron frequency.

By using equation of continuity, we have calculated the number densities of electrons and ions as

$$\frac{\partial n}{\partial t}+\vec{\nabla}.\left(n\vec{\upsilon}\right)=0, \tag{3.3}$$

Current densities of different components have been determined using the relation

$$\vec{J}=ne\vec{\upsilon}. \tag{3.4}$$

To obtain dispersion relation, the wave equation is given as

$$\nabla^2\vec{E}-\nabla\left(\vec{\nabla}.\vec{E}\right)+\frac{\omega^2}{c^2}\vec{E}=-\frac{4\pi i\omega}{c^2}\vec{J}. \tag{3.5}$$

3.2.1 OBLIQUE SHEAR ALFVEN WAVE

We consider an elliptically polarized Alfven wave propagating in X-Z plane with electric vectors also in X-Z plane i.e. $\vec{E}=E_x\hat{x}+E_z\hat{z}$ and $\vec{k}=k_x\hat{x}+k_z\hat{z}$, $k_z= k\cos\theta$ and $k_x= k\sin\theta$.

Obtaining x, y, z-components of Eq. (3.2), we calculate the perturbed plasma electron velocities as

$$\upsilon_{e1x} = \frac{ie\omega E_x}{m_e\omega_{ce}^2}, \tag{3.6}$$

$$\upsilon_{e1y} = -\frac{e\,E_x\omega_{ce}}{m_e\omega_{ce}^2}, \tag{3.7}$$

$$\text{and } \upsilon_{e1z} = \frac{eE_z}{m_e i\omega}\ . \tag{3.8}$$

Substituting Eqs. (3.6), (3.7) and (3.8) in Eq. (3.4), we obtain the perturbed plasma electron current densities as

$$J_{e1x} = -n_{eo}\frac{e^2}{m_e}\frac{i\omega E_x}{\omega_{ce}^2}, \tag{3.9}$$

$$J_{e1y} = n_{eo}\frac{e^2}{m_e}\frac{\omega_{ce}E_x}{\omega_{ce}^2}, \tag{3.10}$$

$$\text{and } J_{e1z} = -\frac{n_{eo}e^2E_z}{m_e i\omega}. \tag{3.11}$$

The perturbed plasma ion current densities are obtained from Eqs. (3.9), (3.10) and (3.11), by replacing e by –e, m_e by m_i andω_{ce} by ω_{ci}.

Similarly, the perturbed beam electron velocities are obtained using Eq. (3.2) as

$$\upsilon_{b1x} = \frac{q_b}{m_b}\frac{(\nu - i\bar{\omega})\bar{\omega}E_x}{\omega\left[(\nu - i\bar{\omega})^2 + \omega_{bc}^2\right]} + \frac{q_b}{m_b}\frac{v_{bo}k_x(\nu - i\bar{\omega})E_z}{\omega\left[(\nu - i\bar{\omega})^2 + \omega_{bc}^2\right]}, \tag{3.12}$$

$$\upsilon_{b1y} = -\frac{q_b}{m_b}\frac{\bar{\omega}\omega_{bc}E_x}{\omega\left[(\nu - i\bar{\omega})^2 + \omega_{bc}^2\right]} - \frac{q_b}{m_b}\frac{v_{bo}k_x\omega_{bc}E_z}{\omega\left[(\nu - i\bar{\omega})^2 + \omega_{bc}^2\right]}, \tag{3.13}$$

$$\text{and } \upsilon_{b1z} = \frac{q_bE_z}{m_b(\nu - i\bar{\omega})}, \tag{3.14}$$

where ω_{bc} is the cyclotron frequency of beam particles and $\bar{\omega} = \omega - k_z\upsilon_{bo}$.

The perturbed beam particle current densities calculated using Eq. (3.4) are

$$J_{b1x} = \frac{q_b^2}{m_b}\frac{n_{bo}(\nu - i\bar{\omega})\bar{\omega}E_x}{\omega\left[(\nu - i\bar{\omega})^2 + \omega_{bc}^2\right]} + \frac{q_b^2}{m_b}\frac{n_{bo}v_{bo}k_x(\nu - i\bar{\omega})E_z}{\omega\left[(\nu - i\bar{\omega})^2 + \omega_{bc}^2\right]}, \tag{3.15}$$

$$J_{b1y} = -\frac{q_b^2}{m_b}\frac{n_{bo}\bar{\omega}\omega_{bc}E_x}{\omega\left[\left(\nu - i\bar{\omega}\right)^2 + \omega_{bc}^2\right]} - \frac{q_b^2}{m_b}\frac{n_{bo}v_{b0}\omega_{bc}E_z}{\omega\left[\left(\nu - i\bar{\omega}\right)^2 + \omega_{bc}^2\right]}, \qquad (3.16)$$

and

$$J_{b1z} = \frac{q_b^2}{m_b}\frac{n_{bo}v_{bo}k_x\left(\nu - i\bar{\omega}\right)\bar{\omega}E_x}{\omega\left[\left(\nu - i\bar{\omega}\right)^2 + \omega_{bc}^2\right]} + \frac{q_b^2 n_{bo}}{m_b}\left[\frac{\omega}{\bar{\omega}\left(\nu - i\bar{\omega}\right)} + \frac{v_{bo}^2 k_x^2\left(\nu - i\bar{\omega}\right)}{\omega\bar{\omega}\left[\left(\nu - i\bar{\omega}\right)^2 + \omega_{bc}^2\right]}\right]E_z$$

(3.17)

Substituting Eqs. (3.9), (3.10), (3.11), (3.15), (3.16), (3.17) and corresponding current densities of plasma ions in Eq. (3.5), we obtain

$$\eta E_x + \mu E_z = 0$$
$$\mu E_x + \lambda E_z = 0$$

$$\text{or } \begin{pmatrix} \eta & \mu \\ \mu & \lambda \end{pmatrix}\begin{pmatrix} E_x \\ E_z \end{pmatrix} = 0, \qquad (3.18)$$

where $\eta = -k_z^2 + \frac{\omega^2}{c^2} + \frac{\omega_{pe}^2\omega^2}{c^2\omega_{ce}^2} + \frac{\omega_{pi}^2\omega^2}{c^2\omega_{ci}^2} + \frac{\omega_{pb}^2 i\left(\nu - i\bar{\omega}\right)\bar{\omega}}{c^2\left[\left(\nu - i\bar{\omega}\right)^2 + \omega_{bc}^2\right]}$,

$$\mu = k_x k_z + \frac{\omega_{pb}^2 i v_{bo}k_x\left(\nu - i\bar{\omega}\right)}{c^2\left[\left(\nu - i\bar{\omega}\right)^2 + \omega_{bc}^2\right]},$$

$$\lambda = -k_x^2 + \frac{\omega^2}{c^2} - \frac{\omega_{pe}^2}{c^2} - \frac{\omega_{pi}^2}{c^2} + \frac{\omega_{pb}^2 i\omega^2}{c^2\bar{\omega}\left(\nu - i\bar{\omega}\right)} + \frac{\omega_{pb}^2 v_{bo}^2 k_x^2 i\left(\nu - i\bar{\omega}\right)}{c^2\bar{\omega}\left[\left(\nu - i\bar{\omega}\right)^2 + \omega_{bc}^2\right]}, \qquad (3.19)$$

$$\omega_{pe}^2 = \frac{4\pi n_{eo}e^2}{m_e},\ \omega_{pi}^2 = \frac{4\pi n_{io}e^2}{m_i} \text{ and } \omega_{pb}^2 = \frac{4\pi n_{bo}q_d^2}{m_d}.$$

The dispersion relation can be obtained by taking $\eta\lambda - \mu^2 = 0$. (3.20)

For elliptically polarized mode of propagation, $E_x = \pm iE_z$, which gives the dispersion relation as

$$\left(\omega^2-\omega_s^2\right)=\frac{-\omega_{pb}^2\left[\left(\bar{\omega}^2-k_x v_{bo}\nu\right)\left(\omega_{bc}^2-\bar{\omega}^2\right)-2\bar{\omega}^2\nu\left(k_x v_{bo}+\nu\right)\right]}{\left(\omega_{bc}^2-\bar{\omega}^2\right)^2\left(1+A\right)}$$

$$+i\frac{\bar{\omega}\left[\left(k_x v_{bo}+\nu\right)\left(\omega_{bc}^2-\bar{\omega}^2\right)+2\nu\left(\bar{\omega}^2-k_x v_{bo}\nu\right)\right]}{\left(\omega_{bc}^2-\bar{\omega}^2\right)^2\left(1+A\right)}\quad,$$

(3.21)

where $\omega_{s\mp}^2=\frac{k_z^2c^2\mp ik_xk_zc^2}{\left(1+A\right)}$, (3.22)

and $A=1+\frac{\omega_{pe}^2}{\omega_{ce}^2}+\frac{\omega_{pi}^2}{\omega_{ci}^2}$.

Eq. (3.22) is the modified dispersion relation of RH (subscript-) and LH (subscript+) elliptically polarized oblique shear Alfven wave in absence of beam.

In terms of θ, the angle of propagation of shear Alfven wave with respect to the ambient magnetic field, we can write Eq. (3.22) as

$$\omega_{s\mp}=\omega_A\frac{1}{\sqrt{1-\tan^2\theta/2}}\mp i\omega_A\frac{1}{\sqrt{\cot^2\theta/2-1}}.\qquad(3.23)$$

where $\omega_A=\frac{k_zc}{\sqrt{1+A}}$ is the Alfven frequency. Equation (3.23) indicates that the RH polarized oblique wave damps and the LH polarized oblique wave grows due to obliquity.

The real frequency for both the modes increases with angle θ and the growth (or attenuation) of LH (or RH) waves also increases with angle θ.

From Eq. (3.21), we can say that both fast and slow cyclotron interactions are possible for both LH and RH polarized oblique Alfven waves, in contrast to only slow (or fast) cyclotron interaction for RH (or LH) polarized parallel propagating Alfven waves. In Fig. 1, the dispersion curves of Alfven waves are plotted for different wave propagation angle θ (= 0º, 30º, 45º, 60º and 80º), plotted using Eq. (3.23) along with the beam mode for beam velocity v_{bo} = 1.69 × 10^8 cm/s. The frequencies and the

corresponding parallel wave numbers of the unstable modes obtained from the points of intersection between the beam mode and the plasma modes are given in Table I. The unstable frequency of Alfven waves 'ω' gradually increases while the unstable wave number 'k_z' decreases with increase in the angle of wave propagation θ.

Assuming fast cyclotron interaction and considering perturbed quantities $\omega = \omega_{s\mp} + \Delta$ and $\bar{\omega} = \omega_{bc} + \Delta$, we get from Eq. (3.21)

$$\Delta^3 = \frac{-\omega_{pb}^2 \bar{\omega}^2 \nu}{4\omega_s \omega_{bc}^2 (1+A)} \left(\mp k_x v_{bo} + i\omega_{bc}\right), \tag{3.24}$$

$$\text{or } \Delta = \left[\frac{\omega_{pb}^2 \nu k v_{bo}}{4\omega_s (1+A)}\right]^{1/3} \left(\pm \sin\theta/3 + i\cos\theta/3\right). \tag{3.25}$$

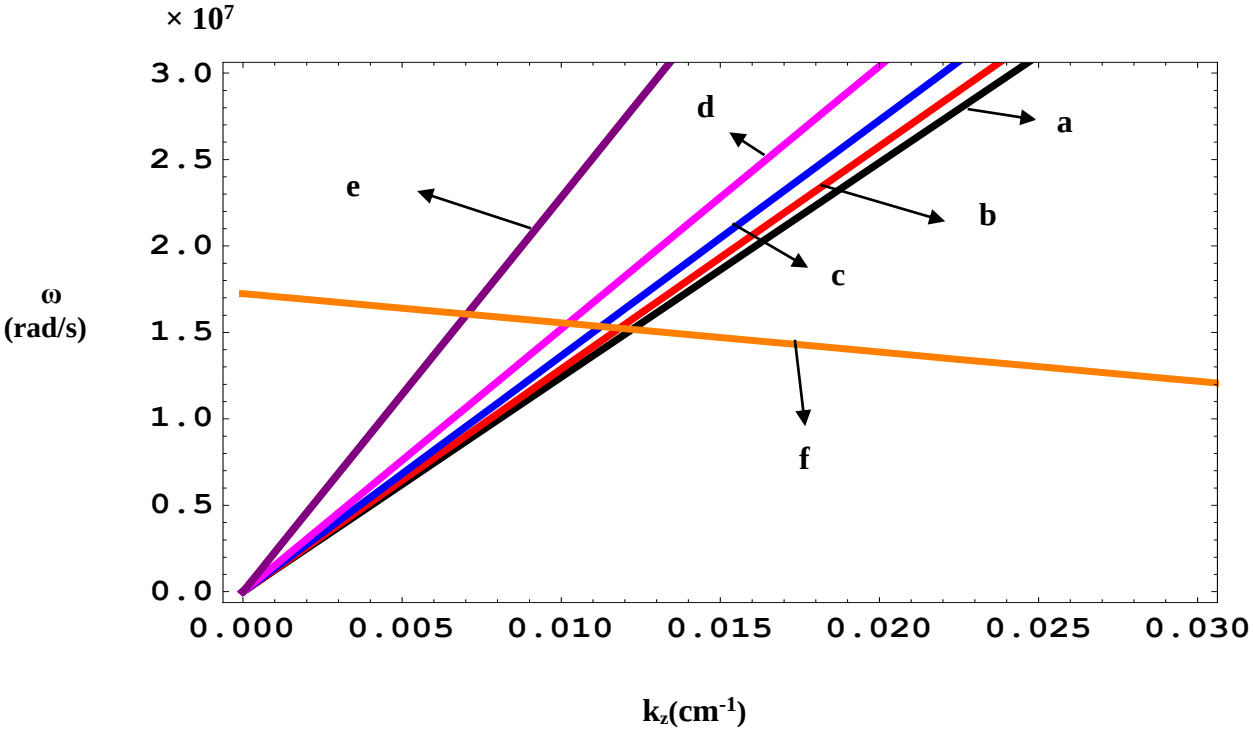

FIG. 3.1 Dispersion curves of oblique shear Alfven wave for different angles of propagation θ (a) 0°, (b) 30°, (c) 45°, (d) 60° and (e) 80° and the beam mode (f) with velocity 1.69×10^8 cms^{-1}.

In Eq. (3.25), a positive imaginary part or the growth rate establishes instability,

while a negative imaginary part indicates damping. A positive (or negative) real part means that the frequency of wave increases (or decreases) on interaction between beam mode and wave mode. The frequency of RH polarized mode increases while the frequency of LH polarized mode decreases with increase in angle of propagation of wave (θ) with respect to ambient magnetic field and both the modes become unstable due to beam-wave interaction. The growth rate increases monotonically as the angle of propagation increases but the increase in maximum growth rate in the presence of beam collisions is nominal. The frequency and growth rate of waves depend mainly on the value of $\left(\frac{\omega + k_z v_{bo}}{k_x v_{bo}}\right)$ [cf. Eq. (3.24)]. $\omega + k_z v_{bo} = \omega_{bc} = k_x v_{bo}$, corresponds to the case of parallel propagation. The frequency increases/decreases for RH/LH polarized waves by a factor of 0.5 as θ varies from 0º to 90º due to beam-wave interaction and the maximum growth rate at θ = 80º becomes 1.3 times of maximum growth rate at θ = 30º.

If the collisions are ignored, Eq. (3.21) becomes

$$\left(\omega^2 - \omega_{s\mp}^2\right) = \frac{\omega_{pb}^2 \left(\omega + k_z v_{bo}\right) k v_{bo}}{\left[\left(\omega + k_z v_{bo}\right)^2 - \omega_{bc}^2\right]\left(1 + A\right)} \exp\left(\mp i\theta\right) \tag{3.26}$$

Assuming perturbed quantities for fast cyclotron interaction, we get

$$\Delta = \left[\frac{\omega_{pb}^2 \left(\omega + k_z v_{bo}\right) k v_{bo}}{4\omega_{bc}\omega_s \left(1 + A\right)}\right]^{1/2} \left(\cos\theta/2 \mp i \sin\theta/2\right) \tag{3.27}$$

Table I (2.1) Angle of propagation, unstable wave numbers and frequencies of oblique shear Alfven waves and maximum growth rates of wave in the absence and presence of beam-plasma collisions.

θ	**0º**	**30 º**	**45 º**	**60 º**	**80 º**
$\mathbf{k_z}$ **(cm^{-1})**	0.01223	0.01184	0.01126	0.01021	0.00704
ω ($\times 10^7 rads^{-1}$)	1.5178	1.5245	1.5342	1.5514	1.6054
ω / ω_{bc}	0.8801	0.8840	0.8896	0.8996	0.9309

γ $(\times 10^5\ s^{-1})$	0	1.94053	3.08662	4.52084	8.08631
γ_{wc} $(\times 10^5\ s^{-1})$ $\nu = 10^4\ s^{-1}$	1.71571	1.75076	1.80275	1.89856	2.24340

Using Eq. (3.26) we plotted in Fig. 3.2, the growth rate of oblique shear Alfven wave with beam collision frequency γ_{wc}(in sec^{-1}) and using Eq. (3.27) we have plotted in Fig. 3.3, the growth rate of oblique shear Alfven wave without collision frequency γ (in sec^{-1}), as a function of k_z(in cm^{-1}) for the same parameters used for plotting dispersion curves. Fig. 3.2 shows that the maximum growth rate as well as the spectrum of the unstable mode increases with increase in angle of propagation θ. Collisions have induced a growth in elliptically X-Z polarized wave for parallel propagation.

In the absence of collisions, for angle of propagation $\theta = 0^o$, the condition is analogous to the interaction of pure Alfven wave, as E_z does not affect the interaction for parallel propagating waves. The frequency then increases and growth rate is zero. The beam generates LH polarized waves and stabilizes the RH polarized wave.

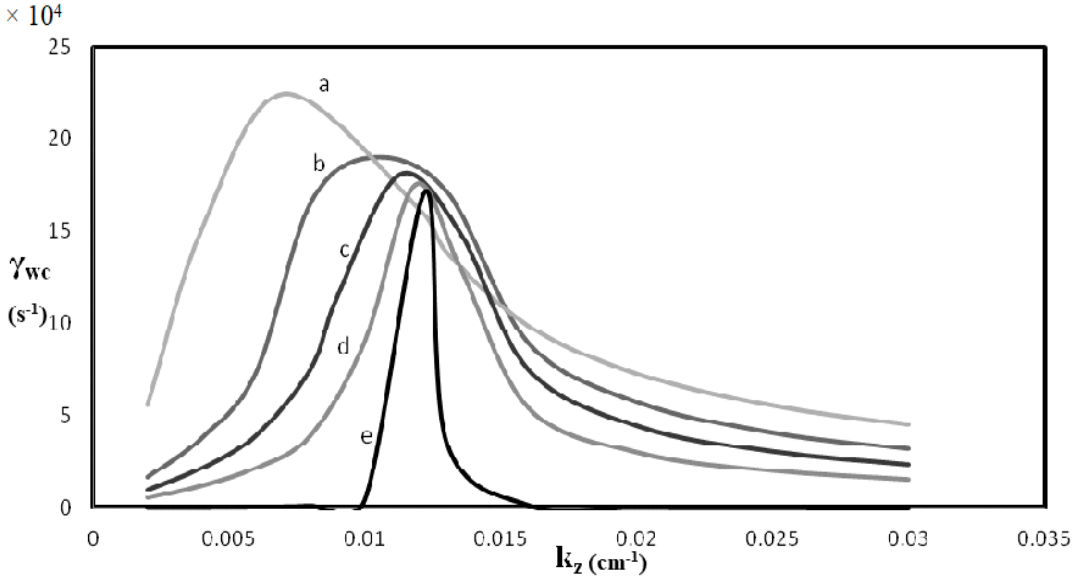

FIG. 3.2 Growth rate γ_{wc}(in sec^{-1}) of the unstable mode as a function of k_z (in cm^{-1}) for different angles (a) 80^0, (b) 60^0, (c) 45^0, (d) 30^0 and (e) 0^0 of propagation of shear Alfven wave in the presence of beam-plasma collisions.

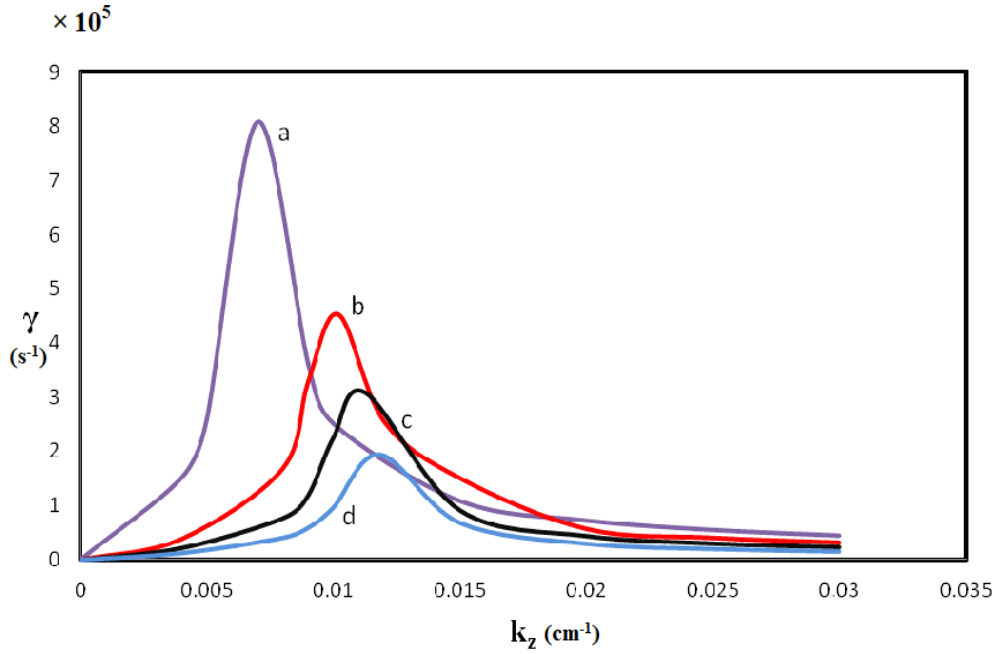

FIG. 3.3. Growth rate γ (in sec^{-1}) of the unstable mode as a function of k_z (in cm^{-1}) for different angles (a) 80^0, (b) 60^0, (c) 45^0 and (d) 30^0 of propagation of shear Alfven wave.

Equation (3.27) shows that the maximum growth rate of the unstable LH polarized oblique Alfven waves occurs at more oblique angles. The produced waves heat /accelerate the plasma ions. On the other hand, the RH polarized oblique Alfven wave loses their energy and heat the beam ions. Li and Lu [22] have also observed similar results using hybrid simulations. The maximum growth rate becomes four-fold as θ changes from 30º to 80º and the unstable wave spectrum decreases with θ. The maximum growth rate of the LH polarized mode excited at nearly perpendicular propagation is 0.05 ω_{bc} occurring at 80º. The maximum frequency of the unstable wave mode decreases slightly with an increase in propagation angle. From Table I, we may conclude that the maximum growth rate values in the presence or absence of beam collisions, increase due to obliquity of wave.

Assuming slow cyclotron interaction and considering perturbed quantities

$\omega = \omega_{s\mp} + \Delta$ and $\bar{\omega} = -\omega_{bc} + \Delta$, we get from Eq. (3.26)

$$\Delta = \left[\frac{\omega_{pb}^2 \bar{\omega}^2 \nu k v_{bo}}{4\omega_s \omega_{bc}^2 (1+A)}\right]^{1/3} \left\{\cos(\pi/6 \mp \theta/3) + i\sin(\pi/6 \mp \theta/3)\right\}. \quad (3.28)$$

The behaviour of RH and LH polarized waves is reciprocal to each other. As the

angle of propagation θ increases, the frequency of RH mode (or LH mode) increases (or decreases), while the growth rate of RH mode (or LH mode) decreases (or increases) by small factors.

In the absence of collisions, for slow cyclotron interaction, we get

$$\Delta = \left[\frac{\omega_{pb}^2 k v_{bo}}{4\omega_s (1+A)} \right]^{1/2} \left(\pm \sin\theta/2 + i\cos\theta/2 \right). \qquad (3.29)$$

The frequency of RH mode increases, while that of LH mode decreases in this interaction, while both the modes grow with time.

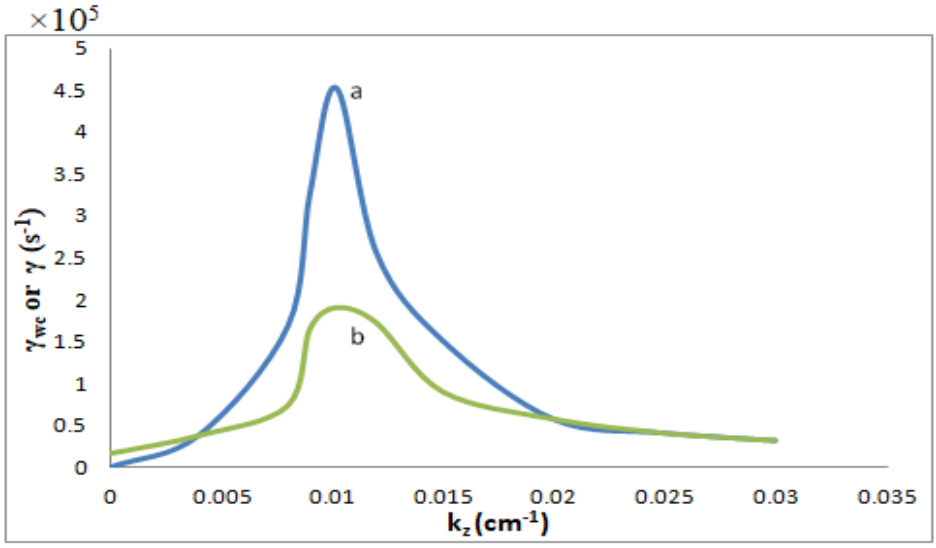

FIG. 3.4. Growth rates (a) γ and (b) γ_{wc} (in sec^{-1}) of the unstable mode as a function of k_z (in cm^{-1}) for an angle of propagation of shear Alfven wave 60^0 in the absence and presence of beam-plasma collisions.

Fig. 3.4 shows the comparison of growth rates of unstable shear Alfven modes in the presence and absence of beam plasma collisions as a function of k_z at wave propagation angle of 60^o, which justifies that the growth rate decreases due to collisions. A rise in the value of ambient magnetic field raises the maximum growth rate in both the cases as shown in Fig. 3.5 and Fig. 3.6.

The variation of growth rate of the unstable mode with the number density of electrons in the plasma is shown in Fig. 3.7 and Fig. 3.8 for different angles of propagation without and with beam plasma collisions. Increase in the number density of electrons decreases the relative density of beam ions in plasma, thus decreasing the growth rate of modes. It can also be seen from the growth rate expressions that an increase in the ion beam velocity increases the growth rate. Similar results for growth

rates have also been observed by Xiang et al. [28] and they have also observed a higher growth rate for RH waves than the LH waves.

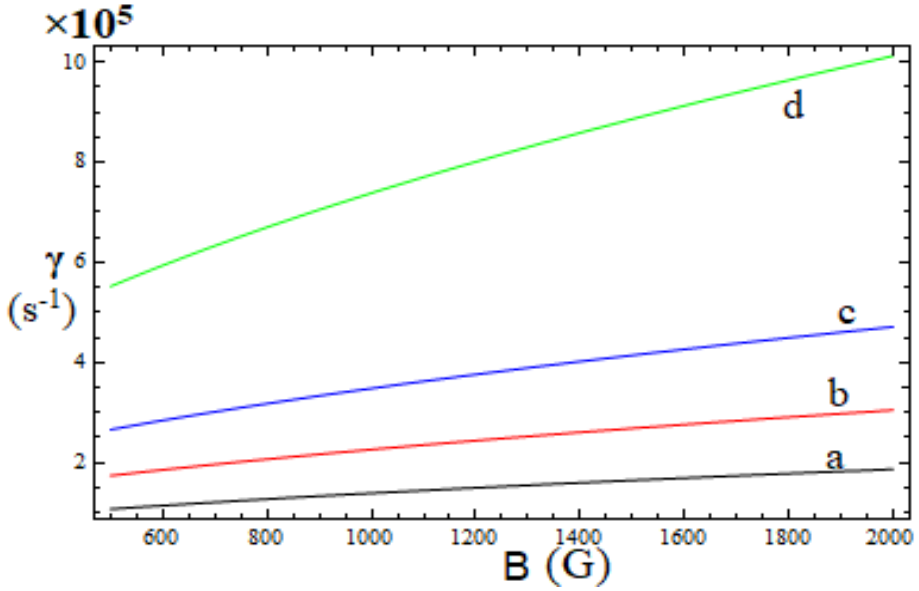

FIG. 3.5 Growth rate γ (in sec^{-1}) of the unstable mode as a function of B (in gauss) for different angles (a) 30^0, (b) 45^0, (c) 60^0 and (d) 80^0 of propagation of shear Alfven wave.

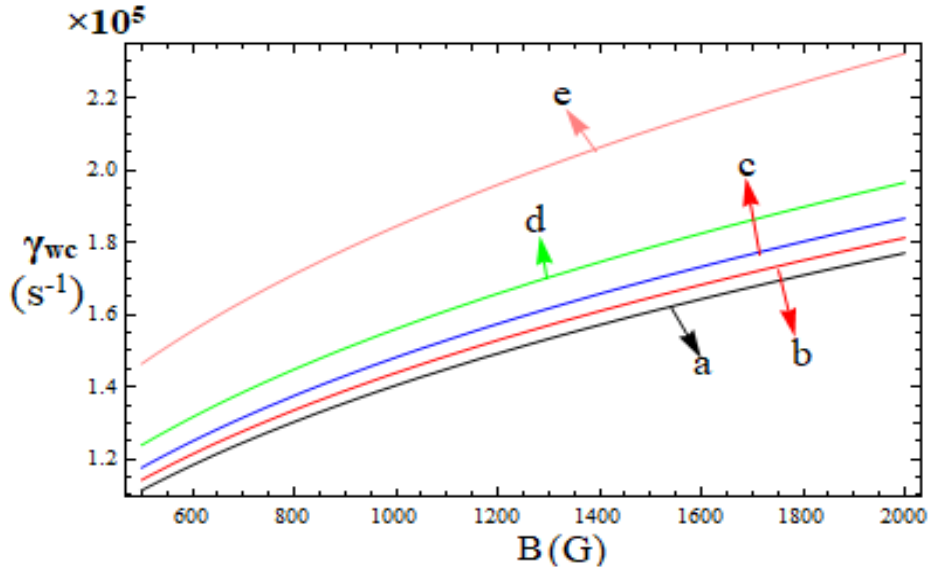

FIG. 3.6 Growth rate γ_{wc} (in sec^{-1}) of the unstable mode as a function of B (in gauss) for different angles (a) 0^0, (b) 30^0, (c) 45^0, (d) 60^0 and (e) 80^0 of propagation of shear Alfven wave in the presence of beam-plasma collisions.

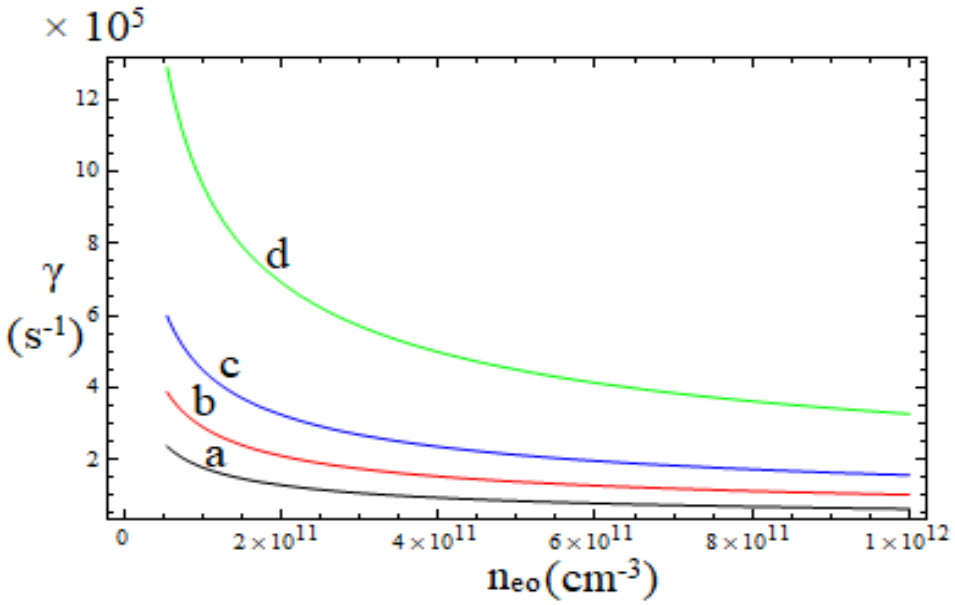

FIG. 3.7 Growth rate γ (in sec^{-1}) of the unstable mode as a function of n_{eo} (in cm^{-3}) for different angles (a) 30^0, (b) 45^0, (c) 60^0 and (d) 80^0 of propagation of shear Alfven wave.

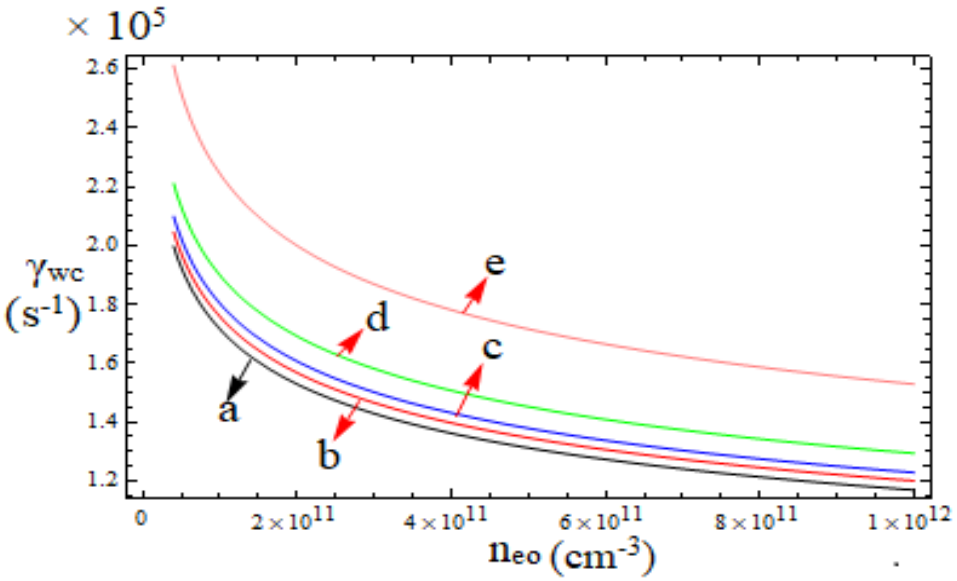

FIG. 3.8 Growth rate γ_{wc} (in sec^{-1}) of the unstable mode as a function of n_{eo} (in cm^{-3}) for different angles (a) 0^0, (b) 30^0, (c) 45^0, (d) 60^0 and (e) 80^0 of propagation of shear Alfven wave in the presence of beam-plasma collisions.

3.3 CONCLUSION

In this paper, we show that an ion beam can efficiently transfer its energy to

plasma through wave generation. The beam ions are resonant both with the parallel as well as oblique shear Alfven modes. The frequency of waves may increase or decrease depending upon the polarization of waves. For oblique shear Alfven waves, the waves grow irrespective of their polarization via beam-wave cyclotron interaction and the beam ions do not show Landau resonance. The numerical values of the growth rate are however, much smaller in the presence of collisions, indicating a collisional damping of waves. The growth rates and frequencies of generated waves are also sensitive to the beam properties. Our results indicate that the growth rates of LH and RH Alfven modes vary with the velocity of ion beam, number density of plasma electrons, ambient magnetic field and collisions in plasma. A stronger magnetic field supports the Alfven wave generation. For, the most unstable mode is the LH polarized oblique Alfven mode and for, it is the RH polarized oblique Alfven mode, indicating a polarization reversal after resonance condition. In this case, the beam- wave interaction could take place only for propagation of Alfven waves and beam ions in opposite direction, with respect to the ambient magnetic field, and only via fast cyclotron interaction. The growth rate is more for parallel shear Alfven waves as compared to oblique shear Alfven waves, making them the dominant modes. The study of oblique modes may find application within the Earth's bow shock as well as to basic plasma processes and are important in the thermodynamics of minor ions in the solar wind.

The collision of beam ions with plasma components affects the growth rate as well as the frequency of generated waves, while the collision between plasma components damps the waves. The effect of beam collisions can be ignored for beam velocities more than ~108 cm/s, but as the velocity of beam decreases, the role of collisions become more and more significant and decrease the growth rate of Alfven waves. The effect of beam and plasma collisions becomes more significant for heavy ion beams or in a complex multi-component plasma, which will be a subject of our future work.

REFERENCES

[1] Gekelman W., Vincena, Leneman D. S. and Maggs J., "Laboratory experiments on shear Alfven waves and their relationship to space plasmas," *J. Geophys Res.* Vol. **102**, No. A4, 7225-7236, 1997**.**

[2] Chen L. and Zonca F., "Physics of Alfven waves and energetic particles in burning plasmas," *Rev.Mod. Phys.,* Vol. **88**, No. 1, 015008, 2016.

[3] Jephcott D. F. and Stocker P. M., "Hydromagnetic waves in a cylindrical; plasma: an experiment," *J. Fluid Mech.,* Vol. **13**, No. 4, 587-596, 1962.

[4] Dwivedi A.K, Kumar S. and Tiwari M.S., "Effect of ion and electron beam on kinetic Alfven wave in an inhomogeneous magnetic field," *Astrophys. Space Sci.*, Vol. **350**, No. 2, 547-556, 2014.

[5] Prakash, V., Gupta, R., Sharma, S.C. and Vijayshri, "Excitation of lower hybrid wave by an ion beam in magnetized plasma," *Laser Part. Beams.*, Vol. **31**, No. 4, 747-752, 2013.

[6] Gupta, R., Prakash, V., Sharma, S.C. and Vijayshri, "Interaction of an electron beam with whistler waves in magnetoplasmas," *Laser Part. Beams.*, Vol. **33**, No. 3, 455-461, 2015.

[7] Gupta, R., Prakash, V., Sharma, S.C., Vijayshri and Gupta, D.N., "Resonant ion beam interaction with Whistler waves in a magnetized dusty plasma," *J. Atomic, Molecular, Condensate and Nano Physics.*, Vol. **3**, No. 1, 45-53, 2016.

[8] Prakash, V., Gupta, R., Vijayshri and Sharma, S.C., "Excitation of electromagnetic surface waves at a conductor-plasma interface by an electron beam," *J. at. mol. condens. nano phys*., Vol. **3**, No.1, 35-43, 2016.

[9] Prakash, V. and Sharma, S. C., "Excitation of surface plasma waves by an electron beam in a magnetized dusty plasma," *Phys. Plasmas.*, Vol. **16**, No. 9,93703, 2009.

[10] Prakash, V., Sharma, S.C., Vijayshri and Gupta, R., "Surface wave excitation by a density modulated electron beam in a magnetized dusty plasma cylinder," *Laser Part. Beams***.,** Vol.**31**, 411-418, 2013.

[11] Shoucri, M.M. and Gagne, R.R.J., "Excitation of lower hybrid waves by electron beams in finite geometry plasmas. Part 1. Body waves," *J. Plasma Phys.*, Vol. **19**, No. 2,281-294, 1978.

[12] Rubab, N. and Jaffer, G., "Excitation of dust kinetic Alfven waves by semi-relativistic ion beams," *Phys. Plasmas.*, Vol. **23**, No. 5, 053701, 2016.

[13] Shevchenko, V.I., Galinsky, V.L. and Ride, S.K., "Excitation of left-hand-polarized nonlinear Alfven waves by an ion beam in a plasma," *J. Geophys. Res.* Vol. **107**, No. A11, 1-12, 2002.

[14] Amagishi, Y. and Tanaka, M., *Phys.*, "Ion-neutral collision effect on an Alfven wave," *Phys. Rev. Lett.***,** Vol.**71** No. 3, 360-363, 1993.

[15] Tripathi, S.K.P., Compernolle, B.V., Gekelman, W., Pribyl P. and Heidbrink W., "Excitation of shear Alfven waves by a spiraling ion beam in a large magnetoplasma," *Phys. Rev. E.*, Vol. **91**, No. 1, 1-5, 2015.

[16] Zhang, Y., Heidbrink, W.W., Boehmer, H., McWilliams, R., Vincena, S., Carter, T.A., Gekelman, W., Leneman, D. and Pribyl, P., "Observation of fast-ion Doppler-shifted cyclotron resonance with shear Alfven waves," *Phys. Plasmas.*, Vol. **15**, No. 10, 102112, 2008.

[17] Soler, R., Ballester, J. L. and Zaqarashvili, T. V., "Overdamped Alfven waves due to ion-neutral collisions in the solar chromospheres," *A & A.*, Vol. 573, 79-91, 2014.

[18] Shukla, P.K. and Stenflo, L., "Periodic structures on an ionic-plasma-vacuum interface,"*Phys. Plasmas.*, Vol. **12**, No. 4, 0845021, 2005.

[19] Shukla, P.K., Yu, M.Y. and Stenflo L., "Growth rates of modulationally unstable ion-cyclotron Alfven waves," *Phys. Scr.*, Vol. **34**, No. 2, 169-170, 1986.

[20] Lu, X.Q., Tang, W. Z., Guo, W. and Gong, X. Y., "A study on interactions between ions and polarized Alfven waves below cyclotron resonance frequency," *Phys.Plasmas.*, Vol. **23**, No. 12, 1-5, 2016.

[21] Hollweg, J. V. and Markovskii, S. A., "Cyclotron resonances of ions with oblique propagating waves in coronal holes & the fast sdolar wind," *J. Geophys. Res.*, Vol. **107**, No. A6, 1-7, 2002.

[22] Li, X. and Lu, Q. M., "Heating and deceleration of minor ions in the extended fast solar wind by oblique Alfven waves," *J. Geophys. Res.*, Vol**. 115**, No. A48, A08105, 2010.

[23] Hellinger, P. and Mangeney, A., "Structure of low mach number oblique shock waves," *Correlated Phenomena at the Sun, in the Heliosphere and in Geospace,* 337-340, 1997.

[24] Hellinger, P. and Mangeney, A., "Electromagnetic ion beam instabilities –oblique pulsation," J. Geophys. Res. Atmos., Vol. **104**, No. A3, 4669-4680, 1999.

[25] Verscharen, D. and Chandran, B.D.G., "The dispersion relations and instability thresholds of oblique plasma modes in the presence of an ion beam," *Astrophys. J.*, Vol. **764**, No. 1, 1-12, 2013.

[26] Maneva, Y.G., Vinas, A.F., Moya, P.S, Wicks, R.T. and Poedts, S., "Dissipation of parallel & oblique Alfven-cyclotron waves- implications for heating of alpha particles in the solar wind," *Astrophys. J.,* Vol. 814, No. 1, 1-15, 2015.

[27] Gao, X., Lu, Q., Li, X., Huang, C. and Wang, S., "Heating of the background plasma by obliquely propagating Alfven waves excited in electromagnetic alpha/proton instability," *Phys. Plasmas.*, Vol. **19**, No. 3, 1-5, 2012.

[28] Xiang, L., Wu, D.J. and Chen, L., "Effect of alpha beams on low-frequency electromagnetic waves driven by proton beams," Astrophy. J., Vol. **869**, No. 64, 1-10, 2018.

CHAPTER 4

Generation of Obliquely Propagating Shear Alfven Wave in Dusty Plasma by Ion Beam

An analytical model based on the fluid treatment on plasmas species and ion beam have been developed to study the interaction of obliquely propagating Shear Alfven wave by an ion beam in a magnetized dusty plasma. Ion beam interacts via cyclotron and Cerenkov interaction with shear Alfven wave only if they counter propagate and co-propagate, respectively. The effect of beam velocity, magnetic field, wave number, dust particle density and dust charge fluctuations have been analyzed in detail. The results are in good agreement with the experimental observations.

4.1 INTRODUCTION

The Alfven waves [1] are very interesting as wave energy is transported directly along magnetic field lines and they may explain the high temperature in the solar corona and high speeds of solar wind. All low frequency currents are shear or compressional Alfven waves responsible for rearranging the current systems in the magnetized plasmas. The current along the magnetic field is due to electrons flow and current across the magnetic field is due to ions because of ion polarization drift in the shear Alfven wave. Gekelman et al. [2] examined that shear Alfven waves emitted from the sources are different from planar magneto-hydrodynamic waves with the cross - field size of the electron inertial length. Tripathi et al. [3] demonstrated experimentally the generation of shear Alfven waves through Doppler shifted cyclotron resonance of a spiraling ion beam, with magnetic fluctuations in a large magnetoplasma. They observed that the beam current is intense enough to excite magnetic perturbations in the ambient plasma when ion beam is injected at a variety of pitch angles with Alfvenic

speeds in the Large Plasma Device (LAPD). They established that ambient plasma density and electron temperature were significantly increased by the beam. In space and variety of laboratory plasmas [4-9], the generation of Alfven wave by Doppler shifted ion cyclotron resonance (DICR) has important roles in exciting sub-cyclotron fluctuations. Zhang et al. [10] studied experimentally the DICR between fast Li+ ions and shear Alfven waves in the He-plasma of the Large Plasma Device.

It is well known that the ion beams dominantly excite the parallel-propagating waves through the "resonant" and "non-resonant" instabilities [11-18]. The growth rates of these instabilities are usually larger than those of the other instabilities while the left hand polarized waves are dominantly excited when the beams are relatively hot and/or weak. Heidbrink [19] analyzed Alfven instabilities driven by energetic particles in toroidally confined plasmas and observed two modes of Alfven instabilities occurring due to resonance between the orbital frequencies of the energetic particles and the wave phase velocity. Compernolle et al. observed experimentally [20] and analytically [21] the Cerenkov radiation pattern of the shear Alfven waves excited by a burst of charged particles propagating along the confinement magnetic fields. Nariyuki et al. [22] showed that a left-hand (LH) polarized Alfven wave excites both LH and right-hand (RH) polarized Alfven waves. The past studies assumed that all the physical quantities depend only on one spatial coordinate parallel to the ambient magnetic field while it was also suggested that obliquely propagating waves excited by the beam instabilities can play important roles in the nonlinear evolution of the system. Moreover, the presence of charged dust particles also modifies the scenario of the Alfven waves [23-28] by enhancing their frequency, modifying the dispersion relation and showing damping effect due to dust charge fluctuation dynamics. Jatenco-Pereira et al. [29] showed the sensible modification of the dispersion relation of Alfven waves in the presence of dust and superthermal particles. They analyzed the competition between different damping processes of kinetic Alfven waves and Alfven cyclotron waves and their applications in the auroral regions of space plasmas, stellar winds and astrophysical plasmas. Cramer and Vladimirov [30] studied that in a dusty plasma, the wave energy propagating at oblique angles to the magnetic field in an increasing density gradient can be effectively damped by the Alfven resonance absorption process. Singh et al. [31] investigated that dust inertial Alfven waves (DIAWs), the obliquely propagating oscillations of dust density with respect to the external magnetic field, have the characteristics of a solitary wave. They showed that an increase in angle of

propagation for sub-Alfvenic DIAWs results in the decrease in amplitude while having no influence on its width and the increase in angle of propagation leads to the decrease in both the amplitude as well as width of the DIAWs in case of super-Alfvenic DIAWs.

In the present paper, we study the interaction of oblique Alfven waves with hydrogen ion beam forced into a magnetized plasma at an angle to the magnetic field. In Section 2, the instability analysis of the shear Alfven wave is discussed for plasma with and without dust grains. The dispersion relation and the growth rate of Alfven waves for cyclotron and Cerenkov interactions are derived and the results are discussed in Section 3. Finally, the conclusion part is given in Section 4.

4.2 INSTABILITY ANALYSIS

Assume a dusty plasma immersed in static magnetic field $\mathbf{B_0} \| \hat{\mathbf{Z}}$ with ion density N_0^i, electron density N_0^e, dust density N_0^d, ion mass m_i, electron mass m_e, dust particle mass m_d, ion charge e, electron charge –e and dust particle charge q_d. A positively charged hydrogen (H^+) beam with charge +e, mass m_b (= m_i) and density N_0^b moves obliquely to the magnetic field through the plasma in the X-Z-plane.

An electromagnetic Alfven wave propagates obliquely through the plasma with electric field

$$\mathbf{E} = \left(E_x \hat{\mathbf{x}} + E_y \hat{\mathbf{y}}\right) e^{-i(\omega t - \mathbf{k}.\mathbf{r})}, \tag{4.1}$$

where $\mathbf{k} = k_X \hat{\mathbf{x}} + k_Z \hat{\mathbf{z}}$ and the magnetic field $\mathbf{B} = c\mathbf{k} \times \mathbf{E}/\omega$.

The equation of motion governing the drift velocity of plasma electrons, plasma ions, dust particles and beam ions is $\frac{\partial \mathbf{v_e}}{\partial t} = -\frac{e}{m_e}\left(\mathbf{E} + \frac{1}{c}\mathbf{v_e} \times \mathbf{B'}\right) - \frac{T_e}{m_e N_0^e}\nabla n_e$

$$\text{or} -i\omega \mathbf{v_e} = -\frac{e\mathbf{E}}{m_e} - \frac{e}{m_e c}\mathbf{v_e} \times \mathbf{B}_0 - v_{te}^2 \frac{\nabla n_e}{N_0^e}, \tag{4.2}$$

where $v_{te}\left(=\left(T_e/m_e\right)^{1/2}\right)$ is the electron thermal velocity, $\mathbf{B'} = \mathbf{B_0} + \mathbf{B}$ and v_{td}, $v_{ti} << v_{te}$.

In the absence of the wave, $\mathbf{v_i} = 0$ and $\mathbf{v_e} = 0$ and when wave is present, **E** and **B** of the

wave behave as small or perturbed quantities and result in perturbed velocities $\mathbf{v}^i$, $\mathbf{v}^e$, $\mathbf{v}^d$ and $\mathbf{v}^b$ for plasma ions, plasma electrons, dust particles and beam ions, respectively.

From linear response of electrons to shear Alfven wave for frequency $\omega_{cd} << \omega << \omega_{ci} << \omega_{ce}$, Eq. (4.2) gives the perturbed velocities and perturbed electron density as

$$v_x^e = \frac{c\,(\mathbf{E}_\perp \times \boldsymbol{\omega}_{\mathbf{ce}})}{B_0 \omega_{ce}}, \tag{4.3}$$

$$v_z^e = \frac{eE_z}{im_e\omega} + \frac{v_{te}^2 k_z n_e}{\omega N_0^e}, \tag{4.4}$$

$$\text{and } n_e = N_0^e \frac{iek_z E_z}{m_e k_z^2 v_{te}^2}. \tag{4.5}$$

From linear response of ions to shear Alfven wave, Eq. (4.2) yields the perturbed ion velocities and perturbed ion density as

$$v_x^i = -\frac{i\omega}{\omega_{ci}}\frac{cE_x}{B_0} + \frac{c(\mathbf{E}_\perp \times \boldsymbol{\omega}_{\mathbf{ci}})}{B_0\omega_{ci}}, \tag{4.6}$$

$$v_z^i = -\frac{eE_z}{im_i\omega}, \tag{4.7}$$

$$\text{and } n_i = N_0^i \frac{iek_z E_z}{m_i\omega^2} - N_0^i \frac{ick_x E_x}{B_0\omega_{ci}}. \tag{4.8}$$

Similarly, linear response of dust to shear Alfven wave yields perturbed velocities and perturbed density of dust particles as

$$v_x^d = -\frac{iq_d\,E_x}{m_d\omega} + \frac{q_d(\boldsymbol{\omega}_{\mathbf{cd}} \times \mathbf{E}_\perp)}{m_d\omega^2}, \tag{4.9}$$

$$v_z^d = \frac{q_d E_z}{im_d\omega}, \tag{4.10}$$

and $n_d = -N_0^d q_d \frac{ik_x E_x}{m_d \omega^2} - N_0^d q_d \frac{ik_z E_z}{m_d \omega^2}$. (4.11)

Using quasi-neutrality condition $n_i e + n_d q_d + N_0^d q_d' = n_e e$, where q_d' is perturbed dust charge, the following previous works is given as

$$q_d' = \frac{|I_{0e}|}{i(\omega + i\eta)}\left(\frac{n_i}{N_0^i} - \frac{n_e}{N_0^e}\right), \tag{4.12}$$

where I_{0e} is the electron current, $\eta = 0.01\omega_{pe} a\, N_0^e / \lambda_D N_0^i$ is the dust charging rate, a is dust particle size and $\lambda_D = v_{te}/\omega_{pe}$ is the Debye length.

Substituting Eqs. (4.5) and (4.8) in (4.12), we get

$$N_0^d q_d' = -\frac{\beta N_0^e e^2}{(\omega + i\eta)}\left[\frac{k_x E_x}{m_i \omega_{ci}^2} + \frac{k_z E_z}{m_e k_z^2 v_{te}^2} - \frac{k_z E_z}{m_i \omega^2}\right], \tag{4.13}$$

where $\beta = \frac{|I_{0e}|}{n}\frac{N_0^d}{N_0^e} = 0.397\left(1 - \frac{1}{\delta}\right)\frac{a}{v_{te}}\omega_{pi}^2 \frac{m_i}{m_e}$ is the coupling parameter that defines the coupling between dust particles and plasma.

We can now determine E_z in terms of E_x using quasi-neutrality condition as

$$E_z = \frac{-\left[\left(1 + \frac{i\beta}{\omega + i\eta}\right)\frac{N_0^e}{N_0^i}\frac{\omega_{pi}^2}{\omega_{ci}^2} - \frac{\omega_{pd}^2}{\omega^2}\right]k_x E_x}{\left[\left(1 + \frac{i\beta}{\omega + i\eta}\right)\frac{\omega_{pe}^2}{k_z^2 v_{te}^2} - \frac{\omega_{pd}^2}{\omega^2} - \left(1 + \frac{i\beta}{\omega + i\eta}\frac{N_0^e}{N_0^i}\right)\frac{\omega_{pi}^2}{\omega^2}\right]k_z}. \tag{4.14}$$

Linear current densities of electrons, ions and dust particles can be obtained as

$$J_x^e = -N_0^e \frac{e^2}{m_e}\frac{i\omega}{\omega_{ce}^2} E_x, \tag{4.15}$$

$$J_x^i = -N_0^i e\left[\frac{i\omega}{\omega_{ci}}\frac{cE_x}{B_0} + \frac{c\left(\mathbf{E}_\perp \times \boldsymbol{\omega}_{ci}\right)}{B_0\omega_{ci}}\right], \tag{4.16}$$

$$\text{and } J_x^d = N_0^d q_d\left(\frac{iq_d E_x}{m_d\omega}\right). \tag{4.17}$$

Now substituting these Equations in wave equation, we obtain

$$\left[\left(1+\frac{\omega_{pi}^2}{\omega_{ci}^2}\right)\omega^2 - \omega_{pd}^2 - k_z^2c^2\right]E_x - k_x^2k_z^2c^2D^2E_x = 0,$$

$$\text{or } \omega^2 - k_z^2v_A^2\left(1+k_x^2D^2\right) - \omega_{pd}^2\frac{v_A^2}{c^2} = 0, \tag{4.18}$$

where

$$D^2 = \frac{\left[\left(1+\frac{i\beta}{\omega+i\eta}\frac{N_0^e}{N_0^i}\right)\frac{\omega_{pi}^2}{\omega_{ci}^2} - \frac{\omega_{pd}^2}{\omega^2}\right]}{\left[\left(1+\frac{i\beta}{\omega+i\eta}\right)\frac{\omega_{pe}^2}{k_z^2v_{te}^2} - \frac{\omega_{pd}^2}{\omega^2} - \left(1+\frac{i\beta}{\omega+i\eta}\frac{N_0^e}{N_0^i}\right)\frac{\omega_{pi}^2}{\omega^2}\right]k_z^2}. \tag{4.19}$$

Equation (4.18) is the dispersion relation for shear Alfven wave in dusty plasma. The standard dispersion relation of the wave in the absence of dust particles can be retrieved from Eq. (4.18) as

$$\omega_A = k_z v_A\left(1+\frac{k_x^2v_{te}^2m_e}{m_i\omega_{ci}^2}\right)^{1/2}. \tag{4.20}$$

Similarly, we analyzed the linear response of beam hydrogen ions to oblique shear Alfven wave and the perturbed beam hydrogen ion velocities are obtained as

$$v_x^b = -\frac{ei\bar{\omega}E_x}{m_i\left(\omega_{ci}^2-\bar{\omega}^2\right)}\left(1+\frac{v_{boz}k_z}{\omega}\right) + \frac{ev_{boz}i\bar{\omega}k_xE_z}{m_i\omega\left(\omega_{ci}^2-\bar{\omega}^2\right)}, \tag{4.21}$$

$$v_y^b = -\frac{e\omega_{ci}E_x}{m_i\left(\omega_{ci}^2-\bar{\omega}^2\right)}\left(1+\frac{v_{boz}k_z}{\omega}\right)+\frac{ev_{boz}\omega_{ci}k_xE_z}{m_i\omega\left(\omega_{ci}^2-\bar{\omega}^2\right)}, \quad (4.22)$$

$$\text{and } v_z^b = -\frac{ev_{box}k_zE_x}{m_i\omega i\bar{\omega}}-\frac{eE_z}{m_i i\bar{\omega}}\left(1-\frac{v_{box}k_x}{\omega}\right), \quad (4.23)$$

where $\bar{\omega}=\omega-k_zv_{box}-k_zv_{boz}$.

The perturbed beam ion density can be written as

$$n_b=\frac{N_0^be}{m_i}\left[\left(\frac{-v_{box}k_z^2}{\omega i\bar{\omega}^2}-\frac{ik_x}{\left(\omega_{ci}^2-\bar{\omega}^2\right)}-\frac{iv_{boz}k_zk_x}{\omega\left(\omega_{ci}^2-\bar{\omega}^2\right)}\right)E_x-\left(\frac{k_z}{i\bar{\omega}^2}-\frac{v_{box}k_zk_x}{\omega i\bar{\omega}^2}-\frac{iv_{boz}k_x^2}{\omega\left(\omega_{ci}^2-\bar{\omega}^2\right)}\right)E_x\right]. \quad (4.24)$$

The perturbed beam current density along X-direction can be calculated as

$$J_x^b=\frac{-ie^2N_0^b}{m_i\omega}\left[\left(\frac{\left(\omega+k_zv_{boz}\right)\bar{\omega}_zE_x-k_xv_{boz}\bar{\omega}_zE_z}{\left(\omega_{ci}^2-\bar{\omega}^2\right)}\right)-\left(\frac{k_z^2v_{box}^2E_x+k_zv_{box}\bar{\omega}_xE_z}{\bar{\omega}^2}\right)\right], \quad (4.25)$$

where $\bar{\omega}_z=\omega-k_zv_{boz}$ and $\bar{\omega}_x=\omega-k_xv_{box}$.

On substituting this value in the wave equation for X-component, we obtain two possible interactions viz. cyclotron interaction and Cerenkov interaction

4.2.1 For Cyclotron interaction:

Wave Equation becomes

$$\omega^2 - \omega_A^2 = \frac{\omega_{pb}^2 \bar{\omega}_z v_A^2}{c^2\left(\bar{\omega}^2 - \omega_{ci}^2\right)}\left[\omega + k_z v_{boz}\left(1 + k_x^2 D^2\right)\right] \quad . \tag{4.26}$$

From Eq. (4.26), we can say that both fast cyclotron as well as slow cyclotron interactions are possible analytically. Since $\omega < \omega_{ci}$, therefore, fast cyclotron interaction is not possible physically and only slow cyclotron interaction exists i.e. for $\bar{\omega} \approx -\omega_{ci}$ and only if beam propagates opposite to the Alfven wave direction. Similar results have been obtained experimentally by Tripathi *et al*. [3] where shear Alfven wave exists in a direction opposite to the ion beam in a Large Plasma Device by Doppler- shifted ion- cyclotron resonance.

Assuming perturbed quantities, $\omega = \omega_A + i\delta_1$, we get

$$\delta_1^2 = \frac{-\omega_{pb}^2 \bar{\omega}_z v_A^2}{c^2 2\omega_{ci} 2\omega_A}\left[\omega + k_z v_{boz}\left(1 + k_x^2 D^2\right)\right] .$$

The growth rate is found as

$$\gamma^{cyc} = \left[\frac{R}{\left(\bar{\omega}_A^2 - \omega_{ci}^2 + 4\omega_A \bar{\omega}_A\right)} - \frac{\omega_A^2\left(\bar{\omega}_A^2 - \omega_{ci}^2\right)^2}{\left(\bar{\omega}_A^2 - \omega_{ci}^2 + 4\omega_A \bar{\omega}_A\right)^2}\right]^{1/2}, \tag{4.27}$$

and the maximum growth rate is given as

$$\gamma_{max}^{cyc} = \left[\frac{R}{4\omega_A \bar{\omega}_A}\right]^{1/2} \text{for} \, \bar{\omega}_A = -\omega_{ci}, \tag{4.28}$$

$$\text{where} \, R = \frac{\omega_{pb}^2 \bar{\omega}_z v_A^2}{c^2}\left[\omega_A + k_z v_{boz}\left(1 + k_x^2 D^2\right)\right],$$

$$\bar{\omega}_A = \omega_A - k_z v_{box} - k_z v_{boz} \, \text{and} \, \omega_{pb}^2 = \frac{4\pi N_0^b e^2}{m_i} .$$

The imaginary part of δ_1 is obtained as $\mathrm{Im}[\delta_1] = \dfrac{2\omega_A\left(\bar{\omega}_A^2 - \omega_{ci}^2\right)}{\left(\bar{\omega}_A^2 - \omega_{ci}^2 + 4\omega_A\bar{\omega}_A\right)}$ which indicates a decrease in Alfven frequency due to cyclotron interaction.

The threshold for shear Alfven wave growth is

$$|R| > \frac{{\omega_A}^2\left({\bar{\omega}_A}^2 - \omega_{ci}^2\right)^2}{\left({\bar{\omega}_A}^2 - \omega_{ci}^2 + 4\omega_A\bar{\omega}_A\right)}. \tag{4.29}$$

4.2.1 For Cerenkov interaction:

The wave equation becomes

$$\omega^2 - \omega_A^2 = \frac{\omega_{pb}^2 v_A^2 k_z^2 v_{box}^2}{c^2\bar{\omega}^2}\left[1 + k_x^2 D^2 - \frac{k_x\omega D^2}{v_{box}}\right]. \tag{4.30}$$

In this case the interaction is possible for beam propagating in the same direction as the direction of shear Alfven wave.

Assuming perturbed quantities $\omega = \omega_A + i\delta_1$ and $\bar{\omega} = i\delta_1$ i.e. $\omega = \mathbf{k.v} + i\delta_1$, we obtain a cubic equation for δ_1, which is solved for different wave numbers to obtain imaginary and real values of δ_1 , representing frequency and the growth rate of Alfven wave in Cerenkov interaction. The values have been tabulated and analyzed by drawing graphs.

The maximum growth rate in this case becomes

$$\gamma_{max}^{cer} = \frac{\sqrt{3}}{2}\left[\frac{R'}{2\omega_A}\right]^{1/3}, \tag{4.31}$$

where $R' = \dfrac{\omega_{pb}^2 k_z^2 v_A^2 v_{box}}{c^2}\left(k_x\bar{\omega}_A D^2 - v_{box}\right)$.

4.3 RESULTS AND DISCUSSION

We now analyze and discuss the properties of oblique shear Alfven waves in plasma, with as well as without dust particles in the presence of Hydrogen ion beam and

study the influence of ion beam and dust particles on real frequencies and growth rates of waves. This study in dusty plasma can be important to explosion generated relativistic plasmas and can also play an important role in exciting sub-cyclotron fluctuations in a variety of space plasmas and in laboratory [3]. We have chosen plasma parameters from the experiment [3] conducted on the LAPD for excitation of shear Alfven waves by a spiraling ion beam and typical dust plasma parameters i.e. $N_0^i = 1.5\times10^{11}\,cm^{-3}$, $N_0^e = N_0^i/\delta$, where δ is the relative density of negatively charged dust particles varied from 1 to 7, $q_d = 1000\,e$, $v_{te} = 9.4\times10^7\,cms^{-1}$, dust particle radius, $a = 10^{-4}\,cm$, $N_0^b = 5\times10^9\ cm^{-3}$, $m_i/m_e = 7344$, $m_d/m_i = 2.5\times10^{11}$, $\omega_{pe}^2 = 4\pi N_0^e e^2/m_e$, $\omega_{pi}^2 = 4\pi N_0^i e^2/m_i$, $\omega_{pd}^2 = 4\pi N_0^d q_d^2/m_d$, B_0= 1800 G, and the beam velocity v_{b0} = (0.2-2)× 10^8 cm/s. The Hydrogen beam spirals down the ambient plasma oblique to the magnetic field direction with initial velocity components in X-Z plane as considered in experimental study.

Using Eq. (4.20), we have plotted Fig. 4.1 displaying normalized frequency and beam modes versus normalized parallel wave number $k_z c/\omega_{pi}$ for cyclotron interaction between counter propagating wave and beam. For smaller beam velocities, the unstable frequency and the unstable wave number increases indicating that a high velocity beam is needed to excite low frequency oblique Alfven waves. Fig.4.1 shows that a beam with velocity less than 2×10^7 cm/s may excite ion cyclotron waves.

3-D picture of Fig. 4.2 shows normalized growth rate of the wave as a function of normalized perpendicular and parallel wave numbers via cyclotron interaction. The growth rate first increases, shows a maxima and then decreases along the magnetic field but it increases gradually across the magnetic field. The domain of growth rate also increases with perpendicular wave number.

In Fig. 4.3, we have plotted the growth rate for cyclotron interaction as a function of normalized parallel wave number for different beam ion velocity using Eq. (4.27). The average growth domain remains almost same for different beam velocities but the maximum growth rate decreases with increase of beam velocity. For low beam velocity, the shear Alfven wave strongly interacts and grows at a faster rate for the cyclotron interaction owing to its low frequency and the maximum growth rate is obtained for

nearly same value of k_z.

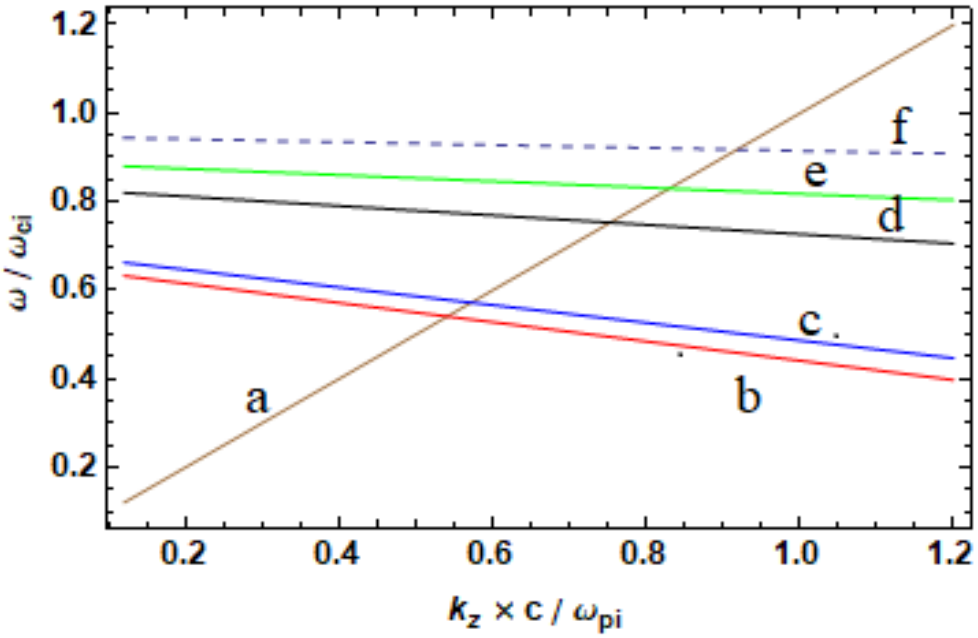

Fig. 4.1 Dispersion curve (a) of Shear Alfven wave and various beam modes with beam ion velocities (b) v_{b0} =1.84 × 10^8 cm/s (c) v_{b0} =1.69 × 10^8 cm/s (d) v_{b0} =9 × 10^7 cm/s (e) v_{b0} =6 × 10^7 cm/s (f) v_{b0} =2.8 × 10^7 cm/s for cyclotron interaction between wave and beam.

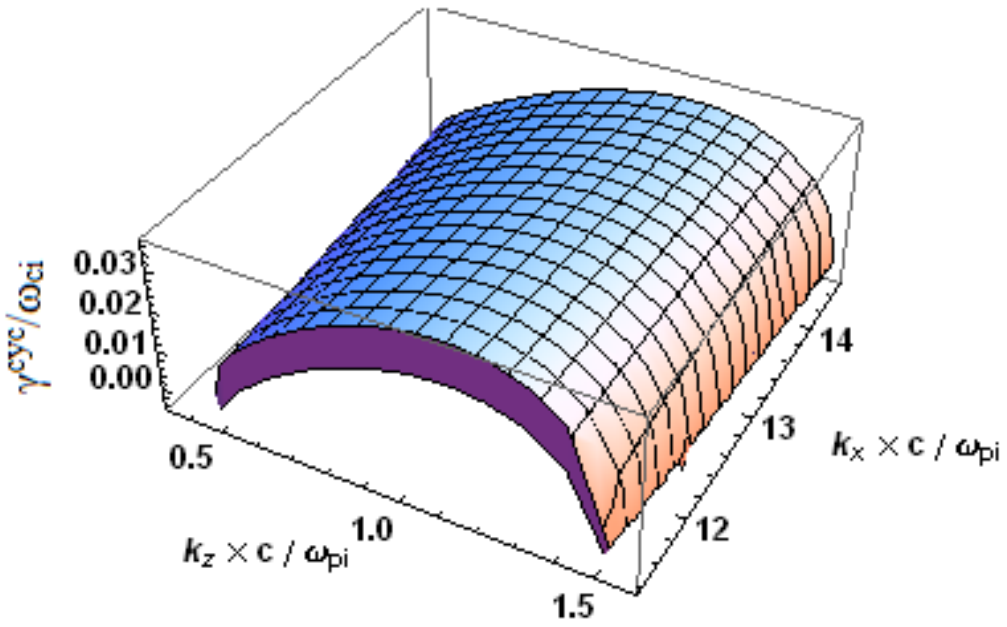

Fig. 4.2 Normalized growth rate γ^{cyc}/ω_{ci} versus normalized parallel and perpendicular wave numbers.

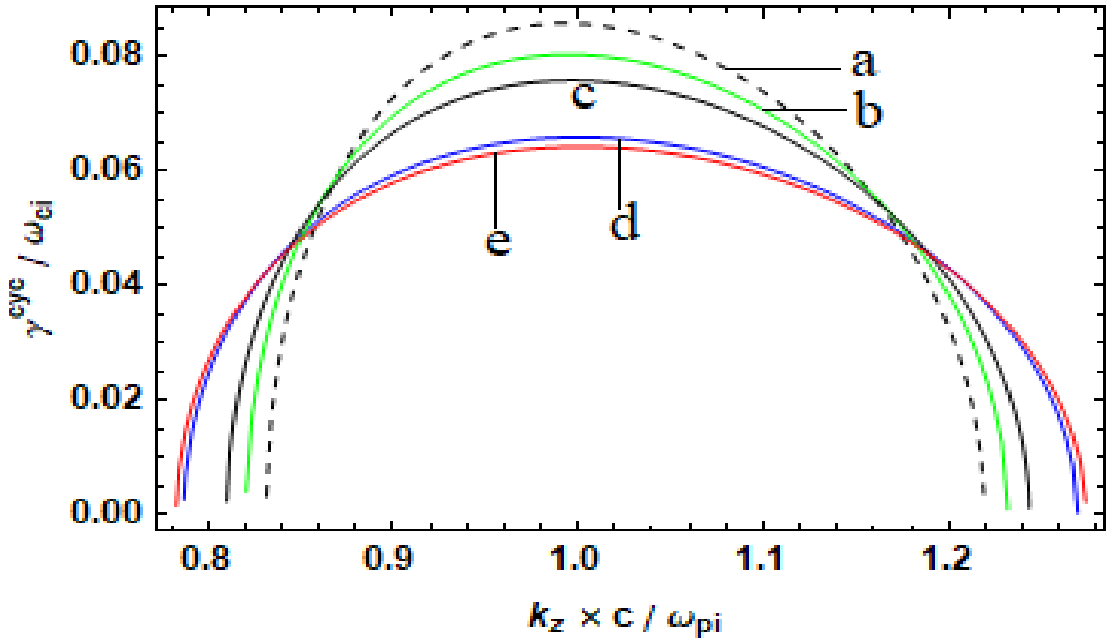

Fig. 4.3 Normalized growth rate γ^{cyc}/ω_{ci} versus normalized parallel wave number for different beam velocities (a) 2.8×10^7 cms^{-1} (b) 6.0×10^7 cms^{-1} (c) 9.0×10^7 cms^{-1} (d) 1.69×10^8 cms^{-1} (e) 1.84×10^8 cms^{-1}.

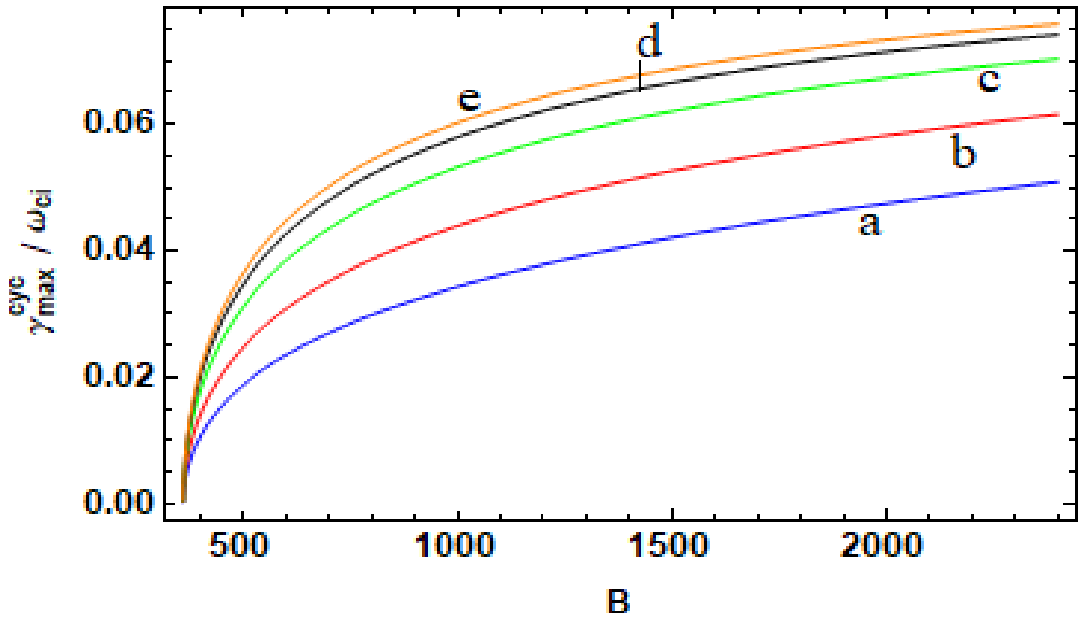

Fig. 4.4 Normalized growth rate γ^{cyc}_{max} versus static magnetic field B in Gauss for different parallel wave numbers (a) 0.001 (b) 0.002 (c) 0.004 (d) 0.006 (e) 0.0075 (in cm^{-1}) of unstable shear Alfven wave.

Using Eq. (4.28), we have plotted graph for maximum growth rate for cyclotron interaction as a function of ambient magnetic field for different values of $k_z$in Fig.4. 4. The growth rate enhances with the magnetic field and its dependence on the latter

increases with increasing parallel wave number.

In Fig. 4.5, we theoretically observed that normalized frequency of shear Alfven wave increases with decrease in the beam velocity which propagates in opposite direction of the ambient magnetic field which is compatible with unstable frequencies of Fig.4.1.

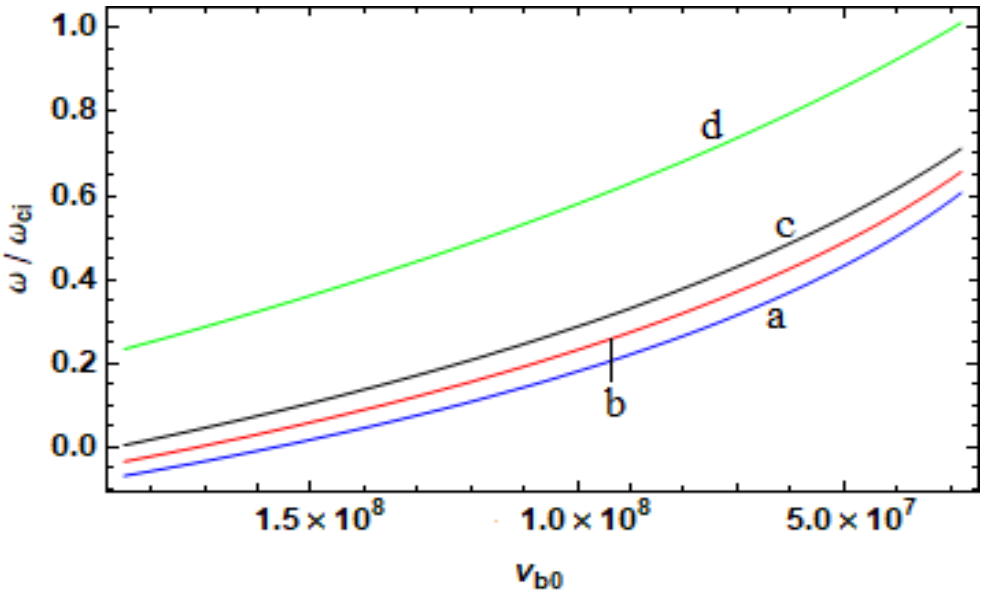

Fig. 4.5 Normalized wave frequency ω/ω_{ci} of the shear Alfven wave versusbeam velocity (cm/s) for different parallel wave number k_z (Cyclotron interaction) (a) 0.008 (b) 0.009 (c) 0.010 (d) 0.015 (in cm^{-1}).

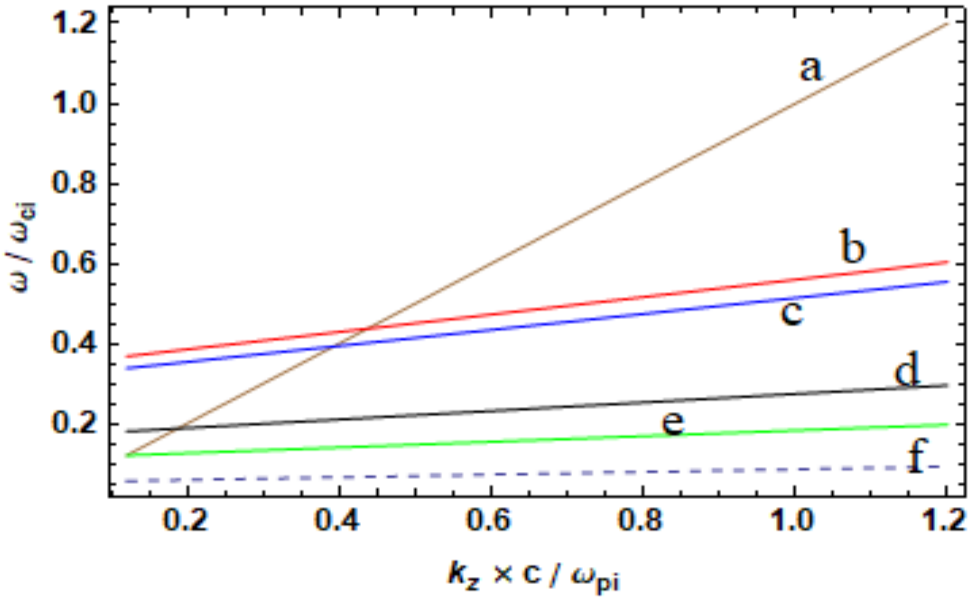

Fig. 4.6. Normalized dispersion curve (a) of Shear Alfven wave for various beam modes with different beam ion velocities (b) $v_{b0} = 1.84 \times 10^8$ cm/s (c) $v_{b0} = 1.69 \times 10^8$ cm/s (d) $v_{b0} = 9 \times 10^7$ cm/s (e) $v_{b0} = 6 \times 10^7$ cm/s (f) $v_{b0} = 2.8 \times 10^7$ cm/s for Cerenkov interaction.

Using Eq. (4.20), we have plotted the dispersion curves of the shear Alfven wave in Fig. 4.6 with different beam mode for Cerenkov interaction for the same parameters as in Fig.1. When ion beam moves along the direction of magnetic field, beam interacts strongly at comparatively higher velocities and hence wave frequency increases with beam velocity antagonistically to the case of cyclotron interaction.

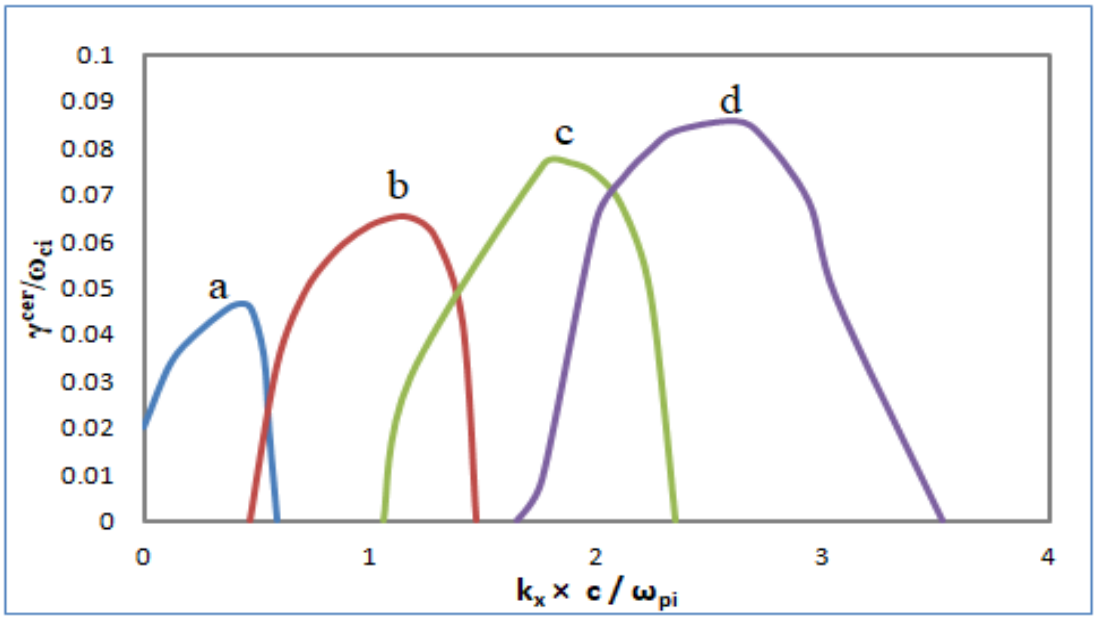

Fig. 4.7 Normalized growth rates γ^{cer}/ω_{ci} versus normalized perpendicular wave numbers for various normalized parallel wave numbers $k_z \times c / \omega_{pi}$ (a) = 0.12 (b) = 0.35 (c) = 0.59 (d) = 0.82.

We have plotted Fig.4.7 by calculating the real values of δ_1 from Eq. (4.30) i.e., the growth rate of instability for Cerenkov interaction vs normalized perpendicular wave numbers for different values of normalized parallel wave number. We inferred from Fig.4.7 that the value of growth rate is higher at higher values of k_x and k_z.

From Eq. (4.31), Fig.4.8 has been plotted showing variation of maximum growth rate with normalized perpendicular wave number for different beam velocity. At higher beam ion velocity, maximum growth rate for Cerenkov interaction increases slowly with k_z while it grows with faster rate for comparatively lower beam velocity.

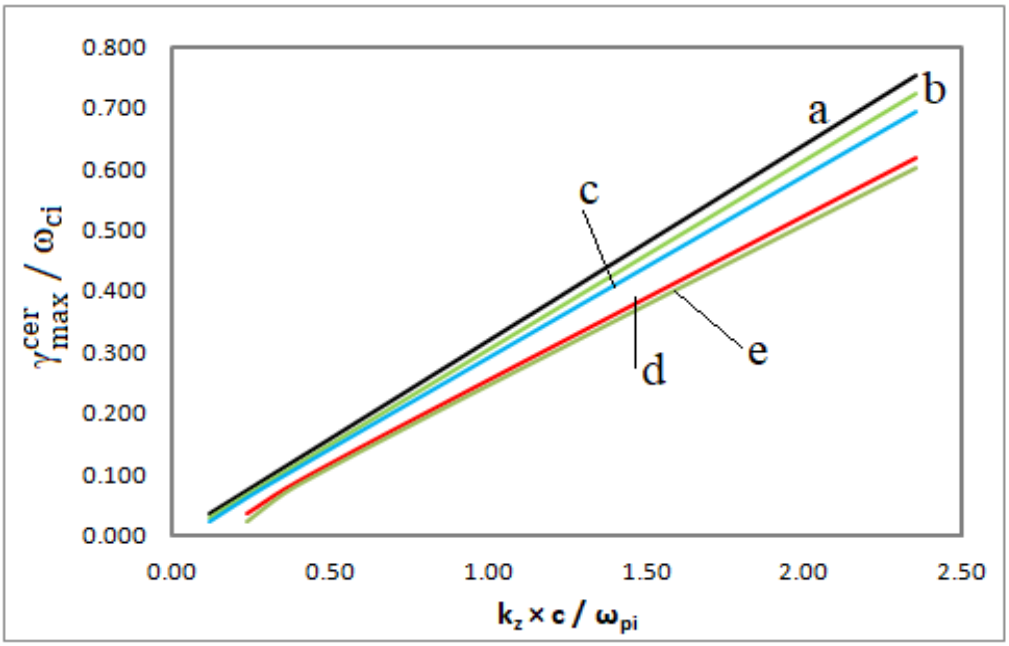

Fig. 4.8. Normalized maximum growth rate γ^{cyc}_{max} versus normalized perpendicular wave number for different beam velocities, v_{b0} (a) 2.8×10^7 cm/s (b) 6×10^7 cm/s (c) 9×10^7 cm/s (d) 1.6×10^8 cm/s (e) 1.84×10^8 cm/s.

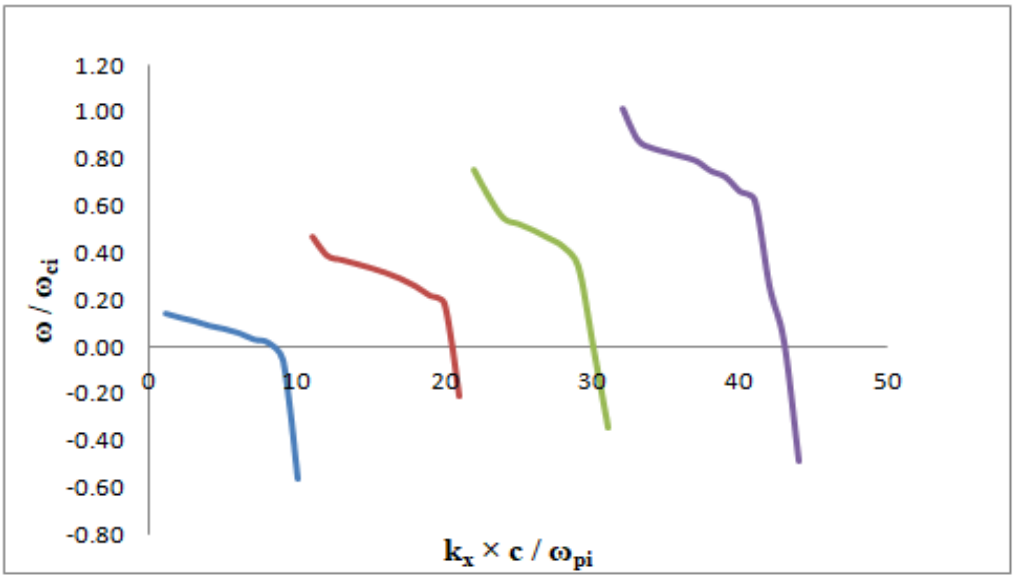

Fig. 4.9. Normalized shear Alfven wave frequency ω/ω_{ci} versus normalized perpendicular wave numbers $k_x\times c/\omega_{pi}$ at different normalized parallel wave numbers, $k_z\times c/\omega_{pi}$ (a)= 0.12 (b) = 0.35 (c) = 0.59 (d) = 0.82.

We have used imaginary part of δ_1 from Eq. (4.30) to plot Fig.4.9. It shows a decrease in the frequency of shear Alfven wave in Cerenkov interaction with the increase in the value of k_x.

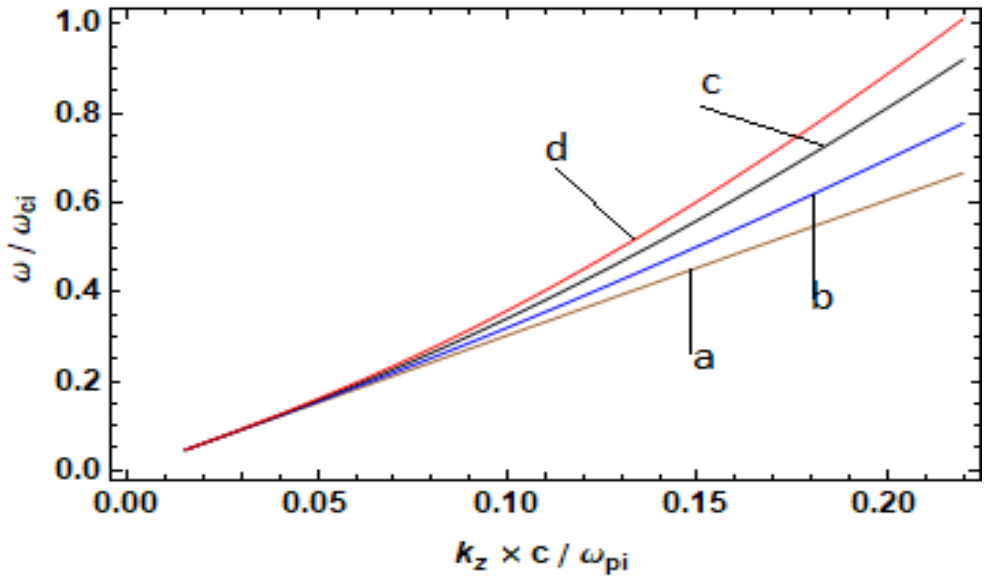

Fig. 4.10 Dispersion curves of shear Alfven wave frequency in dusty plasma at (a) δ = 1 (b) δ = 2 (c) δ = 5 (d) δ = 7.

To study the dust effects in the magnetized plasma on the ion beam interaction with the shear Alfven wave we used typical dusty plasma parameters. We have plotted Fig. 10 for the dispersion relations of shear Alfven wave in dusty plasma for different values of δ using Eq. (18). It shows a rise in the alfvenic wave frequency in the dusty plasmas with increase in relative density of dust grains.

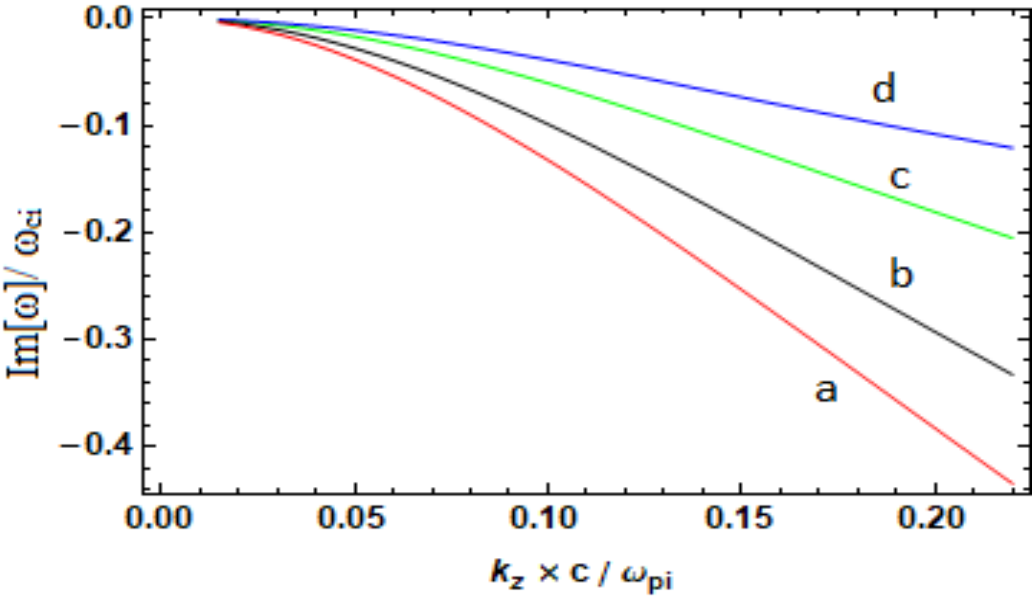

Fig. 4.11 Decrease in frequency of shear Alfven wave due to dust charge fluctuations in plasma for (a) δ=7 (b) δ=5 (c) δ=3 (d) δ=2.

The addition of dust grains in plasma increases the frequency of the shear Alfven wave, however, the dust charge fluctuations act as a source of frequency decline as shown in Fig. 4.11, plotted by using imaginary value of frequency from Eq. (18). More the number of dust grains, higher is the rate of decrease of frequency with parallel wave number.

Fig. 4.12 has been plotted using Eq. (4.27) to show variation of maximum growth rate in cyclotron interaction with the normalized k_z for different values of δ. It may be inferred that maximum growth rate is higher at higher value of δ for a given k_z.

With the use of Eq. (4.31), we have plotted Fig.4.13 illustrating normalized maximum growth rate for Cerenkov interaction with the rise of normalized wave number for different values of δ. We have obtained higher value of maximum growth rate for higher value of δ for a given k_z in Cerenkov interaction also, like in the case of cyclotron interaction but the value of normalized maximum growth rate is more in the case of Cerenkov interaction than cyclotron interaction.

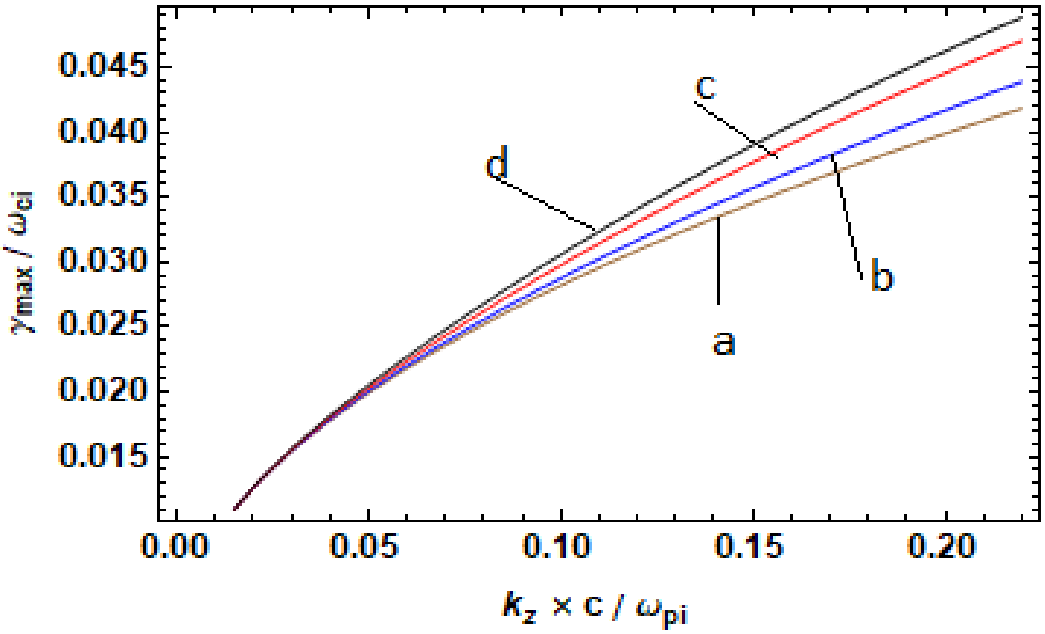

Fig.4. 12 Normalized maximum growth rate for cyclotron interaction versus normalized wave number at (a) δ=1 (b) δ=2 (c) δ=5 (d) δ=7

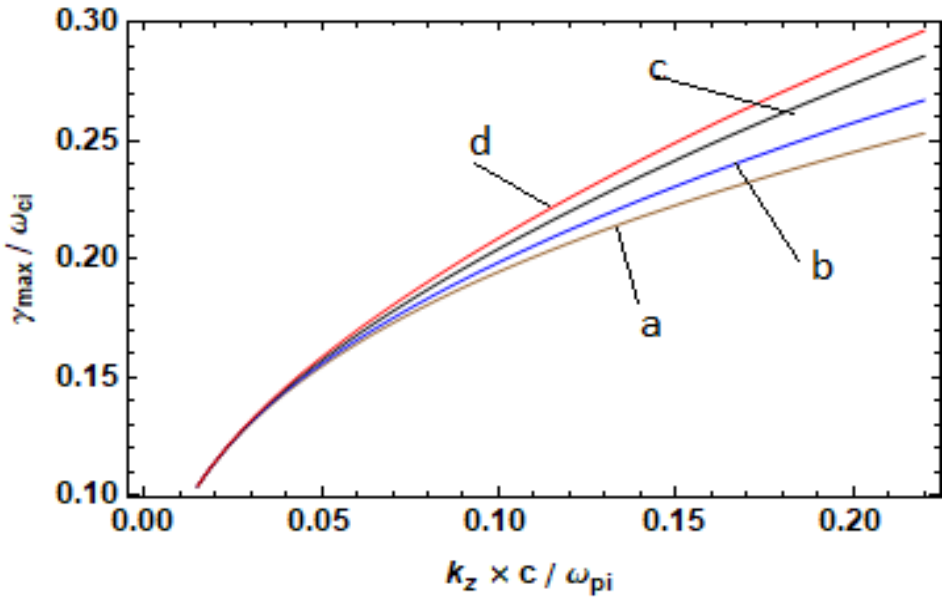

Figure 4.13. Normalized maximum growth rate for Cerenkov interaction versus normalized wave number at (a) δ = 1 (b) δ = 2 (c) δ = 5 (d) δ = 7

4.4 CONCLUSION

Generation of obliquely propagating Shear Alfven wave through Hydrogen ion beam has been observed theoretically. We have used first order perturbation theory to study the interaction between the beam and the plasma mathematically. Ion beam particles interact with shear Alfven wave only when it propagates in opposite direction with the wave via cyclotron interaction and in same direction via Cerenkov interaction. We have derived the dispersion relation and the growth rate of the shear Alfven wave in both the cases. We present the theory on instabilities in the presence of hydrogen ion beam in a magnetized plasma which is in good agreement to the results of experiment performed by Tripathi *et al.* [3]. In addition, we have studied the effect of dust charge fluctuations on beam-shear Alfven wave interaction. The shear Alfven wave generation has important role in exciting sub-cyclotron fluctuations in laboratory and space plasmas. In the solar corona, the Alfven waves dissipate their energy and transfer their momentum to the solar wind particles, accelerating the solar wind streams at the Earth's orbit. Thus Alfven waves play an important role in driving stellar winds. The winds of super-giant stars contain significant amount of dust particles, therefore our work may be useful for evaluating the effect of dust on damping of Alfven waves to accelerate solar wind. The results we have obtained should also be useful for understanding the Alfven wave propagation and absorption in dusty interstellar clouds, planetary dust rings and the Earth's mesopause.

REFERENCES

1. H. Alfven, Nature **1942,** *150*, 405.
2. W. Gekelman, Vincena, D. S. Leneman, J. Maggs, Geophys. Res. **1997,***102***,** 7225.
3. S. K. P. Tripathi, B. V. Compernolle, W. Gekelman, P. Pribyl, W. Heidbrink, Phys. Rev. E. **2015**, *91***,** 0131091.
4. P. K. Shukla, L. Stenflo, Phys. Plasmas. **2005,***12***,** 0845021.
5. P. K. Shukla, M. Y. Yu, L. Stenflo, Phys. Scripta **1986,** *34*, 169.
6. Xing-Qiang Lu, Wei-Zhong Tang, Wei Guo, Xue-Yu Gong, Phys. Plasmas. **2016,***23*, 122114.
7. P. K. Shukla, R. P. Sharma, Phys. Rev.A. **1982,** *25***,** 2816.
8. J. V. Hollweg, S. A. Markovskii, J. Geophys. Res. **2002,** *107*, SSH1.
9. X. Li, Q. M. Lu, J. Geophys. Res. **2010,** *115*, A081051.
10. Y. Zhang, W. W. Heidbrink, H. Boehmer, R. McWilliams, S. Vincena, T. A. Carter, W.Gekelman, D. Leneman, P. Pribyl, Phys. Plasmas. **2008**, *15*, 102112.
11. Y. Amagishi, M. Tanaka, Phys. Rev. Lett**. 1993,** *71*, 360.
12. A.K Dwivedi, S. Kumar, M. S. Tiwari, Astrophys. Space Sci. **2014,** *350***,** 547.
13. R. Gupta, V. Prakash, S. C. Sharma, Vijayshri, Laser Part. Beams. **2015**, *33*, 455.
14. R. Gupta, V. Prakash, S. C. Sharma, Vijayshri, D. N. Gupta, J. Atomic, Molecular, Condensate and Nano Physics **2016**, *3*, 45.
15. V. Prakash, R. Gupta, Vijayshri, S. C. Sharma, J. Atomic, Molecular, Condensate and Nano Physics **2016,** *3*, 35.
16. V. Prakash, S.C. Sharma, Phys. Plasmas **2009,** *16***,** 93703.
17. V. Prakash, R. Gupta, S.C. Sharma, Vijayshri, Laser Part. Beams. **2013**, *31*, 747.
18. V. Prakash, S. C. Sharma, Vijayshri, R. Gupta, Laser Part. Beams **2013,** *31***,** 411.
19. W. W. Heidbrink, Phys. Plasmas. **2008,** *15*, 055501.
20. B. V. Compernolle, G. J. Morales, W. Gekelman, Phys. Plasmas. **2008,***15*, 082101.
21. B. V. Compernolle, W. Gekelman, P. Pribyl, Phys. Plasmas. **2006,***13*, 092112.
22. Y. Nariyuki, T. Hada, K. Tsubouchi, J. Geophys. Res.:Space Phys. **2009,***114*, A07102.
23. N. Rubab, G. Jaffer, Phys. Plasmas. **2016,** *23***,** 0537011.
24. P. Varma, N. Shukla, P. Agarwal, M. S. Tiwari, J. Phys.: Conference Series **2010,***208*, 012034.
25. A. C. Das, A. K. Misra, K. S. Goswami, Phys. Rev. E, **1996,***53*, 4051.

26. J. Shrivastava, M. S. Tiwari, Ind. J. Radio Space Phys. **2004,***33*, 25.
27. M. C. Juli, R. S. Schneider, L. F. Ziebell, Phys. Plasmas. **2005,***12*, 052109.
28. M. Jamil, H. A. Shah, M. Salimullah, K. Zubia I. Zeba, Ch. Uzma, **2010,***17*, 073703.
29. V. Jatenco-Pereira, A. C.-L. Chian, N. Rubab, Nonlin. Processes Geophys. **2014**, 21, 405.
30. N. F. Cramer, S. V. Vladimirov, Publ. Astron. Soc. Aus. **1997**, 14, 170.
31. M. Singh, K. Singh, N. S. Saini, Pramana – J. Phys. **2021**, 95:197, 1.

CHAPTER 5

Beam-driven Growth of Lower Hybrid Wave in a Magnetized Relativistic Beam-Plasma System

In this chapter, a problem based on fluid theory of parametric decay of lower hybrid wave in a magnetized relativistic beam plasma system has been studied. The nonlinear coupling of lower hybrid wave via beam mode excitation is numerically analyzed. The growth rates of beam driven instability in different beam density regions namely Compton regime and Raman regime have been obtained with the dependency of parametric instabilities on the local plasma parameters.

5.1 INTRODUCTION

A relativistic beam-plasma system can support a variety of plasma modes via momentum and energy conservation. The interaction of an electron beam (propagating with relativistic velocity) and plasma has been used for plasma heating in fusion and many other applications because the relativistic electron beam can have high-energy density, which can be transferred to the target plasma efficiently [1-3]. Several experiments have been carried out to study the interactions between a plasma and an electron beam [4,5]. The plasma can be excited in several modes of oscillations. Some modes grow in amplitude at the cost of the beam energy, which can be a subject of study in fusion related research.

Earlier experiments [6-8] have studied the electron beam injection with low energies into the magnetosphere from sounding rockets. However, the relativistic beams have proven to be more stable than low energy beams due to lower beam density requirements for a fixed beam current [1,9,10]. Relativistic beam-plasma instabilities have attracted many theoretical [11-13] and experimental works [4,5], as they excite

plasma wave and couple energy between beam and plasma. A phase matching between beam electrons and wave is required as long as possible. For beam energy interaction, Cerenkov resonance has this desirable property of maintaining synchronization.

These studies are very helpful to understand similar processes occurring in nature and in man-made devices. Lower hybrid (LH) waves are crucial in exploring the space and fusion plasmas. They are highly electrostatic with large k-vector with frequency downshift by the magnetic field. These waves are formed in the lower frequency limit of the electron whistler branch. Space observations also show that LH waves play a prominent role in radio communication in earth's magnetosphere.

The mechanism for transferring beam energy by the beam itself to the plasma has been an issue of research [14,15]. This energy transfer can be done via parametric instability at (or above) the lower hybrid frequency whenever an electron beam is injected parallel to the magnetic field in a plasma. Growth rates of parametric instabilities are dependent on the plasma conditions, mainly the plasma beta and the pump wave, also called as mother wave properties, amplitude and polarization. Lizunov*et al.* experimentally showed that decay instabilities have very low threshold and high growth rates [16]. With the use of axial and spiralling electron and ion beams, LH waves have been studied analytically and experimentally by many researchers [17-20]. The LH waves give rise to various non-linear phenomena, e.g. modulational instabilities, harmonic generation and parametric instabilities [21-24]. It has been presented by number of theoretical investigations that excitation of LH wave can be achieved by two counter propagating cosh-Gaussian laser beams in a magnetized plasma [25, 26]. Moreover, it has also been shown analytically that two copropagating super-Gaussian laser beams in a collisional plasma excite electron Bernstein wave [27, 28]. Varma and Kumar [29] have shown that the ponderomotive force exerted by pump wave on the electrons has potential to drive electron Bernstein wave in homogenous and inhomogeneous plasmas. The pre-existing electrostatic wave present in plasma aids cosh- Gaussian laser absorption in itself with magnetic field [30].

In this article, we study the non-linear coupling of lower hybrid wave in a relativistic beam plasma system in the presence of a magnetic field and the electron beam. The lower hybrid wave $(\omega_p, \boldsymbol{k}_p)$ acts as a pump and imparts energy and momentum to the plasma electrons. The decay of large amplitude lower hybrid wave into lower-hybrid sideband wave and beam mode drives the instability. The sideband

wave couples with the plasma density perturbation [associated with the low frequency mode $(\omega_B, \boldsymbol{k}_B)$] and produces nonlinear density fluctuations. In a result, the sideband lower hybrid wave $(\omega_s, \boldsymbol{k}_s)$ is excited, where $\omega_s = \omega_p - \omega_B$, $k_s = k_p - \boldsymbol{k}_B$. The sideband couples with the pump wave to produce a ponderomotive force on plasma electrons, driving the beam mode and the low frequency mode.

We present our work in two sections: In Section 2, the instability analysis following the plasma fluid approach has been done. The growth rate of the beam driven parametric instability in Compton and Raman regimes has been estimated. The discussion of results and conclusion are briefed in Section 3.

5.2 ANALYTICAL MODEL

We consider a plasma of electron density n_e and ion density n_i. The plasma is immersed in a magnetic field **B** along the z-direction. An electron beam of densityn_B interacting with this plasma. The electron beam velocity is assumed $v_B\hat{z}$. The electron beam propagates with the relativistic speed, where the Lorentz factor is defined as $\gamma_0 = (1 - v_B^2/c^2)^{-1/2}$ with c is the velocity of light in vacuum. On ignoring finite boundary effects, we write the electric potential of the lower hybrid (LH) wave as

$$\varphi_p = \varphi_{p0} e^{-i(\omega_p t - \boldsymbol{k_p} \cdot \boldsymbol{x})}, \tag{5.1}$$

where$\boldsymbol{k_p} = k_{p\perp}\hat{\boldsymbol{x}} + k_{pz}\hat{\boldsymbol{z}}$,$\omega_p = \omega_{LH}\left(1 + (k_{pz}^2 m_i)/(k_p^2 m)\right)^{1/2}$, $\omega_{LH} = \frac{\omega_{pi}}{1+\omega_{pe}^2/\omega_c^2}$, ω_{pe} and ω_c are the plasma electron, $\omega_{pe}^2 = \frac{4\pi n_e e^2}{m_e}$and electron cyclotron frequencies, $\omega_c = \frac{eB}{m_e c}$ and ω_{pi} is plasma ion frequency, $\omega_{pi}^2 = \frac{4\pi n_i e^2}{m_i}$.

The equation of motion in simple form, governing the plasma particle motion can be written as

$$m\frac{\partial \boldsymbol{v}}{\partial t} + m\boldsymbol{v}\cdot\nabla\boldsymbol{v} = -e\,\boldsymbol{E} - \frac{e}{c}\boldsymbol{v}\times\boldsymbol{B},$$

where $\boldsymbol{v}$ is the particle velocity and **B** is the applied magnetic field**.** If all forces are balance in equilibrium, then we can take $\boldsymbol{v}_{io} = 0$ and$\boldsymbol{v}_{eo} = 0$. In the presence of a wave, the plasma equilibrium can be modified and, in that case, the perturbed quantities can be written as$\boldsymbol{v_{i1}}$,$\boldsymbol{v}_{e1}$, and $\boldsymbol{v}_{b1}$ for plasma ions, plasma electrons and beam particles, respectively.

On linearizing the equation of motion, we can obtain

$$\frac{\partial \boldsymbol{v}_1}{\partial t} = -\frac{e\,\boldsymbol{E}}{m} - (\boldsymbol{v}_o + \boldsymbol{v}_1) \times \hat{\boldsymbol{z}}\omega_c,$$

The plasma density also follows the equation of continuity

$$\frac{\partial n}{\partial t} + \nabla.(n\boldsymbol{v}) = 0,$$

On solving the equations of motions and continuity equation, the velocity and density perturbations due to the LH wave in the presence of beam mode and the magnetic field can be written as

$$\boldsymbol{v}_{B1\perp} = \frac{ie\varphi_p}{m\bar{\omega}^2}\left[\boldsymbol{k}_{p\perp} \times \boldsymbol{\omega_c} + i\left(\omega_p - k_{pz}v_B\right)\gamma_0 \boldsymbol{k}_{p\perp}\right], \tag{5.2}$$

$$\boldsymbol{v}_{B1z} = \frac{-e\varphi_p \boldsymbol{k}_{pz}}{m\bar{\omega}(\gamma_0+\gamma_1)}, \tag{5.3}$$

where $\bar{\omega} = \omega_p - k_{pz}v_B$, $\gamma_1 = (\gamma_0^3/c^2)v_B^2$, and

$$n_{B1} = \frac{-e\varphi_p}{m} n_B \left[\frac{\gamma_0 k_{p\perp}^2}{\bar{\omega}^2} + \frac{k_{pz}^2}{\bar{\omega}^2(\gamma_0+\gamma_1)}\right]. \tag{5.4}$$

Here, symbols ⊥ and ‖ represent perpendicular and parallel velocity components with respect to the applied magnetic field **B.** Sideband LH wave also perturbs beam electrons. Corresponding perturbed velocities and density can be obtained from Eqs. (5.2), (5.3) and (5.4) with $\omega_p$replaced by ω_s, $\mathbf{k}_p$ replaced by $\mathbf{k}_s$, giving$\mathbf{v_B} = 0$.

Pump LH wave and sideband LH wave couple to excite a low-frequency ponderomotive force on beam electrons [3], which can be written as

$$\boldsymbol{F}_{Bz} = \frac{-m}{2}\left[\boldsymbol{v}_{B1\perp}^*.\nabla_\perp \boldsymbol{v}_{Bsz} + \boldsymbol{v}_{Bs\perp}.\nabla_\perp \boldsymbol{v}_{B1z}^*\right]. \tag{5.5}$$

The perpendicular ponderomotive force is usually weak($\omega_p << \omega_c$) and is strongly suppressed by the magnetic field.

Substituting all values using Eqs. (5.2), (5.3) and simplifying Eq. (5.5), we get

$$\boldsymbol{F}_{Bz} = \frac{-e^2}{2m}\varphi_p^*\varphi_s \frac{(k_{s\perp}.\boldsymbol{k}_{p\perp} \times \boldsymbol{\omega_c})}{\bar{\omega}\omega_s\omega_c^2(\gamma_0+\gamma_1)}\left[\bar{\omega}k_{Bz} - k_{pz}(\omega_B - k_{Bz}v_B)\right]. \tag{5.6}$$

Therefore, ponderomotive potential on beam electrons can be written as

$$\varphi_B = \frac{-e}{2m\omega_c^2}\varphi_p^*\varphi_s \frac{(k_{s\perp}.k_{p\perp} \times \omega_c)}{ik_{Bz}\bar{\omega}\omega_s(\gamma_0+\gamma_1)}\left[\bar{\omega}k_{Bz} - k_{pz}(\omega_B - k_{Bz}v_B)\right]. \tag{5.7}$$

Similarly, ponderomotive potential on plasma electrons can be written using Eq. (5.7) by taking $\mathbf{v_B}$= 0 as

$$\varphi = \frac{-e}{2m\omega_c^2}\varphi_p^*\varphi_s \frac{(k_{s\perp}.k_{p\perp}\times\omega_c)}{ik_{Bz}\omega_p\omega_s}\left[\omega_p k_{Bz} - \omega_B k_{pz}\right]. \quad (5.8)$$

φ_B and φ perturb beam electrons linearly at (ω_B, $\mathbf{k_B}$). The perturbed velocities and density are obtained using equation of motion that is $m\frac{\partial\gamma\boldsymbol{v}}{\partial t} + m(\boldsymbol{v}\cdot\boldsymbol{\nabla})\gamma\boldsymbol{v} = -e\,\boldsymbol{E}$, where$\boldsymbol{E} = -\boldsymbol{\nabla}(\varphi_B + \varphi)$ as

$$\boldsymbol{v}_{B\perp} = \frac{-e\boldsymbol{k}_{B\perp}(\varphi_B+\varphi)}{m\gamma_0(\omega_B - k_{Bz}v_B)}, \quad (5.9)$$

$$\boldsymbol{v}_{Bz} = \frac{-e\boldsymbol{k}_{Bz}(\varphi_B+\varphi)}{m\gamma_0(\omega_B - k_{Bz}v_B)}, \text{ and} \quad (5.10)$$

$$n_B = \frac{-k_B^2\omega_{pB}^2}{4\pi e(\gamma_0+\gamma_1)}\left(\frac{k_{Bz}}{k_B}\right)^2\frac{(\varphi_B+\varphi)}{(\omega_B - k_{Bz}v_B)^2} \quad (5.11)$$

The two ponderomotive potentials also perturb plasma electrons linearly and using equation of motion without considering relativistic factor, resulting in perturbed quantities given as:

$$\boldsymbol{v}_{e\perp} = \frac{-ie}{m\omega_c^2}(\boldsymbol{k_B}_{\perp}\times\boldsymbol{\omega}_c + i\boldsymbol{k}_{B\perp}\omega_B)(\varphi_B+\varphi) \quad (5.12)$$

$$\boldsymbol{v}_{ez} = \frac{-e\boldsymbol{k}_{Bz}}{m\omega_B}(\varphi_B+\varphi) \quad (5.13)$$

$$n_e = \frac{k_B^2\omega_p^2}{4\pi e\omega_c^2}\left(\frac{k_{B\perp}^2}{k_B^2} - \frac{\omega_p^2}{\omega_B^2}\frac{k_{Bz}^2}{k_B^2}\right)(\varphi_B+\varphi) \quad (5.14)$$

Substituting linear beam electron density perturbation and linear plasma electron density perturbation in Poisson's Eq., we get

$$\in\varphi = \frac{\omega_{pB}^2}{(\gamma_0+\gamma_1)}\left(\frac{k_{Bz}}{k_B}\right)^2\frac{\varphi_B}{(\omega_B - k_{Bz}v_B)^2} + \frac{\omega_p^2}{\omega_B^2}\left(\frac{k_{Bz}}{k_B}\right)^2 - \frac{\omega_p^2}{\omega_c^2}\left(\frac{k_{B\perp}}{k_B}\right)^2\varphi, \quad (5.15)$$

where $\in\varphi = -\chi_B\varphi_B - \chi_e\varphi$ and $\in = 1 + \chi_B + \chi_e$.

Nonlinear density perturbation at (ω_s, $\mathbf{k}_s$) to beam electrons and plasma electrons can be calculated using the continuity equation as

$n_B^{NL} = \frac{k_s.v_B}{2\omega_s}n_B$and $n_e^{NL} = \frac{k_s.v_0}{2\omega_s}n_e$.

Substituting in Poisson's Equation, we get

$\in_s\varphi_s = \frac{-4\pi e}{k_s^2}(n_e^{NL} + n_B^{NL})$,

where

$$\in_s = 1 + \frac{\omega_p^2}{\omega_c^2}\left(\frac{k_{s\perp}}{k_s}\right)^2 - \frac{\omega_p^2}{\omega_s^2}\left(\frac{k_{sz}}{k_s}\right)^2. \quad (5.16)$$

Multiplying nonlinear coupled Eqs. (5.15) and (5.16), we obtain the nonlinear dispersion relation as:

$$\in\in_s = \frac{k_z^2 c_s^2}{4\omega_s^2}\left(\frac{u}{c_s}\right)^2 \frac{\omega_{pB}^2 sin^2\theta}{(\gamma_0+\gamma_1)(\omega_B - k_{Bz}v_B)^2}\left[1 - \frac{k_{pz}}{k_{Bz}}\frac{\omega_B}{(\omega_p - k_{pz}v_B)}\right], \quad (5.17)$$

where $u = \frac{ek_0|\varphi_p|}{m\omega_c}$, θ is the angle between $\boldsymbol{k}_{s\perp}$ and $\boldsymbol{k}_{p\perp}$, and c_s is the speed of sound.

Solving Eq. (5.17) for the Compton and Raman regimes:

5.2.1 Compton Regime

In this case, the beam density is small, thus we have $\in \approx 1$. Hence, we neglect the self-consistent potential of the beam in comparison with the ponderomotive potential. Hence Eq. (5.17) can be rewritten as

$$(\omega_B - k_{Bz}v_B)^2(\omega_s^2 - \omega_{s1}^2) = \frac{u^2\omega_{pB}^2 k_{Bz}^2 sin^2\theta}{4(\gamma_0+\gamma_1)}\left[1 - \frac{k_{pz}}{k_{Bz}}\frac{\omega_B}{(\omega_p - k_{pz}v_B)}\right]\left[1 + \frac{\omega_p^2}{\omega_c^2}\frac{k_{s\perp}^2}{k_s^2}\right]^{-1}.$$

Taking $\omega_B = k_{Bz}v_B + \Delta_c$ and $\omega_s = \omega_{s1} + \Delta_c$, where Δ_c defined as frequency mismatch.

Now, the growth rate of instability can be calculated as

$$\gamma_c = \frac{\sqrt{3}}{2}\left[\frac{u^2\omega_{pB}^2 k_{Bz}^2 sin^2\theta}{8\omega_{s1}(\gamma_0+\gamma_1)}\left(1 - \frac{k_{pz}}{k_{Bz}}\frac{\omega_B}{(\omega_p - k_{pz}v_B)}\right)\right]^{\frac{1}{3}}\left[1 + \frac{\omega_p^2}{\omega_c^2}\frac{k_{s\perp}^2}{k_s^2}\right]^{-\frac{1}{3}}, \quad (5.18)$$

where $\omega_{s1} = \omega_p \frac{k_{sz}}{k_s}\left[1 + \frac{\omega_p^2}{\omega_c^2}\frac{k_{s\perp}^2}{k_s^2}\right]^{-\frac{1}{2}}$.

Eq. (5.18) indicates that in the weak beam density regime, the growth rate of instability is proportional to one-third power of electron beam density. To see the variation in growth rate with wave number, wave frequency, beam frequency, beam velocity and magnetic field, we normalize growth rate by beam frequency and wave number by parallel pump wave number.

The parameters used for plotting the graphs are: electron plasma density n_e = (10^{11}-10^{15}) cm^{-3}, ω_p = 0.1 ω_{pe} and 0.2 ω_{pe}, ω_{pB} = (0.2-0.6) ω_{pe}, k_{pz}=*3* ω_p/c, θ = 90°, v_B= (0.1-0.8) c, magnetic field B = (10-50) kG and velocity of sound c_s= 10^{-5} c.

In Fig. 5.1, we plot instability growth rate in Compton regime $\frac{\gamma_c}{\omega_{pB}}$with the wave number k_{Bz}/k_{pz}at ω_p=0.1ω_{pe} and 0.2ω_{pe}. The instability growth rate increases with the wave number of the low-frequency wave as well as the pump frequency. These results show the evolution of the instability with the growth of the interacting waves.

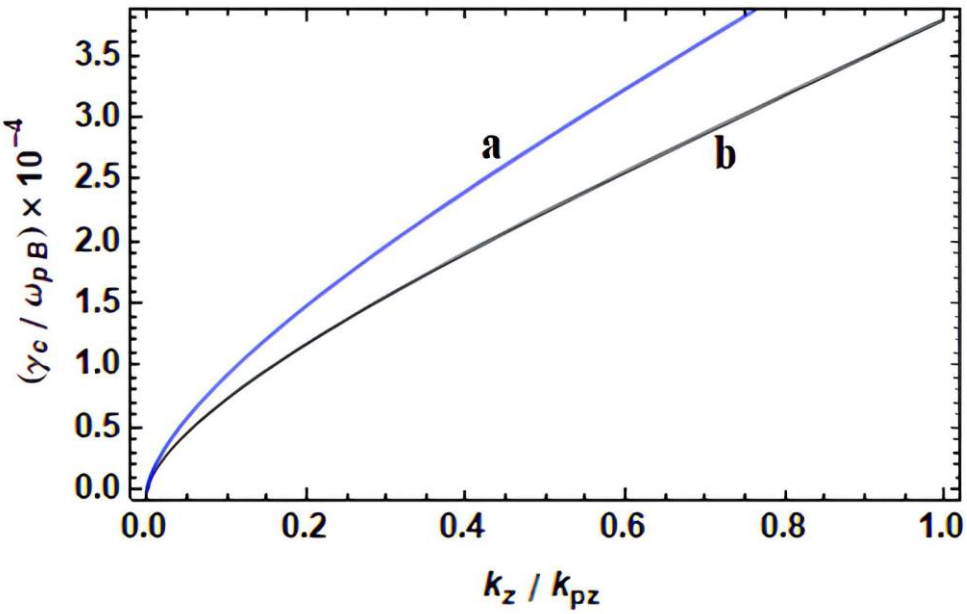

Fig. 5.1 Variation of instability growth rate of LH wave in the Compton regime for different wave frequencies, (a) $\boldsymbol{\omega_p = 0.2\omega_{pe}}$ and (b) $\boldsymbol{\omega_p = 0.1\omega_{pe}}$.

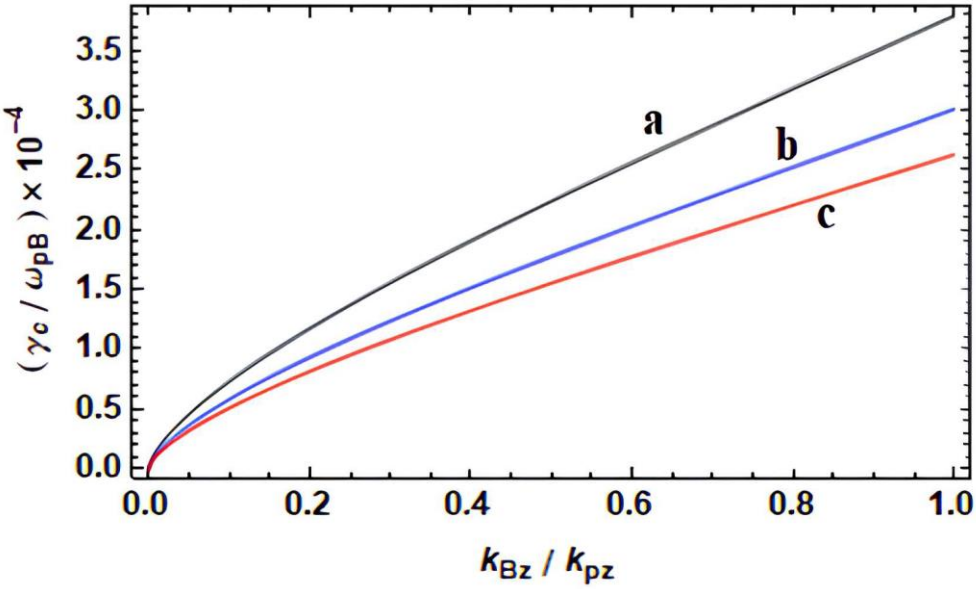

Fig. 5.2 Variation of instability growth rate of LH wave in the Compton regime for different beam frequencies, (a) $\boldsymbol{\omega_{pB} = 0.2\,\omega_{pe}}$, (b) $\boldsymbol{\omega_{pB} = 0.4\,\omega_{pe}}$, and (c) $\boldsymbol{\omega_{pB} = 0.6\,\omega_{pe}}$.

Fig. 5.2 shows the instability growth rate in Compton regime for different beam density. The growth rate of instability increases with the beam density. The sideband couples with the beam mode via Cerenkov interaction to generate parametric instability. The frequency of sideband is upshifted due to negative energy beam mode. An increase in the density of plasma electron further enhances the instability growth rate.

The growth rate dependence on relativistic beam velocity is shown in Fig. 5.3. For a beam counter propagating with the pump LH wave, the sideband frequency is upshifted. For lower wave numbers, the rate of growth of instability with beam velocity is higher. The instability growth rate approaches to the peak due to beam velocity and then starts deceasing. The threshold wave number for the peaked growth rate decreases for higher beam velocity. For a beam co-propagating with the pump LH wave, the side-band frequency is downshifted. To see the role of the applied magnetic field, we depict the instability growth rate for different magnetic field in Fig.5.4. The growth rate increases with the magnetic field. The reason behind this fact is the enhanced growth of the sideband LH wave.

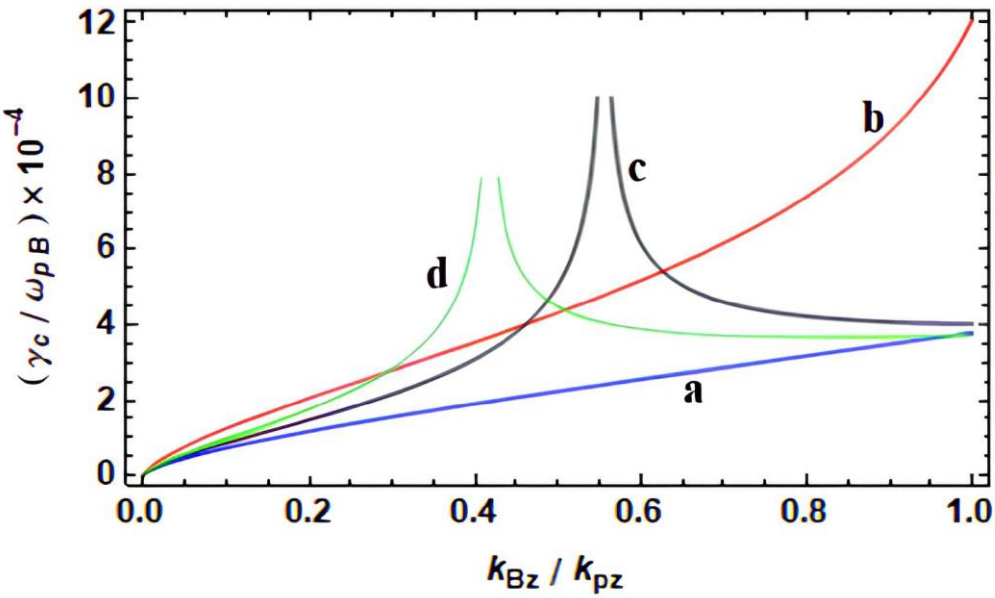

Fig. 5.3 Instability growth rate of LH wave in the Compton regime with the wave number of the beam mode for different beam velocities, (a) $\boldsymbol{v_B = -0.1c}$, (b) $\boldsymbol{v_B = -0.3c}$, (c) $\boldsymbol{v_B = -0.6c}$, and (d) $\boldsymbol{v_B = -0.8c}$.

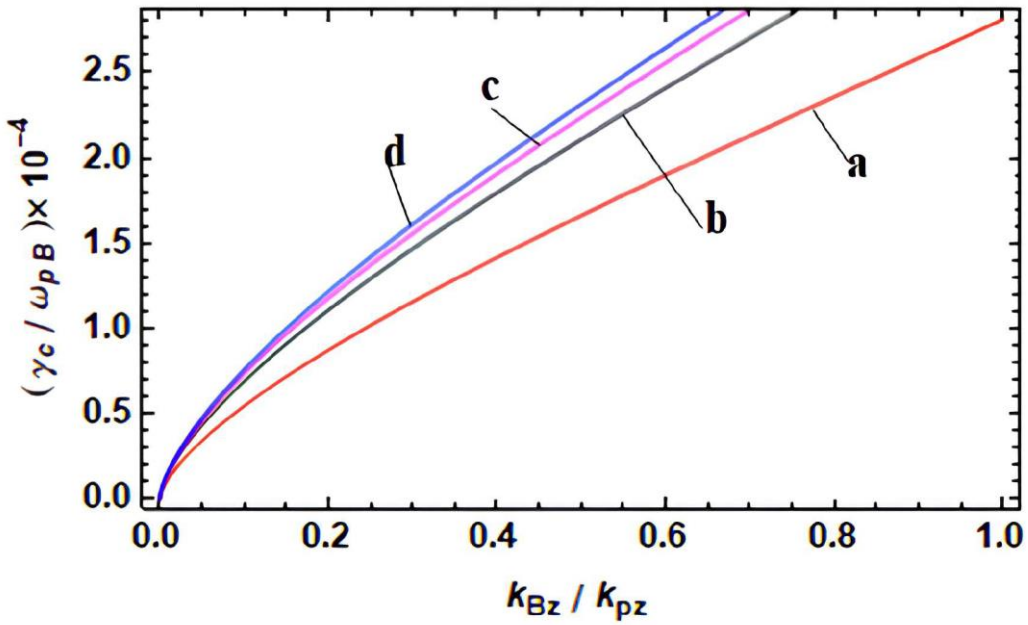

Fig. 5.4 Instability growth rate of LH wave in the Compton regime for different magnetic field strength, (a) **B = 10 kG**, (b) **B = 20 kG**, (c) **B = 30 kG**, and (d) **B = 50 kG**.

5.2.2 Raman Regime

For high beam density we have$\in \approx 0$. For this case, self-consistent potential becomes very high than the ponderomotive one. Therefore, Eq. (5.17) can be written as

$$(\omega_B - \omega_{B1})(\omega_s^2 - \omega_{s1}^2) = -\frac{u^2\omega_{pB}^2 k_{Bz}^2 sin^2\theta}{8(\gamma_0+\gamma_1)k_{Bz}v_B}\left[1 - \frac{k_{pz}}{k_{Bz}}\frac{\omega_B}{(\omega_p - k_{pz}v_B)}\right]\left[1 - \frac{\omega_p^2}{\omega_B^2}\frac{k_{Bz}^2}{k_B^2}\right]^{-1} \times \left[1 + \frac{\omega_p^2}{\omega_c^2}\frac{k_{s\perp}^2}{k_s^2}\right]^{-1}.$$

Taking $\omega_B = \omega_{B1} + \Delta_rand\omega_s = \omega_{s1} + \Delta_r$, the growth rate can be calculated as

$$\gamma_R = \left[\frac{u^2\omega_{pB}^2 k_{Bz}^2 sin^2\theta}{16\omega_{s1}(\gamma_0+\gamma_1)k_{Bz}v_B}\right]^{\frac{1}{2}}\left[1 - \frac{k_{pz}}{k_{Bz}}\frac{\omega_B}{(\omega_p - k_{pz}v_B)}\right]^{\frac{1}{2}}\left[\left(1 - \frac{\omega_p^2}{\omega_B^2}\frac{k_{Bz}^2}{k_B^2}\right)\left(1 + \frac{\omega_p^2}{\omega_c^2}\frac{k_{s\perp}^2}{k_s^2}\right)\right]^{\frac{-1}{2}}, \quad (5.19)$$

where,

$$k_B^2 = \frac{\omega_{pB}^2 k_{Bz}^2}{2(\gamma_0+\gamma_1)k_{Bz}v_B}\left[\frac{1}{2}k_{Bz}v_B - \omega_p\frac{k_{sz}}{k_s}\left(1 + \frac{\omega_p^2}{\omega_c^2}\frac{k_{s\perp}^2}{k_s^2}\right)^{-\frac{1}{2}} + \omega_0\right]^{-1} + \frac{\omega_p^2}{\omega_B^2}k_{Bz}^2 \quad (5.20)$$

and $\omega_{B1} = \frac{1}{2k_{Bz}v_B}\left[k_{Bz}^2 v_B^2 - \frac{\omega_{pB}^2 k_{Bz}^2}{(\gamma_0+\gamma_1)k_B^2}\left(1 - \frac{\omega_p^2}{\omega_B^2}\frac{k_{Bz}^2}{k_B^2}\right)^{-1}\right]$

To determine the instability growth rate $\left(\frac{\gamma}{\omega_{pB}}\right)$in Raman regime, we solve Eqs. (5.19) and (5.20) using mathematical method as was done in the case of Compton regime.

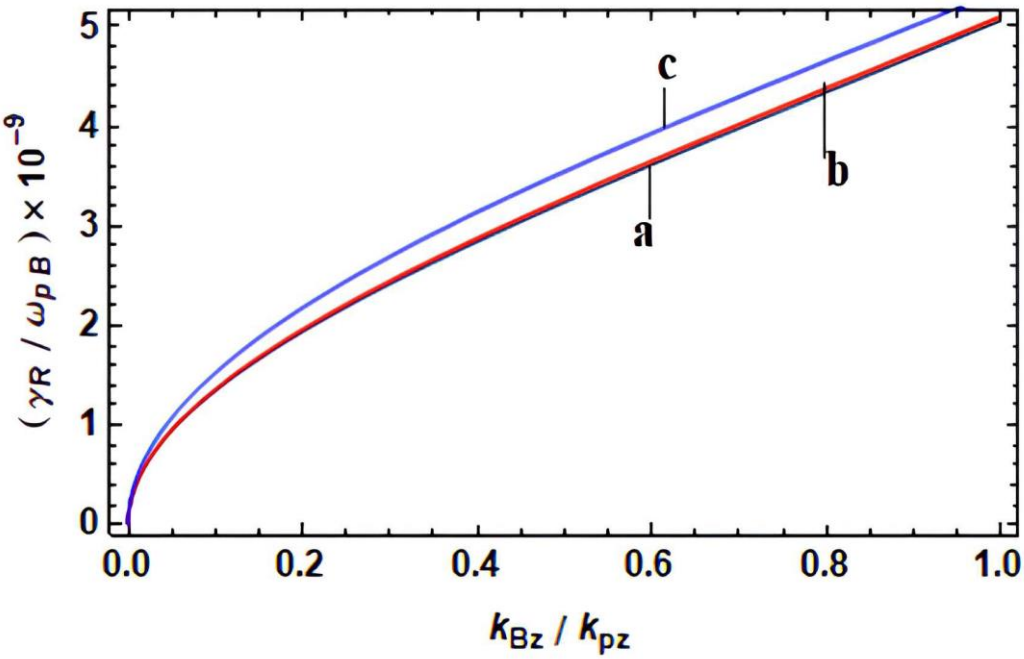

Fig. 5.5 Instability growth rate of LH wave in Raman regime for different plasma frequencies, (a) $\boldsymbol{\omega_p = 0.1\omega_{pe}}$, (b) $\boldsymbol{\omega_p = 0.8\omega_{pe}}$, and (c) $\boldsymbol{\omega_p = 2\omega_{pe}}$.

The normalized growth rate in Raman regime is plotted in Fig.5.5 with the wave number of the beam mode for different values of pump wave frequency. The instability grows with the beam wave number but varies slowly with pump density. These results reveal that the plasma density plays a crucial role in determining the instability growth rate. It is worth to note that the present theory predicts the propagation of LH waves in high-density plasma, because this condition permits to exceed the cut-off for LH waves. At high density, the reason to survive the instability of LH wave is the operating conditions supported by the magnetic field. At higher plasma density, the growth of parametric insatiability of LH wave is sufficiently high to overcome the convective losses, which are intrinsic in parametric instability.

Fig.5.6 shows the instability growth rate with the beam density. The higher beam density supports the growth of the pump wave and hence, the instability growth rate

increases with the beam density. Fig.5.7 depicts the velocity dependence of instability growth rate. As the counter propagating beam velocity increases, instability grows and reaches a maxima at lower velocity for same wave number as compared to growth rate in Compton regime. The variation with magnetic field is almost same in both the regimes but numerical values are smaller for Raman regime.

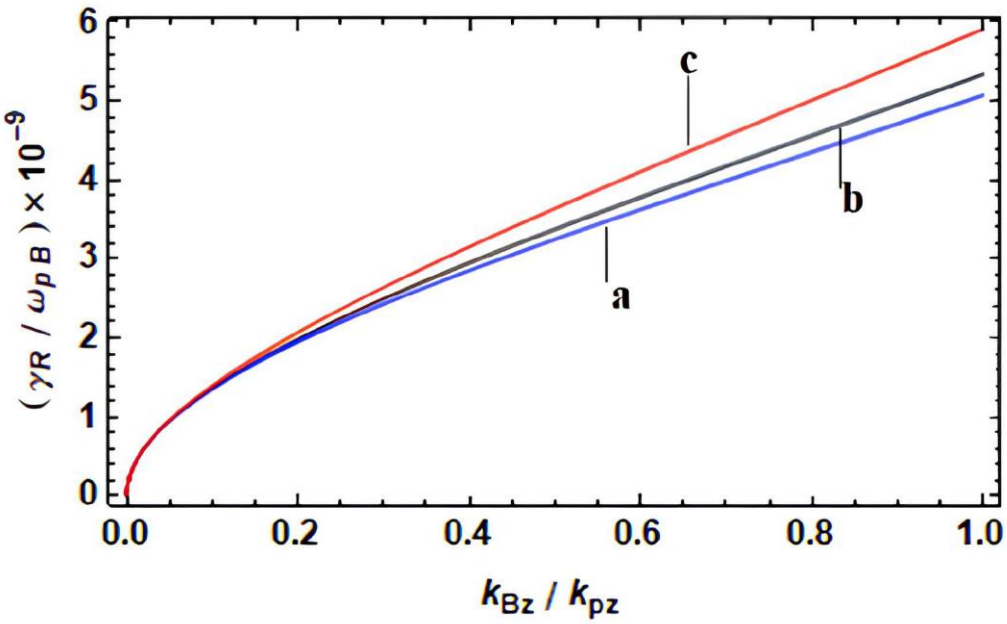

Fig. 5.6 Instability growth rate of LH wave in Raman regime for different beam frequencies, (a) $\boldsymbol{\omega_{pB} = 0.2\ \omega_{pe}}$, (b) $\boldsymbol{\omega_{pB} = 0.4\ \omega_{pe}}$, and (c) $\boldsymbol{\omega_{pB} = 0.6\ \omega_{pe}}$.

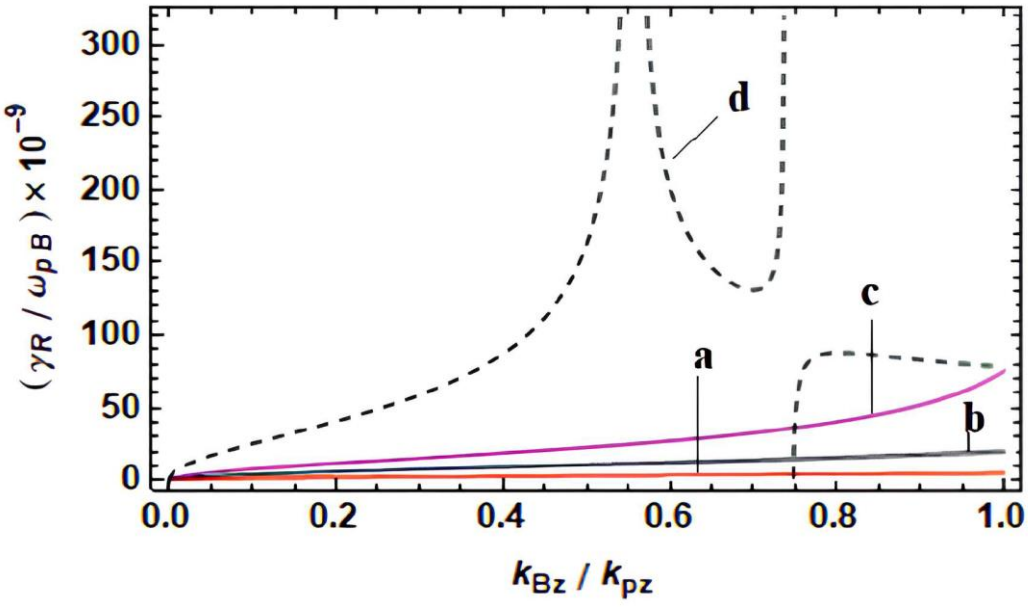

Fig. 5.7 Instability growth rate of LH wave in Raman regime for different beam velocities, (a) $\boldsymbol{v_B = -0.1c}$, (b) $\boldsymbol{v_B = -0.2c}$, (c) $\boldsymbol{v_B = -0.4c}$, and (d) $\boldsymbol{v_B = -0.6c}$.

It has been previously analyzed that the parametric instability of LH wave strongly depends on the magnetic field. We here in Fig.5.8 plot the instability growth rate in Raman regime for different magnetic field strength. The magnetic field assists the instability growth rate because the magnetic field supports the sideband LH wave.

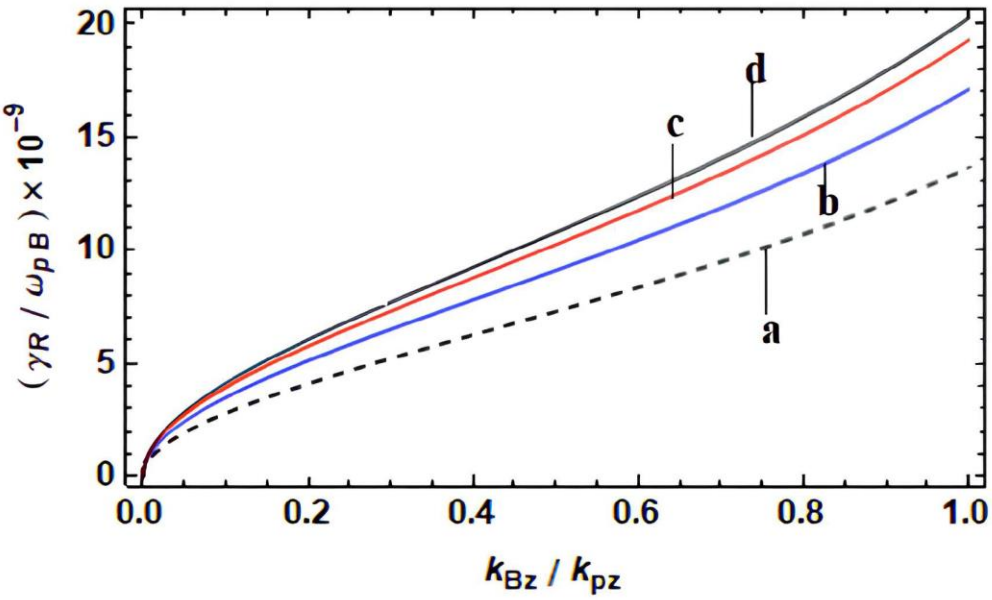

Fig.5.8 Instability growth rate LH Wave in Raman regime for different magnetic field, (a) B= 5kG, (b) B= 10kG, (c) B= 20kG, and (d) B= 50kG.

5.3 CONCLUSION

Using fluid approach, a systematic calculation of the parametric instability of the LH wave in a relativistic and magnetized beam-plasma system has been investigated. The growth rate of parametric instability driven by the lower-hybrid wave is strongly dependent on the local plasma and beam parameters. These results predict that the plasma electron dynamics in the presence of a relativistic electron beam plays a dominant role in determining the beam-coupling producing parametric instability of the LH wave.

The negative energy electron beam supports the instability in various ways. The signature of high growth rates of LH wave is the necessary condition for broadening the launched LH spectrum in fusion plasma. The results shown here provide several optimizations of the instability growth of the LH wave in a relativistic and magnetized

beam plasma system, which may be crucial for the penetration of the coupled LH power in a magnetized plasma.

REFERENCES

[1] N. J. Sircombe, R. Bingham, M. Sherlock, T. Mendonca, and P. Norreys, Plasma Phys. Control. Fusion **50,** 065005 (2008).

[2] G. Praburam, V. K.Tripathi, and V. K. Jain, Phys. Fluids**31,** 3145 (1988).

[3] D. N. Gupta and A. K. Sharma, Laser and Particle Beams **22,** 89 (2004).

[4] R. Kodama et al., Nat. **412,** 798 (2001).

[5] J. Hornubia et al., Laser Part. Beams **22,** 129 (2004).

[6] T. Johzaki et al., Laser Part. Beams **25,** 621 (2007).

[7] W. N. Hesset al., Geophys. Res. **76,** 6067 (1971).

[8] R. A. Hendricksonet al., Nat. **230,** 564 (1971).

[9] J. R. Winckleret al., Am. Geophys. Union **70,** 657 (1989).

[10] T. Neubert et al., J. Geophys. Res. Phys. **107,** SIA 9-1 (2002).

[11] T. Neubert and B. E. Gilchrist, Adv. Space Res. **34,** 2409-2412 (2004).

[12] M. Tabak et al., Phys. Plasmas **12,** 057305 (2005).

[13] H. Saberi and B. Maraghechi, Plasma Phys. Controlled Fus. **55,** 055011 (2009).

[14] S. C. Zhang, Phys. Plasmas **16,** 093107 (2009).

[15] M. Porkolabet al., Phys. Rev. Lett. **38,** 230 (1977).

[16] K. Yatsui and T. Imai., Phys. Rev. Lett. **35,** 1279 (1975).

[17] G. V. Lizunovet al., J. Geophys. Res. **106,** 24755 (2001).

[18] S. C. Sharma et al., Phys. Plasmas. **5,** 3161 (1998).

[19] C. Krafft et al., Phys. Plasmas **7,** 4423 (2000).

[20] D. I. Maslennikovet al., Plasma Physics Report **26,** 139 (2000).

[21] A. S.Volokitin and C. Krafft, Phys. Plasmas. **8,** 3748 (2001).

[22] J. Chang et al., Phys. Rev. Lett. **27,** 1263 (1971).

[23] N. Ahmad and M. Ahmad, Res. Rev.: J. Pure App. Phy. **4** 35 (2001).

[24] J. G. Wang et al., Fusion Eng. Des. **32–33,** 141 (1996).

[25] A. Varma and A. Kumar, Optik. **231,**166326 (2021).

[26] A. Kumar et. al., Opt. Quantum Electron. **54** (2022)

[27] A. Varma and A. Kumar, Optik. **240,** 166872 (2021)

[28] A. Kumar et. al., Laser Phys. **31** 106001 (2021)

[29] A. Varma and A. Kumar, Optik **228,** 166212 (2021)

[30] A. Kumar et. al., Optik**273**, 170436 (2023)

CHAPTER 6

Conclusion and Future Prospective

This chapter summarizes the findings of the research and identifies their implications for the future.

6.1 CONCLUSION

Plasma and dusty plasma waves can be stabilized or destabilized when they interact with electron or ion beams, and collisions generally have a stabilizing effect on them. The shear Alfven wave instability depends on the free energy stored in the particle distribution function in a velocity space, and in a magnetized plasma, ion neutral collisions result in the change of its dispersion relation. we have studied the reaction of oblique shear Alfven waves with an ion beam forced into magnetized plasma parallel and at an angle to the magnetic field in the present thesis. The results obtained from theoretical fluid models are found to be in good agreement with the experimental observations and theoretical predictions of various authors and may found applications for astrophysical and fusion plasmas. It has already been observed in the previous sections that dust plays a vital role in exciting the new collective phenomenon or in modifying the existing wave phenomenon in a plasma due to their variable size and charge. In this work, the role of dust dynamics and charge fluctuations as well as the parameters of external ion beam source, magnetic field has been theoretically investigated in excitation of various plasma wave modes and instabilities. Besides it, the non-linear coupling of lower hybrid waves in a relativistic beam plasma system in the presence of a magnetic field and the electron beam has been also studied. The conclusions drawn from the research work done in the present thesis have been

summarized as follows:

- The study describes an abnormal Doppler resonance with an electron beam in a magnetized plasma that causes a plane polarized Alfven wave to decay nonlinearly. There are two different wave propagation modes: The Alfven wave mode, with a frequency lesser than plasma ion frequency ω_{ci}, and the electron cyclotron wave mode, with a frequency approaching ω_{ce}. The waves and electron beam communicate through both normal and abnormal Doppler resonance. The plane polarized Alfven wave's frequency is increased by the normal resonance interaction, but its amplitude does not increase or decrease. The frequency does not fluctuate and the wave stabilizes in anomalous resonance contact. In this work, it is also described how the frequency and growth rate of plasma electrons vary with magnetic field and number density. With an increase in plasma electron number density, the wave's phase velocity and unstable frequency drop.

- Plasma instability is brought on by energetic electron or ion beams. When an ion beam interacts with magnetoplasmas, the dispersion relation of Alfven waves changes depending on the plasma and beam characteristics because the ion beam may effectively transmit energy to the plasma. The Shear Alfven waves are only affected by the beam's particles when they counter-propagate one another and, via an action called fast cyclotron interaction, destabilize left-hand polarized modes for parallel waves and left-hand as well as right-hand polarized modes for oblique waves. Right-hand (RH) and left-hand (LH) polarized oblique Alfven modes are affected differentially by collisions between beam ions and plasma constituents in terms of the growth rate and frequency of produced Alfven waves. The LH polarized oblique Alfven mode is the most unstable mode for ($\omega + k_z v_{bo} > \omega_{bc}$), whereas the RH polarized oblique Alfven mode is for ($\omega + k_z v_{bo} < \omega_{bc}$), and hence they exhibit a polarization reversal after resonance. The growth rates are correlated with the increase in propagation angle, according to numerical data. Because of the obliquity of the wave, the maximum growth rate values rise in the presence or absence of the beam. The frequency and growth rate of the waves produced are both impacted by the collision of beam ions with plasma constituents. For

beam velocities greater than or equal to 10^8 cm/s, the influence of beam collisions may be disregarded. However, as the beam velocity drops, the significance of collisions increases and they damp the Alfven waves more and more.

♠ Depending on the properties of the beam, dust grains, and plasma, the ion beam-dusty plasma interaction results in considerable variations in the dispersion relation of the shear Alfven wave. When hydrogen ion beam particles counter-propagate and co- propagate with a shear Alfven wave, they interact with through cyclotron interaction and Cerenkov interaction with the wave respectively. Perpendicular currents are produced by the contact, which also results in changes in plasma and beam densities. It has been discussed about how the beam speed, magnetic field, wave number, dust particle density, and dust charge fluctuations affect the situation. As the beam velocity increases, both the wave frequency and maximum growth rate decrease, with the changes being different for parallel and perpendicular wave numbers. While the dust charge variations cause damping, the dust particles increase the frequency and maximal growth rate. The findings and experimental observations are well congruent.

♠ Through beam mode, the non-linear coupling of lower hybrid wave is excited. The decay of large amplitude lower hybrid wave into lower-hybrid sideband wave and beam mode drives the instability. The lower-hybrid wave $(\omega_p, \boldsymbol{k}_p)$ imparts energy and momentum to the electrons of the target plasma. By interacting with electron velocity and producing a non-linear current due to the pump wave, the density fluctuation coupled with the electron beam mode drives a sideband $(\omega_s, \boldsymbol{k}_s)$. The decay of large amplitude lower hybrid wave into lower-hybrid sideband wave and beam mode drives the instability. A ponderomotive force is applied to plasma electrons by the excited sideband wave when it interacts with the pump wave. The low frequency mode at $(\omega_B, \boldsymbol{k}_B)$, which is driven by this coupling, is known as the beam mode. The dependence of parametric instabilities on the local plasma characteristics has been used to determine the rate of growth of the beam driven instability in various beam density

regions. This result indicates that electron dynamics in the presence of a relativistic electron beam play a major role in the beam coupling that results in parametric instability of the LH wave.

6.2 FUTURE PROSPECTIVE

The following information clarifies a few current research-related issues that could be explored later.

- The theoretical investigations can be extended to study nonlinear behaviour of different waves and instabilities.
- The interaction of electron beam or ion beam with plasma waves in magnetized plasma can excite many instabilities, which are helpful for understanding the stability confinement and heating of the plasma
- The investigations can be extended for the astrophysical plasma parameters as well as the theories of bounded plasmas can be extended for the fusion devices parameters.
- The study of oblique modes is very important in the thermodynamics of minor ions in the solar wind and may also find application within the Earth's bow shock as well as to basic plasma processes.
- The studies on the instabilities generated by cyclotron resonances of ions with obliquely propagating waves in solar wind and coronal holes.
- The shear Alfven wave generation has an important role in exciting sub-cyclotron fluctuations in laboratory and space plasmas. In the solar corona, the Alfven waves dissipate their energy and transfer their momentum to the solar wind particles, accelerating the solar wind streams at the Earth's orbit. Thus, Alfven waves play an important role in driving stellar winds. The winds of super-giant stars contain a significant amount of dust particles; therefore, our work may be useful for evaluating the effect of dust on the damping of Alfven waves to accelerate solar wind and understanding the Alfven wave propagation and absorption in dusty interstellar clouds, planetary dust rings, and the Earth's mesopause.
- Several optimizations of the instability growth of the LH wave in a relativistic and magnetized beam plasma system can be investigated which may be crucial for the penetration of the coupled LH power in a magnetized plasma.
- Dusty plasma systems can be used to study "nano-dynamic" behavior of systems at the kinetic level, e.g. physics of liquids, phase transitions, etc.

Moreover, many more the low frequency waves and instabilities having dust particle gravitational effects are yet to be analyzed for the similar plasma conditions.